UNIVERSITEIT VAN PRETORIA
UNIVERSITY OF PRETORIA
YUNIBESITHI YA PRETORIA

Effects of vascular endothelial growth factor receptor-1 inhibition on vasculogenic mimicry and the metabolic profile of breast cancer cells *in vitro*

by

Nare Pretty Sekoba

A thesis submitted in partial fulfilment for the degree of

Doctor of Philosophy (Physiology)

In the

Department of Physiology

School of Medicine

Faculty of Health Sciences

University of Pretoria

Supervisor: Prof P Mabeta

Co-supervisor: Prof M.S. Pepper

2023

Declaration of Originality and Plagiarism

University of Pretoria

Faculty of Health Sciences

Department of Physiology

Title of project:

Effects of vascular endothelial growth factor receptor-1 inhibition on vasculogenic mimicry and the metabolic profile of breast cancer cells *in vitro*

I, Nare Sekoba (student number: 11213354), declare that:

I understand what plagiarism is, and I am aware of the University's policy in this regard.

I declare that this dissertation is my own original work. Where other people's work has been used (either from a printed source, the internet, or any other source), this has been properly acknowledged and referenced in accordance with departmental requirements.

I have not used work previously produced by another student or any other person to hand in as my own.

I have not allowed and will not allow anyone to copy my work with the intention of passing it off as his or her own work.

Signature:

……

Acknowledgements

"**A man's mind plans his way, but the LORD directs his steps and establishes them"**

(Proverbs 16:9)

Alone this journey seemed impossible, but with the love, support and encouragement of the following people, it was made possible.

- I would love to express my deepest gratitude to Professor P Mabeta (lead Supervisor) for her immense dedication, guidance, and support towards this project.
- I appreciate the support and guidance provided by my co-supervisor, Professor MS. Pepper. I cannot thank you enough, Professor P Becker, for your patience and guidance when it came to data analysis.
- The financial assistance of the National Research Foundation (NRF) towards this research is hereby appreciated and acknowledged. Opinions expressed and conclusions arrived at are those of the author and are not necessarily to be attributed to the NRF. The National Research Foundation (Dr P. Mabeta, project 114403) funded this project.
- To my fellow laboratory mate, Lebogang, thank you for your immense support and advise.
- My family, especially my sister, Promise, thank you for your prayers that forever strengthen my soul.
- To my late mom, lehlotlo la bophelo baka, thank you.
- My husband, Lentsoane, for your immense and moral support and for pushing me to be the best version that I can possibly be. To my daughter and Son, Tsholofelo, and Jojo, we did it; thank you for your understanding and support, mommy.

Above all, I would love to thank the Great God of St. Engenas.

I dedicate this Thesis to my late mom.

Executive summary

Female breast cancer is the leading diagnosed cancer globally and the fifth leading cause of cancer mortality worldwide. The ability of breast cancer cells to form vessel-like structures through vasculogenic mimicry (VM) contributes to cancer progression. Vasculogenic mimicry provides a route for the transportation of blood and nutrients, which sustains the growth and survival of breast tumours. Thus, in patients with breast cancer, VM is associated with high tumour grade, metastasis, and poor prognosis. The steps involved in VM include the proliferation and migration of cancer cells, their invasion of the extracellular matrix, and finally, the formation of tube-like structures. The vascular endothelial growth factor receptor-1 (VEGFR-1) signalling pathway is involved in VM, and targeting VEGFR-1 might have clinical relevance and warrants consideration when designing targeted therapies for breast cancer.

Vascular endothelial growth factor receptor-1 is also associated with the metabolic adaptation of cancer cells, as observed in cancer patients who show a correlation between vascular endothelial growth factor A/VEGFR-1 expression and serum lactic acid levels. Indeed, VEGFR-1 promotes the Warburg effect associated with an enhanced acidic environment, which also induces the degradation and remodelling of the extracellular microenvironment.

Therefore, the aim of the study was to investigate the effects of VEGFR-1 inhibition on the steps associated with VM, namely, cell growth, migration, invasion, and metabolism in breast cancer cells *in vitro* using VEGFR-1 inhibitors (ZM 306416 and sunitinib malate).

Human breast cancer cell lines, MCF-10A, MCF-7, and MDA-MB 231 cells were maintained in an incubator at a temperature of 37^0C and in a humidified atmosphere containing 5% CO_2. The effect of VEGFR-1 inhibition on cell viability was measured using the crystal violet assay on MCF-10A (a non-cancerous breast cell line), and breast cancer cell lines, MCF-7 and MDA-MB-231. For subsequent experiments, MDA-MB-231 cells were used as a model of investigation because profound effects (being highly responsive to the drugs of investigation) were observed with this

cell line. Light microscopy was employed to study cell morphology. The effect of VEGFR-1 inhibition on cell migration and invasion was assessed using the scratch assay and the Boyden chamber, respectively. The optimisation of liquid chromatography with the tandem mass spectrometry method for the simultaneous assay of metabolites in cell culture preparations was determined. Lastly, the effects of treatment on the metabolic profile of breast cells were assessed using liquid chromatography with tandem mass spectrometry, enzyme-linked immunosorbent assay, and a pH meter/electrode.

The results demonstrated that sunitinib malate had great efficacy and potency than ZM 306416, as sunitinib malate is a multi-kinase inhibitor. Overall, inhibiting VEGFR-1 reduces cell growth and alters breast cancer cell morphology. In addition, inhibiting the VEGFR-1 signalling pathway attenuates migration and invasion possibly by reducing ATP formation and the extracellular fluid acidity. Optimisation of mass spectrometry in terms of achieving mass ratio and ionisation mode of analytes (glucose-6-phosphate, fructose-6-phosphate, pyruvate, lactate, and glutamate) was achieved, however the optimisation of liquid chromatography was challenging, although it was discovered that analytes of interest in this study should be analysed using the Luna NH2 column to achieve retention and high separation. This study has formed the basis for further investigation of VEGFR-1 targeting in reducing VM and altering metabolic patterns in breast cancer to improve the treatment of this disease.

Keywords: Metabolic reprogramming, tumour growth, vascular endothelial growth factor receptor-1, vasculogenic mimicry

Research Output

Participation in conferences

The 39th congress of the International Union of Physiological Sciences (IUPS), Beijing, China (May 2022)

Poster: Effects of vascular endothelial growth factor receptor-1 inhibition on the metabolic patterns of breast cancer cells. Sekoba NP & Mabeta P.

University of Pretoria, Faculty of Health Sciences, Faculty Day (August 2022)

Poster: Effects of vascular endothelial growth factor receptor-1 inhibition on the metabolic patterns of breast cancer cells. Sekoba NP & Mabeta P.

University of Fort Hare, PhD seminar series, East London, Eastern Cape (October 2022)

Speaker: The clinical relevance of vasculogenic mimicry in breast cancer. Sekoba NP & Mabeta P.

University of Fort Hare, Research week of Excellence, East London, Eastern Cape (November 2022)

Speaker: Effects of vascular endothelial growth factor receptor-1 inhibition on the metabolic patterns of breast cancer cells. Sekoba NP & Mabeta P.

Table of Contents

Declaration of Originality and Plagiarism i

Acknowledgements ii

Executive summary iii

Research Output v

List of Figures x

List of Tables xiii

Abbreviation List xiv

CHAPTER 1: LITERATURE REVIEW 1

1.1. Introduction 1

1.1.1. Risk factors associated with breast cancer 4

1.1.1.1. Female gender and age 4

1.1.1.2. Genetic mutation/heredity 4

1.1.1.3. History of high-risk pathology 4

1.1.1.4. Radiation 5

1.1.1.5. Reproductive factors 5

1.1.1.6. Exogenous hormones 5

1.1.1.7. Obesity and physical activity 6

1.1.1.8. Alcohol 6

1.1.2. Breast cancer classification 6

1.1.2.1. Histological type 8

1.1.2.3. Receptor status 10

1.1.2.3.1. Luminal 11

1.1.2.3.2. Triple-negative breast cancer 11

1.1.3. Breast cancer and the vasculature 12

1.2. The origin of vasculogenic mimicry 13

1.2.1. Vasculogenic mimicry and breast cancer 15

1.2.2.1. Regulators of vasculogenic mimicry in breast cancer....17
1.2.2.2. Techniques applied to detect vasculogenic mimicry....19
1.2.2.3. Vasculogenic mimicry and patient outcome in breast cancer....20
1.3. Metabolism....23
1.3.1. Breast cancer cell metabolism....23
1.3.1.1. Changes in glucose metabolism....23
1.3.1.1.1. Isoforms of glycolytic enzymes....24
1.3.1.1.1.1. Hexokinase II....25
1.3.1.1.1.2. Phosphofructokinase-1....25
1.3.1.1.1.3. Pyruvate kinase M2....26
1.3.1.1.2. Phosphate pentose pathway....26
1.3.1.1.3. Lactate Production....26
1.3.1.2. Activation of glutaminolysis....27
1.3.1.3. Metabolic rewiring and breast cancer subtypes....29
1.3.1.3.1. Luminal subtype....29
1.3.1.3.2. Triple-negative breast cancer subtype....31
1.3.1.4. Regulator of metabolic reprogramming and vasculogenic mimicry....32
1.3.1.5. Treatment that targets vasculogenic mimicry in breast cancer....33
1.4. Targeted therapy....35
1.4.1. Small molecule inhibitors....36
1.4.1.1. Sunitinib malate and ZM 306416....36
1.5. Problem statement....38
1.6. Aim....38
1.7. Objectives....38
CHAPTER 2: MATERIALS AND METHODS....40
2.1. Study design....40
2.2. General materials and cell culture maintenance....41
2.2.1. Cell lines....41
2.2.2.1. MCF 7....41
2.2.2.2. MDA-MB-231....41

2.2.3. Reagents....42
2.2.4. Cell culture maintenance procedure....42
2.2.4.1. Maintenance and subculturing....42
2.2.5. Compound preparation....43
2.3. Experimental methods....43

2.3.1. Crystal violet assay....43
2.3.3. Migration assay....46
2.3.4. Invasion assay....47
2.3.5. Liquid chromatography mass spectrometry....49
2.3.5.1. Sample preparation....51
2.3.5.2. Preparation of standards....52
2.3.5.3. Mass spectrometry method optimisation....52
2.3.5.4. Liquid chromatography method development....53
2.3.6. Adenosine triphosphate assay....54
2.3.7. Extracellular pH....56
2.3.8. Statistics....56
CHAPTER 3: RESULTS....58

3.1. Cell viability....58

3.1.1. Effect of ZM 306416 and Sunitinib malate on the viability of MCF-10A cells....58
3.1.2. Effect of ZM 306416 and Sunitinib malate on the viability of MCF-7 cells....62
3.1.3. Effect of ZM 306416 and Sunitinib malate on the viability of MDA-MB-231 cells....66
3.2. Morphological studies....70

3.3. Cell Migration....73

3.4. Invasion....78

3.5. Liquid chromatography and mass spectrometry....80

3.5.1. Mass spectrometry optimisation....80
3.5.2. Liquid chromatography optimisation....85
3.5.2.1. C18 amide column....85
3.5.2.2. IEC QA-825 column....86
3.5.2.3. Luna HILIC column....86

3.6. Adenosine triphosphate assay 89

3.7. Extracellular pH 92

CHAPTER 4: DISCUSSION 94

CHAPTER 5: CONCLUSION 107

5.1. Future Studies 111

REFERENCES 112

Appendix I: PhD committee letter 138

Appendix II: Ethics letter 139

Appendix III: Language editor certificate 140

Appendix IV: Turnitin report 141

List of Figures

Figure 1.1. Illustration of normal breast architecture……...7

Figure 1.2. Molecular subtypes stratified according to prognosis……...12

Figure 1.3. Timeline on some of the contributions made to understanding vasculogenic mimicry……...16

Figure 1.4. VEGF A/VEGFR-1 signals via the PI3K pathway to cleave the 5y2 chain by activating MMP 2 and 14 and upregulates VE-cadherin and EphA2 to form vasculogenic mimicry channels……18

Figure 1.5. Glycolysis pathway in breast cancer cell…….....24

Figure 1.6. Lactate production and its role in tumour progression…….27

Figure 1.7. The role of glutamine in tricarboxylic acid cycle in the presence of hypoxia……28

Figure 1.8. Breast cancer metabolism……30

Figure 1.9. Molecular structure of small molecular inhibitors. …….....37

Figure 2.1. Flow diagram illustrating the study design…….40

Figure 2.2. Flow diagram of a scratch assay…….46

Figure 2.3. The principle of transwell invasion assay illustrated using Boyden chamber, which mimics invasion *in vivo*……48

Figure 2.4. Flow diagram depicting the preparation and reading of the ATP assay……55

Figure 3.1. Effect of ZM 306416, sunitinib malate and nocodazole on the viability of MCF-10A cells after 24, 48 and 72 hours of treatment……...60

Figure 3.2. Effect of ZM 306416, sunitinib malate and nocodazole on the viability of MCF-7 cells after 24, 48 and 72 hours of treatment …….....64

Figure 3.3. Effect of ZM 306416, sunitinib malate and nocodazole on the viability of MCF-10A cells after 24, 48 and 72 hours of treatment …….....67

Figure 3.4. Morphological images of MDA-MB-231 cells after 24 hours of treatment……...71

Figure 3.5. Morphological images of MDA-MB-231 cells after 48 hours of treatment……71

Figure 3.6. Representative scratch assay images over a 22-hour period……....74

Figure 3.7. Sunitinib malate reduces cellular migration……77

Figure 3.8. Invasion assay of MDA-MB-231 cells after 48 hours of treatment with sunitinib malate……...79

Figure 3.9(A). LC-MS/MS chromatogram of glucose-6-phosphate…….....80

Figure 3.9(B). LC-MS/MS chromatogram of fructose-6-phosphate…….....81

Figure 3.9(C). LC-MS/MS chromatogram of pyruvate…….....82

Figure 3.9(D). LC-MS/MS chromatogram of lactate…….....83

Figure 3.9(E). LC-MS/MS chromatogram of glutamate…….....84

Figure 3.10. C18 amide chromatography of fructose-6-phosphate, glucose-6-phosphate, pyruvate, lactate and glutamate……...85

Figure 3.11. IEC QA-825 chromatography of fructose-6-phosphate, glucose-6-phosphate, pyruvate, lactate and glutamate……...86

Figure 3.12. Luna HILIC chromatography of fructose-6-phosphate, glucose-6-phosphate, pyruvate, lactate and glutamate……...87

Figure 3.13. ATP standard curve……89

Figure 3.14(A). The effect of sunitinib malate on the ATP levels in MCF-7 cells…….……90

Figure 3.14(B). The effect of sunitinib malate on the ATP levels in MDA-MB-231 cells……91

Figure 4.1. Postulated mechanism of ZM 306416 and sunitinib malate in inhibiting breast cancer cell growth……...97

Figure 4.2. Anti-migratory, -invasive, and -vasculogenic mimicry properties of sunitinib malate……100

Figure 4.3. Effect of sunitinib malate on the metabolic patterns of MDA-MB-231 cells……105

Figure 5.1. The integrative mechanism of inhibiting VEGFR-1 and its effects on the steps that constitute vasculogenic mimicry (growth, migration, and invasion) in breast cancer cells……110

List of Tables

Table 1.1. Estimated changes in the age-standardised rate of the incidence rate of breast cancer from 2008 to 2020……2

Table 1.2. Estimated changes in the age-standardised rate of the mortality rate of breast cancer from 2008 to 2020…….....3

Table 1.3. Histological types and their characteristics…….....…9

Table 1.4. Vasculogenic mimicry and its association with prognosis in breast cancer patients……22

Table 1.5 Therapeutic compound which inhibits vasculogenic mimicry in breast cancer in preclinical studies……...34

Table 1.6 Potential drugs targeting vasculogenic mimicry in clinical trials in breast Cancer……....35

Table 2.1. Mass spectrometry parameters……53

Table 2.2. Gradient elution method showing total LC run time vs the % mobile phase B……54

Table 3.1. Compound concentrations required for half-maximal growth inhibition of MDA-MB-231 and MCF-7 cells……..69

Table 3.2. Comparison of extracellular pH in breast cancer cells……93

Abbreviation List

ALK	Activin-like kinase
ATCC	American Tissue Culture Collection
ATP	Adenosine triphosphate
BRCA	Breast cancer gene
CAF	Cancer-associated fibroblast
CE	Collision energy
Chk	Checkpoint kinase
CoA	Coenzyme A
CUR	Curtain gas
DDAH 1	Dimethylarginine dimethylaminohydrolase 1
DMBT	(2.3-dimethoxybenzoyl)a,a-D-trehalose
DMEM	Dulbecco's modified eagle's medium
DP	Declustering potential
E2	17β-estradiol
ECM	Extracellular matrix
EGFR	Epidermal growth factor receptor
ELISA	Enzyme-linked immunosorbent assay
EMT	Epithelial to mesenchymal transition

EP	Entrance potential
EphA 2	Ephrin type A receptor 2
ER	Estrogen receptor
FAD^+	Flavin adenine dinucleotide
FADH	Flavin adenine dinucleotide hydrogen
FAK	Focal adhesion kinase
FBS	Foetal bovine serum
GLUT	Glucose transporters
HER2	Human epidermal growth factor receptor 2
HIF	Hypoxia-inducible factor
IDC	Invasive ductal carcinoma
IDC-NOS	Invasive ductal carcinoma not otherwise specified
IDC-NST	Invasive ductal carcinoma, no special type
ILC	Invasive lobular carcinoma
ISV	Ion spray voltage
JAK	Janus kinase
LC-MS/MS	Liquid chromatography with tandem mass spectrometry
LDH	Lactate dehydrogenase
MCT	Monocarboxylate transporter
MMP	Matrix metalloproteinase

mTOR	Mammalian target of rapamycin
NAD	Nicotinamide adenine dinucleotide phosphate
NADPH	Nicotinamide adenine dinucleotide phosphate hydrogen
OXPHOS	Oxidative phosphorylation
PAS	Periodic acid Schiff
PBS	Phosphate buffered saline
PFK	Phosphofructokinase
PFKFB-3	Phosphofructo-2-kinase/fructose-2,6-bisphosphatase
PI3K	Phosphoinositide-3-kinase
PIGF	Placental growth factor
PK	Pyruvate kinase
PlasDIC	Polarization-optical differential interference contrast
PPP	Phosphate pentose pathway
PR	Progesterone receptor
SL1CA 5	Solute carrier family 1 member 5
TCA	Tricarboxylic acid
TEM	Temperature
TNBC	Triple-negative breast cancer
TNM	Tumour size, lymph node and metastasis
VE	Vascular endothelial

VEGF	Vascular endothelial growth factor
VEGFR	Vascular endothelial growth factor receptor
VM	Vasculogenic mimicry
WIBC-9	Human inflammatory breast cancer xenograft

CHAPTER 1: LITERATURE REVIEW

1.1. Introduction

Breast cancer is the most common cancer diagnosed in females worldwide, increasing from 1.3 million estimated new incidence cases in 2008 to 2.3 million estimated new cases in 2020 [1-2]. Although there is an increasing trend of incidence rate globally, in some developed countries, the reported incidence and mortality rate are lower than the global average and are relatively stable and decreasing, as depicted in **Table 1.1.** and **Table 1.2.** [3-4]. In African countries such as middle Africa (32.7 per 100 000 females), the incidence rate is low compared to other continents such as Europe (Western Europe (90.7 per 100 000 females) and America (Northern America 89.4 per 100 000 females), although the incidence rate is rising in some parts of Africa as shown in **Table 1.1.** [2]. The low incidence rate presented in Africa does not necessarily present a low-risk breast cancer continent, as the age-standardised mortality rate of Africa ranked highest globally in 2020 [2,5].

In low-and middle-income countries, including South Africa, 1 in 26 females in their lifetime are at risk of being diagnosed with breast cancer [6]. There are several challenges that contribute to the high diagnosis-to-mortality ratio in low and middle-income countries in Africa, such as poor health infrastructure, lack of population awareness and delayed health-seeking behaviour, among others [6-7]. As shown in **Table 1.1.**, reported by GLOBOCAN 2020, Southern Africa and Northern Africa present with the highest incidence rate compared to the other African sub-regions [2,8-9]. Of note is that Africa's incidence and mortality rate from 2008 to 2020 depicts an increasing trend. Therefore, the burden of breast cancer is projected to double in Africa by 2030 with ageing, population growth and adoption of unhealthy lifestyles [1,10].

Table 1.1. Estimated changes in the age-standardised rate of incidence rate of breast cancer from 2008 to 2020 [1-2, 8-9]

	Incidence				
	2008	2012	2018	2020	% Increase
Europe					
Western Europe	89.9	96.0	92.6	90.7	0.9
Northern Europe	84	89.4	90.1	86.4	2.9
Southern Europe	68.9	74.5	80.3	79.6	15.5
Eastern Europe	45.3	47.7	54.5	57.1	26.0
America					
Northern America	76.7	91.6	84.8	89.4	16.6
South America	44.3	52.1	56.8	56.4	27.3
Asia					
Western Asia	32.5	42.8	45.3	46.6	43.4
Eastern Asia	25.3	27.0	39.2	43.3	71.1
South-Eastern Asia	31	34.8	38.1	41.2	32.9
South-Central Asia	24	28.2	25.9	26.2	9.2
Africa					
Eastern Africa	19.3	30.4	29.9	33.0	71.0
Middle Africa	21.3	26.8	27.9	32.7	53.5
Western Africa	31.8	38.6	37.3	41.5	30.5
Northern Africa	32.7	43.2	48.9	49.6	51.7
Southern Africa	**38.1**	**38.9**	**46.2**	**50.4**	**32.3**

Table 1.2. Estimated changes in the age-standardised rate of the mortality rate of breast cancer from 2008 to 2020 [1-2, 8-9]

	Mortality				
	2008	2012	2018	2020	% Increase
Europe					
Western Europe	17.5	16.2	15.5	15.6	-10.9
Northern Europe	17.8	16.4	14.1	13.7	-23.0
Southern Europe	15.3	14.9	13.3	13.3	-13.1
Eastern Europe	16.9	16.5	15.5	15.3	-9.5
America					
Northern America	14.8	14.8	12.6	12.5	-15.5
South America	13.2	14.0	13.4	14.0	6.1
Asia					
Western Asia	14.3	15.1	13.6	16.0	12.0
Eastern Asia	6.3	6.1	8.6	9.8	55.6
South-Eastern Asia	13.4	14.1	14.1	15.0	11.9
South-Central Asia	12	13.5	13.6	13.1	9.2
Africa					
Eastern Africa	11.4	15.6	15.4	17.9	57.0
Middle Africa	13.1	14.9	15.8	18.0	37.4
Western Africa	18.9	20.1	17.8	22.3	18.0
Northern Africa	17.8	17.4	18.4	18.8	5.6
Southern Africa	**19.3**	**15.5**	**15.6**	**15.7**	**-18.7**

1.1.1. Risk factors associated with breast cancer

Breast cancer begins with abnormal proliferation of breast cells that replicate to form a malignant tumour that eventually metastases to other parts of the body such as the lung, bone, liver and brain [11-12]. Signs of breast cancer include a lump in the breast, a change in breast shape, dimpling of the breast skin, nipple discharge and/or a red scaly patch of skin [13]. The etiology of breast cancer is complex. However, there are well-recognised risk factors that are associated with the risk of developing breast cancer, which are discussed below:

1.1.1.1. Female gender and age

The risk of females developing breast cancer is approximately a hundred times greater than that of males [14].

The risk of developing breast cancer increases with age. It is estimated that there is 1 in 1, 732 probability of developing breast cancer in the next ten years for a woman with a current age of 20 years. This raises to 1 in 69 and 1 in 26 for individuals aged 40 and 70 years, respectively [13-14].

1.1.1.2. Genetic mutation/heredity

Inherited mutations account for 5 to 10% of breast cancer cases. Breast cancer gene *(BRCA)1* and *BRCA2* mutation are associated with increased susceptibility to breast cancer. It is suggested that all women having a first-degree female relative with breast cancer are at risk, with risk increasing with the younger age of the relative's diagnosis [8,14].

1.1.1.3. History of high-risk pathology

Women who have previously been diagnosed with breast cancer are at a two to five times increased risk of developing a second primary breast cancer. Again, women with previous proliferative lesions with atypia, such as atypical ductal hyperplasia or atypical lobular hyperplasia, are at five times increased risk of developing breast cancer [14-15].

1.1.1.4. Radiation

Ionizing radiation is an environmental exposure for which there is well-established evidence of carcinogenicity for breast cancer. Exposure to radiation is now from diagnostic medical imaging, including radiographs, fluoroscopy, and computed tomography. Women, who have been previously treated with radiation therapy, for example, for lymphoma or bone tumours in childhood, are at greater risk of developing breast cancer [16-17].

1.1.1.5. Reproductive factors

Breast cancer is a hormonally dependent malignancy. Abnormal levels of estrogen have been associated with breast carcinogenesis through a proliferative impact on breast tissue [18]. Thus, it is hypothesised that greater exposure to estrogen and androgens increases the likelihood of developing breast cancer [14]. Younger age at menarche and older age at menopause subject women to longer exposure to estrogen and androgens, and therefore, it has been associated with an increased risk of hormone receptor-positive breast cancer [14,19].

Number of pregnancies has been inversely associated with a relative risk of luminal-like breast cancer [20]. However, women older than 20 years and giving birth to their first child have a higher risk of developing breast cancer than nulliparous women. The latter is substantiated by speculation that a full-term pregnancy at an early age may reduce the likelihood of tumour initiation by causing further maturation of breast epithelial cells, while a full-term pregnancy at a later age may promote the growth of existing tumour cells [14,19].

1.1.1.6. Exogenous hormones

Long duration of oral contraceptive use (>10 years) has been associated with a slight increase in the risk of triple-negative breast cancer (TNBC) [20]. Additionally, Ellingjord-Dale *et al*. (2017) had observed that intrauterine device usage for more than 10 years is associated with breast cancer risk. This was further supported by a Finnish study of levonorgestrel-releasing intrauterine devices and breast cancer, which reported that levonorgestrel-releasing intrauterine devices were

associated with an increased risk of breast cancer [20]. One hypothesis is that levonorgestrel-releasing intrauterine devices have substantial progestogenic and androgenic effects, which could contribute to this increased breast cancer risk with intrauterine device use [21].

1.1.1.7. Obesity and physical activity

Obesity, measured by body mass index is associated with an elevated risk of postmenopausal breast cancer [14,17]. Body fat in postmenopausal women is the main source of estrogen secretion via the aromatisation of androgens. As previously mentioned, high levels of estrogen are directly proportional to breast cancer risk [18].

Increased physical activity may reduce the risk of breast cancer by reducing the level of body fatness and through reducing estrogen levels [17].

1.1.1.8. Alcohol

In a large-pooled analysis of 20 studies, including 37, 191 breast cancer cases, alcohol consumption of ≥30 g/day was associated with a relative risk of 1.32 (95% CI 1.23–1.41) when compared with 0 g/day of alcohol consumption. Moreover, it appears that alcohol consumption has an effect on both estrogen-positive tumours and estrogen-negative malignancies [22]. The proposed mechanism explaining the relationship between breast cancer and alcohol consumption involves alcohol metabolism, by which alcohol is converted to acetaldehyde by alcohol dehydrogenase which is expressed in the breast tissue. Acetaldehyde is genotoxic and is considered to increase breast cancer risk by damaging DNA. Another common proposal is that alcohol increases breast cancer risk via alterations in circulating estrogen levels [23].

1.1.2. Breast cancer classification

Breast cancer is a heterogeneous and complex disease with different biological features and clinical behaviours [24-25]. Clinically, several factors such as morphological classification (nuclear grade, tubular grade, mitotic index, histological grade and architectural characteristics), clinical

pathologies parameters (tumour size, lymph node involvement and metastasis) and molecular classification are used to categorise patients with breast cancer to assess prognosis and recommend the appropriate treatment [13,26].

Therefore, to understand breast cancer development, it is important to reflect on the normal architecture of the breast.

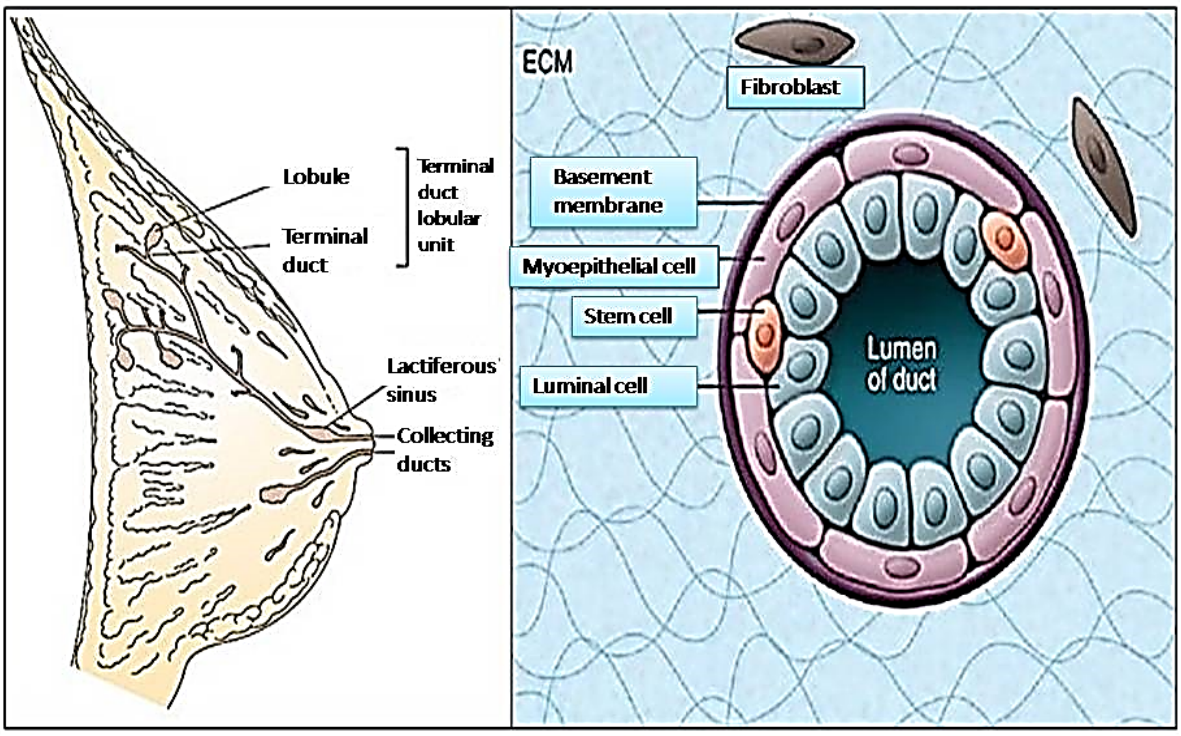

Figure 1.1. Illustration of normal breast architecture. **(A)** The structure of lobules as they connect to a common terminal interlobular duct. **(B)** The structural lining of the duct. *Reprinted with permission from Bertos & Park [27].*

Each lobe of the breast arises from multiple lobules, which connect to a common terminal interlobular duct. These ducts then continue to their outlet at the nipple. Histologically, lobules and ducts are lined by a single layer of luminal epithelial cells, surrounded by transversely oriented myoepithelial cells. A basement membrane separates these structures from the surrounding tissue, or stroma (**Figure 1.1.**) [27].

1.1.2.1. Histological type

Breast cancer arises in the epithelial lining of the ducts (85%) or lobules (15%) in the breast glandular tissue [28]. Initially, tumour growth is confined locally within the breast, which is referred to as carcinoma *in situ.* In contrast, invasive carcinoma penetrates the surrounding tissues and may be associated with distant metastasis [13,29]. These growth patterns form part of the histological type, which further describes breast cancer's morphological and cytological patterns associated with distinctive clinical outcomes [26,30].

According to the 4th edition of the World Health Organization, the histological classification of breast cancer comprises 21 subtypes of invasive breast carcinoma [31]. Invasive ductal carcinoma not otherwise specified (IDC-NOS)/ no special type (IDC-NST) and invasive lobular carcinoma (ILC) represents the vast majority of breast cancers [26-27]. Breast cancer special types (categorised as medullary, tubular, apocrine, mucinous, inflammatory and papillary types) account for the remaining cases of breast cancer, which lack sufficient characteristics to be classified as one of the special types; their characteristics are further discussed in **Table 1.3.** [26,31]. These morphological classifications are utilised in the clinical setting and research to investigate therapeutic targets specific to each subgroup [30].

Table 1.3. Histological types and their characteristics

Histological type	Characteristics
Lobular carcinoma *in situ*	Characterised by a population of small aberrant cells with small nuclei, individual private acini and a lack of cohesion between cells
Ductal carcinoma *in situ*	Characterised by the proliferation of malignant cells within the ducts without invasion of surrounding stromal tissues
Invasive lobular carcinoma	Second most common histopathological type, representing approximately 10-20% of all breast malignancies
Invasive ductal carcinoma	Represents roughly 70% of all breast malignancies and penetrates the surrounding tissues, and may be associated with distant metastasis.
Medullary carcinoma	Characterised by sharp tumour borders and lymphoid infiltration
Mucoid carcinoma	Characterised by large amounts of extracellular mucous
Papillary carcinoma	Characterised with well-differentiated papillary structure
Inflammatory carcinoma	Is a rare and aggressive form of breast cancer and occurs in 1-2% of all breast malignancies.
Tubular carcinoma	Are usually small (about 1 cm or less) and made up of tube-shaped structures
Apocrine carcinoma	A rare malignant adnexal neoplasm that most commonly arises in areas with high apocrine gland

1.1.2.2. Grade and the tumour size, lymph node and metastasis system

The histological grade is also used in classifying breast cancer into biological and clinically meaningful subgroups. Grading compares the appearance of the breast cancer cells to the appearance of normal breast tissue [13]. It is an assessment of the degree of differentiation (i.e. tubule formation and nuclear pleomorphism) and proliferative activity of a tumour [24]. Cells are described as well-differentiated (low grade), moderately differentiated (intermediate grade), and poorly differentiated (high grade) as the cells progressively lose the features seen in normal breast cells. Cancerous cells are poorly differentiated or undifferentiated as cell division becomes uncontrolled and cell nuclei become less uniform. Poorly differentiated cancers have the worst prognosis as they are highly aggressive and tend to metastasise [13,32].

Breast cancer staging uses the tumour size, lymph node and metastasis (TNM) system, which is based on tumour size, whether or not the tumour has spread to the lymph node and whether the tumour has metastasis [13,33].

- Stage 0 is a pre-cancerous, either ductal carcinoma *in situ* or lobular carcinoma *in situ*.
- Stage 1-3 are within the breast or regional lymph node.
- Stage 4 is metastatic cancer that has the worst prognosis.

1.1.2.3. Receptor status

Gene expression profiling is another method used to classify breast cancer into various molecular subtypes depending on the presence or absence of receptors. Breast cancer cells have receptors on their surfaces, cytoplasm and nucleus. Chemical messengers such as hormones bind to these receptors causing secondary changes in the cells. These receptors include estrogen receptor (ER), progesterone receptor (PR) and human epidermal growth factor receptor (HER)2 [13,26]. Perou *et al*. [34], in a seminal study, performed cDNA microarray analysis of 38 invasive breast cancer (36 IDC and 2 ILC), 1 ductal carcinoma *in situ*, 1 fibroadenoma and 3 normal breast

samples, and a number of biological replicates from the same patients, and defined an intrinsic gene list . An intrinsic gene list is genes that vary most between tumours from different patients compared to samples from the same tumour/ patients. Hierarchical cluster analysis from the intrinsic gene list revealed the division of the cluster dendrogram into ER-positive and ER-negative breast cancer and the existence of four molecular subtypes of breast cancer: luminal, normal breast-like, HER2 and basal-like (triple-negative). Perou *et al*. (2000) further demonstrated that the ER-positive luminal group could be separated into at least two subgroups; luminal A and luminal B [34]. In this study, luminal and triple-negative subtypes are the focus of the study, as MCF-7 (luminal subtype) and MDA-MB-231 (triple-negative subtype) cell lines were used as experimental models. Together with MCF-10A cells which are normal mammary epithelial cells.

1.1.2.3.1. Luminal

Luminal tumours are positive for estrogen and progesterone receptors, with luminal A being negative for HER2 receptors and luminal B being positive for HER2 [35-36]. MCF-7 breast cell line was established in 1973 at the Michigan Cancer Foundation and is classified as a luminal A breast cancer cell as it expresses ER receptor [37]. Luminal A tumours have been shown to have high levels of expression of ER-activated genes, low levels of proliferation-related genes, to be usually of low histological grade and have a good prognosis compared to their counterpart, luminal B (**Figure 1.2.**). Luminal B cancers are more often of a higher histological grade and have a higher proliferation rate, with a worse prognosis [36,38]. Although the majority of luminal tumours respond well to hormonal intervention due to the presence of specific hormonal receptors in luminal subtype tumours, recurrence after treatment does occur [39].

1.1.2.3.2. Triple-negative breast cancer

Triple-negative tumours do not express ER, PR and HER2 receptors [13,35]. Triple-negative breast cells are the most heterogeneous compared to other subtypes as they are further differentiated into at least; basal, claudin-low, metaplastic breast cancer and interferon-rich (**Figure 1.2.**) [35].

MDA-MB-231 breast cells formed part of the claudin-low (claudin are proteins that form part of tight junctions of the cell) subtype and were established in the 1970s [40]. Claudin-low subtype are characterized by characterised by the low expression of tight-junction claudins and enrichment of epithelial-to-mesenchymal transition (EMT) marker, which contributes to the invasive nature of the tumour subtype [41]. Therefore, clinically claudin-low tumours are clustered as aggressive, invasive and having poor prognosis. Overall, TNBC tumours are more aggressive and have a markedly higher likelihood of being grade III than luminal A tumours [26]. Despite the poor prognosis, only 20% of triple-negative tumours respond better to chemotherapy. However, it should be noted that there is currently no molecular-based targeted therapy for TNBC mainly due to the lack of receptors in TNBC tumours which negates the use of targeted therapy [26].

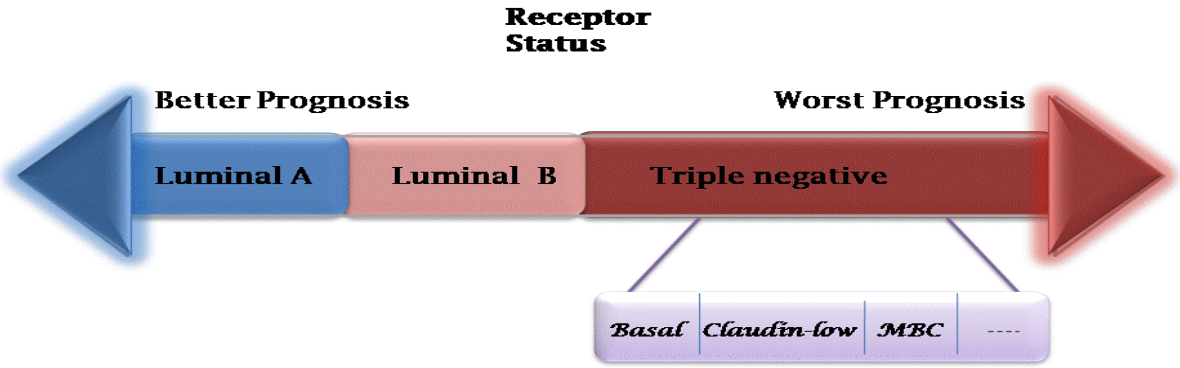

Figure 1.2. Molecular subtypes stratified according to prognosis. Triple-negative tumour is further stratified into basal, claudin-low, metaplastic breast cancer and interferon-rich. MBC; metaplastic breast cancer,- - -; interferon-rich. *Figure drawn by N.P Sekoba using Microsoft PowerPoint, adapted from Dai et al.* [35].

1.1.3. Breast cancer and the vasculature

The vascular phase is characterised by the formation of new vascular channels that enhance tumour cell proliferation, invasion and metastasis. Cancer metastasis involves the dissemination of primary tumour cells into the lymphatic system or vasculature with the aim of colonising

secondary sites [42-43]. Distant metastasis is the main cause of mortality in breast cancer patients [44]. Vasculogenic mimicry (VM), the formation of vascular channels lined by tumour cells with stem cell features that are devoid of endothelial cells [45-46], serves as a driver of metastasis in a polyclonal mouse model of breast tumour heterogeneity [47].Triple-negative breast cancer is prone to form VM channels compared to luminal breast cancer subtype [48]. Therefore, this unique feature incurred by TNBC perpetuates the aggressiveness of TNBC, and enables them to disseminate and invade distant organs, thus increasing the risk of mortality. Consequently, it is imperative to understand the contribution of VM in breast cancer progression.

1.2. The origin of vasculogenic mimicry

The discovery of VM began with the detection of a highly patterned network of extracellular matrix (ECM) in tissue sections of uveal melanoma [46]. Folberg *et al*. [49], using fluorescein-tagged Ulex and laser scanning confocal microscopy, described periodic acid Schiff (PAS) (a stain) -positive loops, networks, and cross-linked parallel vascular patterns. However, it was initially assumed that these patterns represented the remodelled tumour blood vessels [49].

Maniotis *et al*. [46] reconstituted the PAS-positive patterns *in vitro* in a series of experiments and presented a new interpretation from previous findings. Maniotis *et al*. (1999) observed highly invasive primary and metastatic uveal and cutaneous melanoma forming patterned networks of interconnected loops of ECM in 3D cultures containing matrigel or dilute type I collagen in the absence of endothelial cells or fibroblasts. Not only did invasive melanoma cells generate looping patterns, but they also made cords which eventually became hollow for short distances. Therefore, VM could generally be divided into tubular and patterned matrix types [46,50-51].

Maniotis and colleagues, in an *in vitro* study had also observed that these tumour cells, lining non-endothelial channels in tumour mass, also contained red blood cells and conducted fluid [46]. From the observations, it was suggested that aggressive melanoma cells might generate vascular channels that facilitate tumour perfusion. This phenomenon was coined VM on the basis that

these channels were not blood vessels (devoid of endothelial cells) but merely mimicked the function of vessels [51]. This novel phenomenon ignited a spirited debate for several years. Two positive commentaries supporting the significance of Maniotis *et al*. findings were provided by Bissel [52] and Biranga [53], followed by a controversial commentary article by McDonald [54] entitled "Vasculogenic Mimicry: How Convincing, How Novel, and How Significant?"

McDonald [54] lambasted the concept of VM being novel, as the possibility of cancer cells participating in the formation of a blood vessel in tumours had been recognised many years ago before the coining of VM. In 1948, Willis stated that in "rapidly growing tumours, vessels consist of irregular channels lined by endothelium only or by naked tumour cells" [55]. McDonald *et al*. argue that although Willis did not use the terminology of VM he clearly states the concept of tumour cells acquiring a phenotype that allows participation in the formation of blood vessels [54]. An article by Folberg and Maniotis provided similar evidence to McDonald and colleagues, showing that tubular VM is not as novel as others have hinted at non-endothelial cell-lined channels in melanoma and other tumours. However, Folberg and Maniotis further indicated that the patterned matrix-its histogenesis, composition, ultrastructure and role in perfusion, is novel [51].

The physiological function and clinical significance of VM were also debated: In 1996, Pötgens [56] developed a xenograft model of cutaneous melanoma, which contained looping patterns of matrix rich in heparan sulfate proteoglycan. Within 2 minutes of the injection of an intravenous tracer, the tracer material co-localised not only to endothelial cell-lined vessels but also to the looping matrix patterns that did not stain for the presence of endothelium. However, Pötgens considered these patterns to be part of the tumour stroma but did not address the histogenesis of these matrix-rich patterns [56]. Clarijs [57] also used a xenograft mouse model of uveal melanoma, demonstrating intravenous tracer material co-localising not only to blood vessels but also to looping patterns rich in laminin. Clarijs referred to the patterned matrix as a ‘‘fluid-conducting meshwork" [57]. Furthermore, anticoagulant properties were associated with tumour cell-lined

vessels. Specifically, tissue factor, the initiating cell surface receptor of the coagulation cascade (extrinsic coagulation pathway), was found to be regulated by tissue factor pathway 1 inhibitor. This balance between coagulation and anti-coagulation was postulated to facilitate in fluid-conducting capabilities of VM networks [58].

These were some of the gathered findings that illustrated the physiological function and importance of VM; however, much work in understanding VM and the mechanism that drives VM is still needed.

1.2.1. Vasculogenic mimicry and breast cancer

Since the discovery of VM, a plethora of research has been conducted to unravel and comprehend the concept (**Figure 1.3.**). After the discovery of VM in melanoma by Maniotis *et al*. (1999), Tímár and Tóth (2000) observed that breast cancer cells also line vascular channels, although the clinical function of these breast tumour cell-lined vessel-like structures was unknown [46,59]. A year later, Shirakawa and colleagues also observed VM in aggressive inflammatory breast cancer xenografts (WIBC-9), along with the absence of endothelial cells and the absence of central necrosis, indicating the presence of viable tissue in the absence of a traditional intra-tumoural vasculature [60]. Shirakawa and colleagues provided the first evidence indicating the perfusion role of VM in aggressive breast cancer [61]. Furthermore, the authors investigated the hemodynamics of VM and angiogenesis and were able to demonstrate the existence of a connection between VM and angiogenesis in breast cancer [61].

Subsequently, VM facilitates nutrient and oxygen delivery to proliferating tumours by linking with angiogenic vessels and transferring blood from angiogenic vessels to the tumour through this VM - angiogenesis junction [61-62]. Thus, VM as a functional micro-circulation enables the dissemination of breast tumours to distant organs [63].

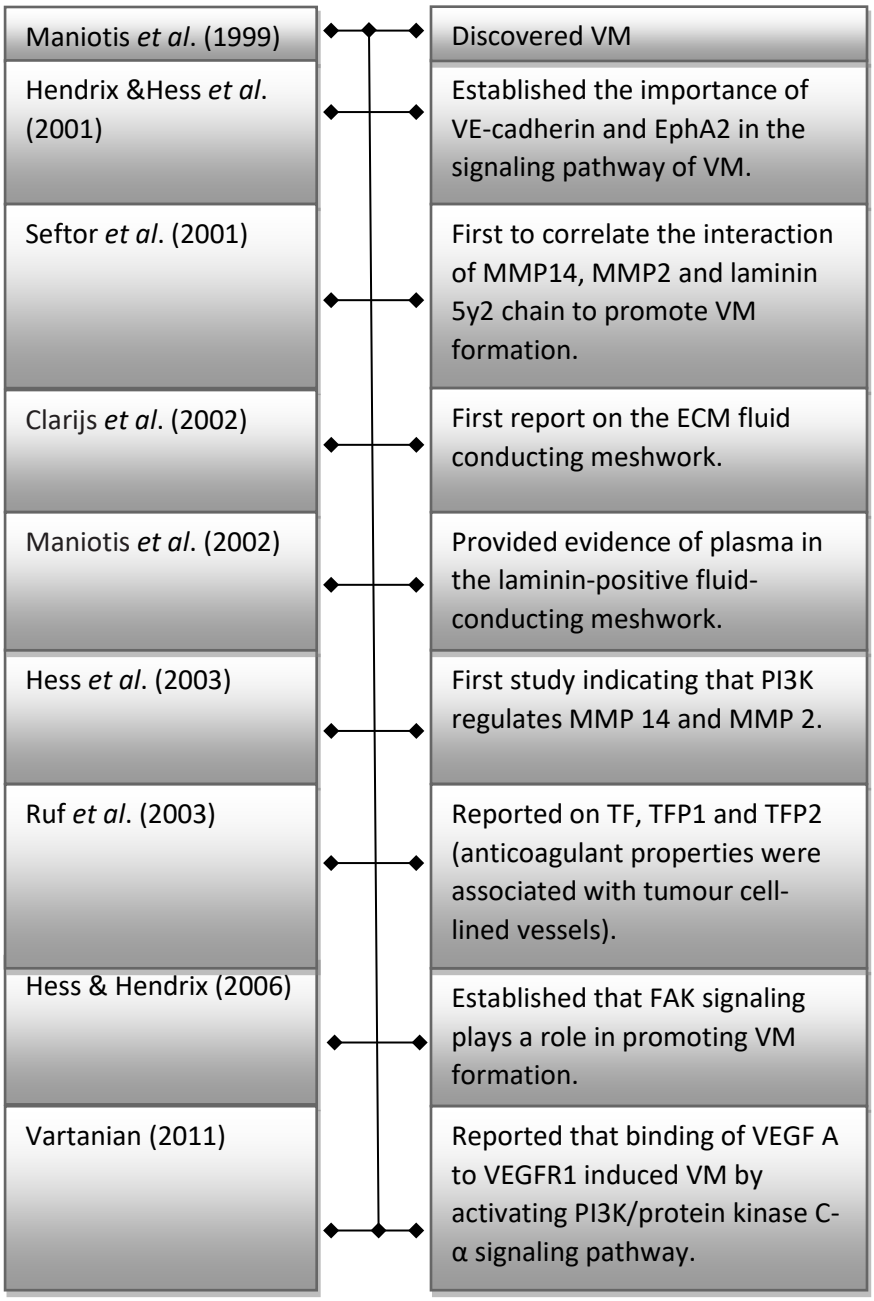

Figure 1.3. Timeline on some of the contributions made to understanding vasculogenic mimicry.

The discovery of key molecules that play a role in the formation of vasculogenic mimicry channels is indicated. The mechanism of vasculogenic mimicry is not yet fully understood. It should be noted that vasculogenic mimicry does not have universal markers. VM; vasculogenic mimicry, VE; Vascular endothelial, EphA2; ephrin type-A receptor 2, PI3K; phosphoinositide 3-kinase, MMP; matrix metalloproteinase, ECM; extracellular matrix, TF; tissue factor, TFP; tissue factor pathway 1 inhibitor, FAK; focal adhesion kinase, VEGF A; vascular endothelial growth factor A, VEGFR-1; vascular endothelial growth factor 1. *Figure drawn by N.P Sekoba using Microsoft PowerPoint*.

1.2.2.1. Regulators of vasculogenic mimicry in breast cancer

As tumours proliferate, vast usage of energy and nutrients are evident, and the alteration of the microenvironment, such as hypoxia and acidity, accompany tumour growth. TNBC adapts to these conditions to sustain proliferation and survive by switching their phenotype (tumour cell plasticity) and initiating VM [64-65]. As breast tumours grow, they tend to develop hypoxia, which triggers a signalling pathway that involves a key transcription factor in tumour development, known as hypoxia-inducible factor (HIF)-1α. Under hypoxic conditions, the HIF-1α protein is translocated into the nucleus, where it combines with the β subunit of HIF-1 to form HIF-1 heterodimer, then activates target genes which trigger VM formation and exacerbates cancer progression and aggressiveness [66]. Vasculogenic mimicry drives tumour growth and metastasis and is associated with poor prognosis in breast cancer [67-69]. Moreover, hypoxia induces breast cancer stemness, a hallmark of VM. This ability of a tumour to acquire a cancer stem-like cell phenotype is a type of phenotypic switching employed by tumours to survive. Another example of phenotypic switching is EMT, through which cells lose epithelial traits (E-cadherin) and gain mesenchymal features (vimentin and N-cadherin) [64,70]. Epithelial-to-mesenchymal transition regulated by HIF-1α mediated factors (SNAIL, SLUG, TWIST 1, ZEB 1) plays a role in VM formation and acquisition of cancer stem-like cell phenotype [64,71]. Furthermore, HIF-1α induces the expression of carbonic anhydrase IX, a pH regulating enzyme, to drive EMT, cancer-stem-like cells and VM formation in TNBC [64].

Upon stabilisation of HIF-1α, carbonic anhydrase IX is not the only gene that is upregulated and overexpressed but also VEGF A which has been associated with VM formation. Binding of VEGF A/VEGFR-1 promotes VM formation in an aggressive and highly invasive breast cancer cell through the phosphoinositide 3-kinase (PI3K) signalling pathway (**Figure1.4.**) [72].

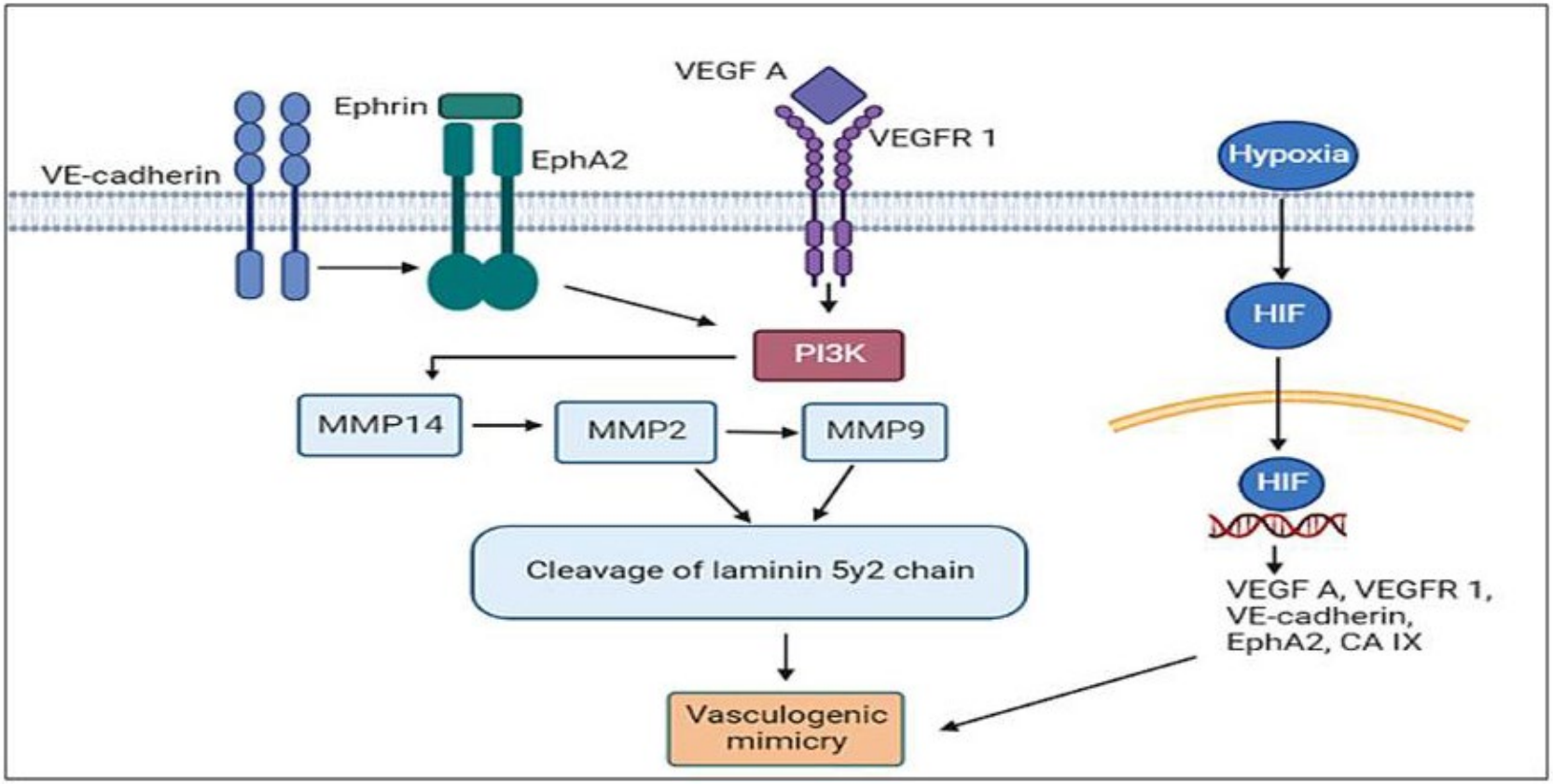

Figure 1.4. VEGF A/VEGFR-1 signals via the PI3K pathway to cleave the 5y2 chain by activating MMP 2 and 14 and upregulates VE cadherin and EphA2 to form vasculogenic mimicry channels. PI3K; phosphoinositide 3-kinase, EphA2; epithelial cell-associated tyrosine kinase receptor, VEGF; Vascular endothelial growth factor; VEGFR, vascular endothelial growth factor receptor; MMP, matrix metalloproteinase, HIF; hypoxia-inducible factor. *Figure drawn by N.P Sekoba using Biorender adapted from Kirschmann et al.* [73].

The formation of VM channels in breast cancer can also be induced via vascular endothelial (VE)-cadherin (a cell-cell adhesion molecule), which co-localises and interacts with another molecule that is overexpressed in VM-forming breast tumours, ephrin type A receptor 2 (EphA2), in the intercellular junctions between cells that forms VM channels [74]. Furthermore, VE-cadherin regulates the phosphorylation of EphA2 at the cell membrane. Phosphorylated EphA2 then targets focal adhesion kinase (FAK) by promoting the localisation of FAK to a new adhesive site, activating PI3K (**Figure 1.4.**) [75-77].

The activated PI3K promotes metalloproteinase (MMP)14, which induces VM channel formation by tumour cells [76]. Metalloproteinase14 is known to activate MMP2, which activates MMP9. Metalloproteinase2 and MMP9 are necessary for cleavage the laminin 5y2 chain, which promotes VM formation. Therefore, targeting the PI3K/MMP pathway might be of clinical benefit.

1.2.2.2. Techniques applied to detect vasculogenic mimicry

The current golden standard for the detection of VM is the immunohistochemical positive PAS and negative CD31 staining of vessel-like structures [78]. PAS-positive channels are externally lined by tumour cells and lack an inner lining of endothelial cells. Thus, the negative CD31 (a marker of endothelial cells), is observed in VM channel formation [79]. In some malignant cancer biopsies, VM can be diagnosed with immunohistochemical staining. In a study using breast cancer exploring the prognostic value of aldehyde dehydrogenase 1 expression and VM in patients with breast cancer, VM formation was examined by CD31/PAS double staining, using formalin-fixed paraffin-embedded tissues from 202 breast cancer patients [80]. In another study, the presence of VM in breast cancer tissues was detected using CD31 and PAS histochemical and immunohistochemical double staining in 134 tissue specimens of IDC [65]. Noteworthy, Immunohistochemical staining does have limitations as it cannot be used to evaluate blood flow in VM channels [81]. Other techniques which have been suggested to detect VM in clinical settings include molecular imaging technologies such as doppler imaging, confocal indocyanine green

angiography and magnetic resonance imaging [78,81]. Molecular imaging technologies detect specific contrasting agents that can enter VM tubes and provides non-invasive imaging. Colour doppler imaging was reported to distinguish the blood flow of endothelial-lined and tumour-cell-lined vasculatures in a study conducted by Ruf *et al.* [58]. Moreover, a study conducted by Frenkel *et al*. (2008) could establish blood flow in VM patterns using confocal indocyanine green [82]. In another study using the dynamic micro-magnetic resonance imaging technique, blood flow through the tumour-cell lined vessels was observed in WIBC-9 breast cancer xenograft used as an experimental model. Clinically, it is important to routinely assess VM using the correct techniques to detect VM, as it is associated with metastasis and therapeutic resistance in breast cancer [83].

1.2.2.3. Vasculogenic mimicry and patient outcome in breast cancer

Various studies have shown that VM is significantly associated with poor overall survival in breast cancer patients [80,84-85]. In a meta-analysis incorporating 8 studies that involved 1, 238 breast cancer patient, the VM-positive patients had a shorter overall survival as compared to those with a VM-negative status [84]. Lower disease-free survival rate was also associated with VM-positive cases compared to their counterpart [80,86]. Thus, VM contributes to therapeutic resistance and recurrence in breast cancer patients.

In HER2-positive breast cancer resistant to trastuzumab exhibited VM formation, promoting metastasis and worsening patient outcomes [87]. Furthermore, VM positive cases were associated with a high rate of hematogenous metastasis, lymph node metastases, high tumour grade, and high Nottingham prognostic index (**see Table 1.4.**) [72,86]. Importantly, VM has been shown to be an independent prognostic factor in breast cancer and is responsible for the aggressiveness and progression of the disease [76].

Regardless of the factors that are known to influence VM formation in breast cancer, additional research must be conducted to further understand the mechanisms underlying VM and use the knowledge gained to improve treatment.

Table 1.4. Vasculogenic mimicry and its association with prognosis in breast cancer patients

Study (publication year)	Number of patients (percentage VM+)	Association	p-value	References
Shirakawa *et al* (2002)	331 (7.9%)	VM group tended to have a higher hematogenous metastases than the non-VM group	p = 0.059	[72]
Liu *et al* (2014)	90 (28.6%)	VM correlated with lymph node metastases	p = 0.004	[86]
		Histological grade	p < 0.001	
		Nottingham prognostic index (NPI) (worse prognosis)	p < 0.001	
		VM correlated with overall survival	p < 0.001	
		VM correlated with disease-free survival	p < 0.001	
Xing *et al* (2018)	202 (16.8%)	VM correlated with disease free survival and overall survival	p = 0015	[80]
		VM presence was higher in triple-negative cases vs. non triple-negative cases	p = 0.003	
Sun *et al*. (2019)	100 (29%)	VM presence was higher in triple-negative cases vs. non triple-negative cases	p = 0.020	[83]
		VM correlated with poorer overall survival	p = 0015	

Abbreviations: VM, vasculogenic mimicry. *Adapted from Andonegui-Elguera et al*. [88].

1.3. Metabolism

Metabolism is the sum of the biochemical reactions in living organisms that either produce or consume energy. Metabolism generally involves three processes; anabolism (synthesising simple molecules into more complex macromolecules), catabolism (The degradation of molecules to release energy), and waste disposal [89]. Energy is derived from nutrients such as carbohydrates, fatty acids, and amino acids, which are essential for energy homeostasis and macromolecular synthesis in humans.

1.3.1. Breast cancer cell metabolism

Metabolic reprogramming is one of the mechanisms employed by cancer cells to achieve indefinite proliferation and invasion [89-90]. Similar to most malignant cells, breast cancer presents with increased aerobic glycolysis and glutaminolysis [11,91].

1.3.1.1. Changes in glucose metabolism

Otto Warburg had observed increased aerobic glycolysis with a ten-fold increase in glucose consumption and a two-fold production of lactate as the end-product, regardless of the oxygen status in cancer metabolism, a phenomenon known as the Warburg effect [91-92]. To achieve the Warburg effect, breast cancer cells exhibit altered expression of different glucose transporters and glycolytic enzymes [91]. Breast cancer overexpresses glucose transporters (GLUT) such as GLUT 1; enabling glucose to cross the plasma membrane and undergo a ten-step reaction catalysed by enzymes to produce pyruvate [11,91]. During glucose deprivation or hypoxia, the expression of VEGF A is upregulated, VEGF A increases GLUT-1 expression, which avails nutrients to tumours and promotes the proliferation of tumours (**Figure 1.5.**) [93].

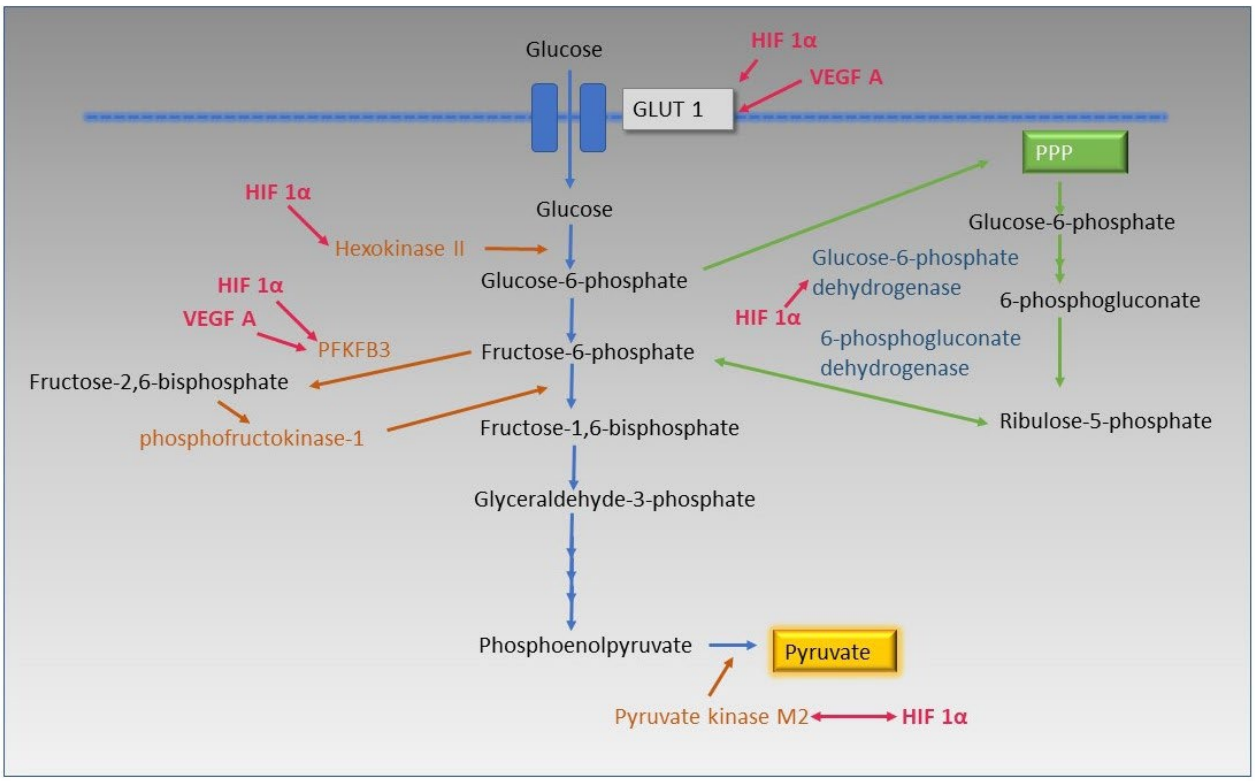

Figure 1.5. Glycolysis pathway in the breast cancer cell. The pink arrows show the effect of VEGF A and HIF-1α on the metabolites of glycolysis. The green arrows indicate the relationship between glycolysis and the phosphate pentose pathway. HIF; hypoxia-inducible factor, VEGF; vascular endothelial growth factor, GLUT; glucose transporter, PPP; phosphate pentose pathway. *Figure drawn by N.P Sekoba using Microsoft PowerPoint, adapted from Penkert et al.* [94].

1.3.1.1.1. Isoforms of glycolytic enzymes

Several of the glycolytic enzymes can express isoforms that are specific to malignant cells. Among the glycolytic enzymes, there are three isozymes (hexokinase II, phosphofructokinase-1 and pyruvate kinase M2) expressed by breast cancer cells which aid in tumour growth and increased metabolism [11,95].

1.3.1.1.1.1. Hexokinase II

Hexokinase catalyzes the first irreversible step of the glycolytic pathway for the phosphorylation of glucose to glucose-6-phosphate with the consumption of adenosine triphosphate (ATP) (**see Figure 1.5.**). Hypoxia-inducible factor 1α, a transcription factor, that facilitates the adaptation of breast cancer cells to hypoxic conditions by increasing the expression of hexokinase, which ultimately contributes to enhanced glycolysis [95]. There are four isoforms of this enzyme, hexokinase I-IV. Malignant cells such as breast cancer cells preferably express the predominant isoform hexokinase II [11,96]. Hexokinase II has a catalytic and regulatory benefit over hexokinase I, and its product glucose-6-phosphate does not inhibit it. Hexokinase II can localise in the cytosol and promote anabolic pathways such as the pentose phosphate pathway (PPP) or on the outer mitochondria and promote glycolysis [11]. The strategic binding of the hexokinase II to the outer mitochondria results in the coupling of ATP produced in mitochondria to phosphorylate glucose in glycolysis. Hexokinase II can also promote cancer by repressing mitochondrial function on cell death, immortalising tumour cells [97]. Hexokinase II overexpression thus renders radio-resistance in MCF-7 and MDA-MB-231 cell lines [11,98].

1.3.1.1.1.2. Phosphofructokinase-1

Phosphofructokinase-1 (PFK-1) catalyses the conversion of fructose 6-phosphate to fructose-1,6-bisphosphate. Fructose 2,6-bisphosphate play regulatory rules on PFK-1 [11]. The enzyme 6-phosphofructo-2-kinase/fructose-2,6 bisphosphatase-3 (PFKFB-3) is overexpressed in breast cancer and positively associates with glycolysis, vascularisation, and tumorigenesis [99-100]. Fructose-2,6 bisphosphatase-3 has a HIF-1α binding region in their promoters [11]. Vascular endothelial growth factor A is associated with an increased expression of PFKFB-3 [101-102]. This enzyme maintains elevated fructose 2,6-bisphosphate levels, which sustains high glycolytic rates by activating PFK-1 (**Figure 1.5.**) [11]. Phosphofrucokinase-1 may exist as homo or heterotetramers of three isoforms, PFKM, PFKL, and PFKP. Breast cancer cells mainly express the P isoform. In

an *in vitro* study, PFKP was shown to be the major isoform in malignant MCF-7 and MDA-MB-231 [11,103].

1.3.1.1.1.3. Pyruvate kinase M2

Pyruvate kinase (PK) is the last enzyme of glycolysis converting phosphoenolpyruvate to pyruvate. There are two specific isoforms: PKM1 and the PKM2 isoform, which promote aerobic glycolysis and are expressed in embryonic and tumour cells [104]. These isoforms are formed by exclusive alternative splicing of PKM gene [105]. Noteworthy, PKM2 acts as a co-activator of HIF-1α (**see Figure 1.5.**) [11].

1.3.1.1.2. Phosphate pentose pathway

One of the advantages of cancer cells preferring aerobic glycolysis over efficient oxidative phosphorylation is the increased anabolic pathway that is observed in glycolysis when glucose is shunted to PPP (**Figure 1.5.**). The PPP provides ribulose-5-phosphate, a substrate for nucleic acid and nicotinamide adenine dinucleotide phosphate hydrogen (NADPH), a precursor for the production of lipids and amino acids [11,106]. NADPH also acts as an anti-oxidant as it reduces the toxicity of reactive oxygen species [106]. The enzymes (glucose-6-phosphate dehydrogenase and 6-phosphogluconate dehydrogenase) involved in PPP have been reported to increase in malignant breast tissue [107]. Overall, the PPP in breast cancer cells has been found to increase by eight-fold compared to normal mammary epithelial tissue. This upregulated pathway renders metastatic cancer resistant to drugs and therapy [108-109].

1.3.1.1.3. Lactate Production

In breast cancer, pyruvate dehydrogenase complex, an enzyme that converts pyruvate to acetyl-CoA; which enters the TCA cycle, is inhibited by pyruvate dehydrogenase kinase-1 [11,110]. Therefore, the greater amount of pyruvate is converted into lactate by lactate dehydrogenase (LDH) A. Pyruvate dehydrogenase kinase-1 and LDH A are activated by HIF-1α (**Figure 1.6.**) [110].The transcription factor, HIF-1α is not only stabilised under hypoxic conditions but also under

normoxic conditions by pyruvate and lactate, which accumulates this transcription factor [111]. The target genes of HIF-1α include GLUT 1 (augments the entry of glucose) and monocarboxylate transporter (MCT) -4; which secrete the accumulated lactate out of the cell [112]. Lactate secretion in the extracellular space drives tumour progression, vascularisation, and metastasis [97,113]. High levels of LDH A in a patient with metastatic colorectal cancer correlates with increased VEGF A and VEGFR-1 expression [114].

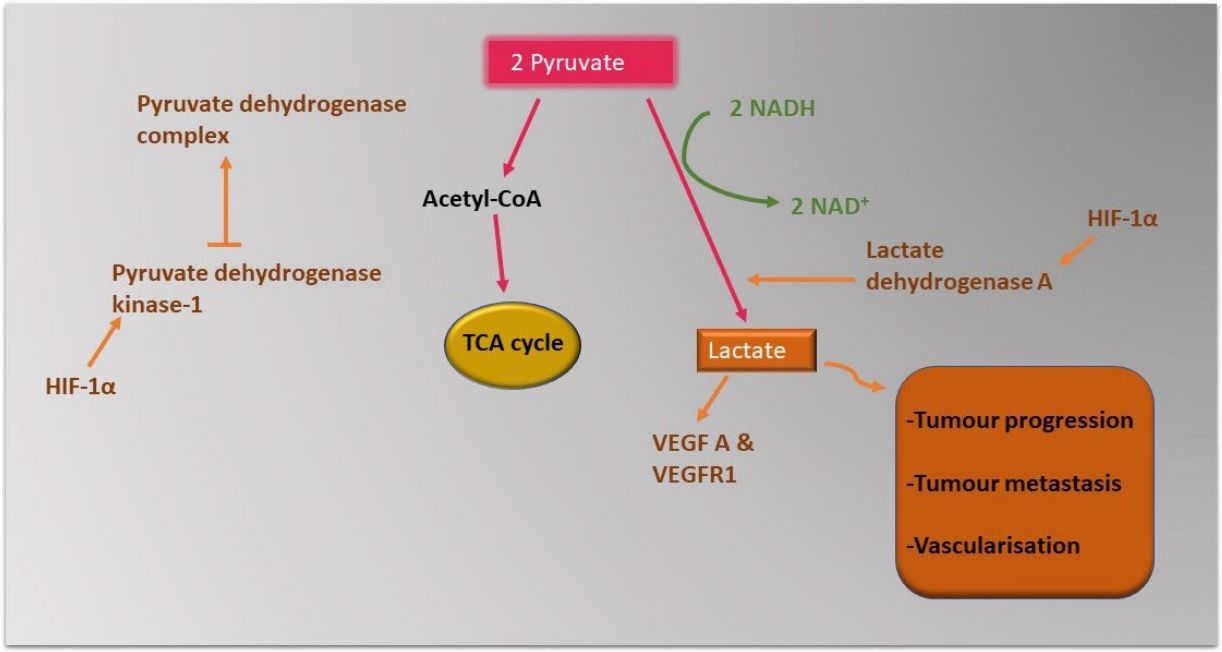

Figure 1.6. Lactate production and its role in tumour progression. TCA; tricarboxylic acid, VEGF; vascular endothelial growth factor, VEGFR; vascular endothelial growth factor receptor, HIF; hypoxia-inducible factor, NADH; reduced nicotinamide adenine dinucleotide, NAD^+; nicotinamide adenine dinucleotide. *Figure drawn by N.P Sekoba using Microsoft PowerPoint* [115-116].

1.3.1.2. Activation of glutaminolysis

Glutamine is a non-essential amino acid in humans because it can be produced from glutamate and ammonia by glutamine synthetase in the liver. Glutamine alone comprises 20% of the total amino acid pool in the blood [11,117]. Breast cancer shows addiction to glutamine and exploits the abundance of glutamine in the body to support biosynthesis, energetics, and homeostasis [11].

Since pyruvate converted to acetyl-CoA is only available in low levels to the TCA cycle, due to the Warburg effect phenotype, glutamine serves as another source to replenish the carbon pool of the TCA cycle [113]. Glutamine enters the cell from the bloodstream through transporters and is then transported into the mitochondria, where it is broken down to glutamate by glutaminase to form α-ketoglutarate, one of the intermediates of TCA cycle (**Figure 1.7.**) [11,92]. The metabolism of glutamine enhances aggressiveness in tumour cells, and the elevated levels of glutamate have been associated with disease outcomes in breast cancer [92]. In hypoxic situations which induces HIF 1-α and play role in enhancing glycolysis, breast cancer cells employ reductive metabolism of glutamine-derived α-ketoglutarate, which constitutes a partial reversal of the TCA cycle to support citrate and fatty acid synthesis [118].

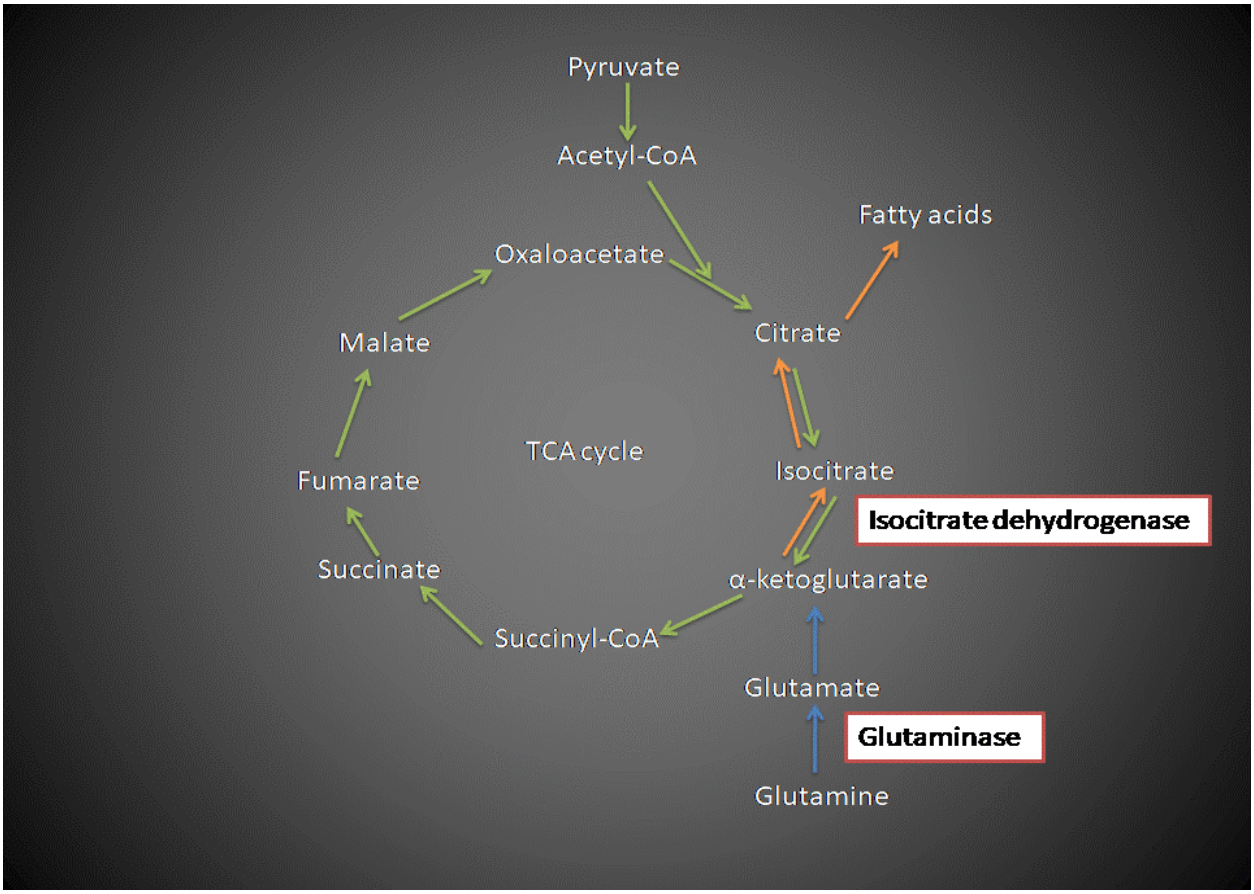

Figure 1.7. The role of glutamine in tricarboxylic acid cycle in the presence of hypoxia. The orange arrows indicate the reductive carboxylate pathway. *Figure drawn by N.P Sekoba using Microsoft PowerPoint, adapted from Corbet and Feron* [118].

1.3.1.3. Metabolic rewiring and breast cancer subtypes

Metabolic alteration is evident in the breast cancer subtypes; however, each subtype has a unique metabolic sig*nature*. Glutamine metabolism, glycolytic rates and metabolite-related proteins differ amongst breast cancer subtypes.

1.3.1.3.1. Luminal subtype

Luminal breast cancer exhibits an intermediate metabolic phenotype in the glycolysis-oxidative phosphorylation (OXPHOS) spectrum [119-120]. In a study conducted by O'Mahony *et al*. [121], they found that MCF-7 cells switch between metabolic pathways (between glycolysis and OXPHOS) depending on the glucose availability and 17β-estradiol (E2) potentiates adaptation. 17β-estradiol, the main estrogen in breast tissue, enhances glycolysis and suppresses the TCA cycle activity in high glucose conditions. Under physiological glucose concentrations, E2 stimulates the TCA cycle via the upregulation of pyruvate dehydrogenase activity and suppresses glycolysis to sustain cell viability and survival [120-122].

Under normoxic conditions luminal subtype relies on ATP production from OXPHOS but increases their glycolytic activity under hypoxia, thus, exhibiting the Pasteur phenotype [123]. The luminal subtype has also been correlated with the reverse Warburg phenotype, in which breast cancer cells rely on glycolytic end products such as lactate and pyruvate supplied by neighbouring cancer-associated fibroblasts (CAFs) [120,124]. The metabolic alteration of CAFs is promoted by the luminal breast cancer subtype by promoting a hypoxic environment through hydrogen peroxide secretion [116,125]. Hydrogen peroxide activates caveolin 1 and HIF-1α, which in turn upregulates glycolysis to produce lactate [116,126]. Lactate is extruded from the CAFs through the upregulation of MCT 4 by breast cancer cells. Conversely, breast cancer cells have expressed MCT 1, enabling

lactate importation produced by CAF [127-128]. Imported lactate can be converted by LDH B to pyruvate, which can be utilised to fuel the TCA cycle [116].

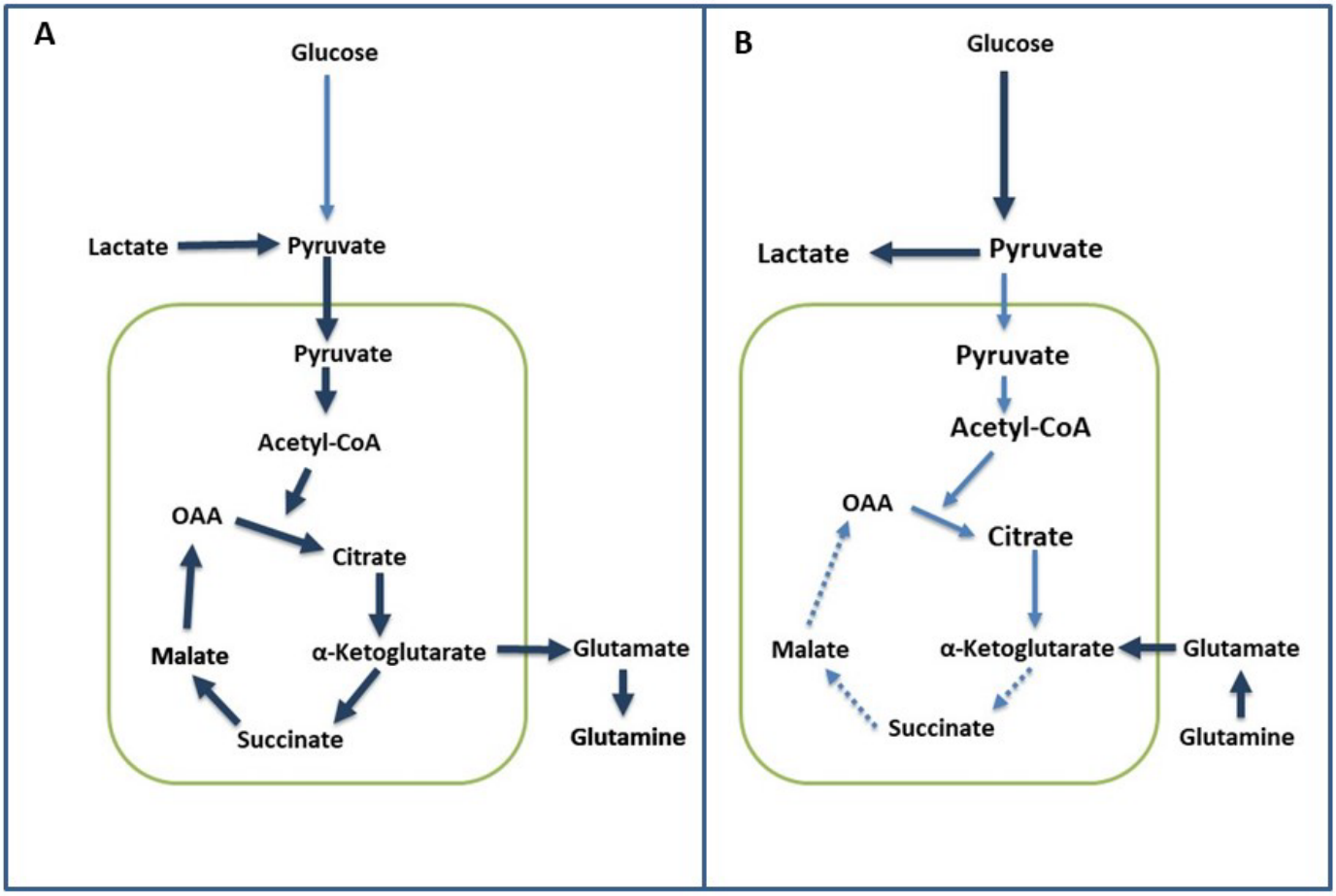

Figure 1.8. Breast cancer metabolism. **A)** Metabolism of estrogen receptor-positive breast cancers. **B)** Metabolism of triple-negative breast cancers. Blue arrows depict the main fluxes within central metabolism, and the dashed lines indicate a down-regulation. *Figure drawn by N.P Sekoba using Microsoft PowerPoint, adapted from Elia et al*. [124].

Overall, luminal subtype breast cancer prefers to utilise the OXPHOS pathway under both normoxic and hypoxic conditions through the Pasteur effect or reverse Warburg type, respectively (**Figure 1.8.**). It should be noted that high proliferating luminal B estrogen receptor-positive breast

cancers display less often a reverse Warburg metabolism compared to slow proliferating luminal A estrogen receptor-positive breast cancers [124]. Thus, high proliferating breast cancer subtypes adapt to high glycolytic rates, which are associated with worse clinical outcomes.

Luminal subtype also expresses high glutamine and low glutamate levels, thus having low glutamate-to-glutamine ratio and lower levels of glutaminolysis [119-120]. This is due to luminal breast cancer cells' lower glutaminase and higher glutamine synthetase expression [116].

1.3.1.3.2. Triple-negative breast cancer subtype

Triple-negative breast cancer tumour has been associated with a greater glycolytic phenotype as compared to both luminal breast cancer subtypes (**see figure 1.8.**) [119]. In a study conducted by Choi *et al* [129]. GLUT 1 was highly expressed in TNBC contrasted to other breast cancer subtypes. Increased glucose uptake is associated with increased glycolysis and intracellular lactic acidosis. Thus, to prevent intracellular acidosis and cell death, TNBC have been shown to highly express carbonic anhydrase IX, which ultimately provides TNBC with an acid-resistant phenotype [122,129]. Additionally, both MCT 1 and MCT 4 transporters are highly expressed in TNBC [130-132]. Triple-negative breast cancer tumour has also been shown to display an increased expression of some of the glycolytic enzymes such as hexokinase II, PKM2 and LDH A, which are correlated with tumour progression and poor prognosis [120,128,132].

Low mitochondrial respiration has also been positively correlated with the TNBC subtype [120]. The TCA cycle and electron transport chain subunits, such as the complex I NDUFB8 and SDHB (the core catalytic subunit of the mitochondrial heterotrimeric complex SDH), are downregulated in MDA-MB-231 cells when compared to MCF-7 cells [128]. The triple-negative subtype has also exhibited a higher NADH/NAD+ ratio than the luminal subtype. This is due to the less oxidation of NADH to NAD+ by the impaired complex I activity and more conversion of NAD+ to NADH during active glycolysis [128,133]. High NADH levels in the TNBC subtype inhibit the pyruvate

dehydrogenase complex, thus, cementing the truncation of the TCA cycle and upregulating the lactic fermentation [134].

Triple-negative breast subtype is glutamine addicted, thus displaying an increased glutaminolysis activity, high glutamate to glutamine ratio and increased expression of glutaminases [11,116,124]. Glutamine metabolism begins with a solute carrier family 1 member 5 (SL1CA5)-dependent transport into cells [135]. Triple-negative breast cancer subtype displays a significant increase in the SL1CA5 transport as compared to luminal breast cancer cells [132]. Loss of glutaminases impairs tumour growth of TNBC but has minimal effect on the growth and metabolic phenotype of luminal subtype [132,136]. This is due to the lack of glutamine synthetase observed in some TNBC.

1.3.1.4. Regulator of metabolic reprogramming and vasculogenic mimicry

The physiological function of breast tumor-lined vessels is in the ability to provide nutrients to the proliferating tumour. An increased glucose flux is associated with VM channel formation in p53-mutated triple-negative breast cancer. PKM2, a rate-limiting enzyme that catalyzes the final step of glycolysis, promotes VM formation by enhancing glucose flux and VE-cadherin expression in p53-mutated triple-negative breast cancer under low phosphorylated-Checkpoint kinase (Chk)2 T68. Activation of Chk2, a multifunctional kinase that modulates the cellular response to DNA damage, results in phosphorylation of Chk2 at the T68 site, which enables coupling of Chk2-PKM2 and nuclear exportation of PKM2 by phosphorylating PKM2 at Ser100. Phosphorylated-PKM2 Ser100 then reduces VM formation by decreasing glucose flux and VE-cadherin [137]. This new metabolic regulatory axis (Chk2-PKM2) is the first link that has established a relationship between metabolic alteration and VM and, thus, has clinical relevance and warrants consideration when designing targeted therapies for breast cancer.

In this study, VEGF A/VEGFR-1 signalling (regulator of both VM and metabolic reprogramming) will be investigated to determine its contribution to metabolic changes and VM formation in breast cancer.

1.3.1.5. Treatment that targets vasculogenic mimicry in breast cancer

Hypoxia is an important inducer of VM formation, and several compounds have been employed to suppress HIF. 6, 6'-bis (2.3-dimethoxybenzoyl)-a,a-D-trehalose (DMBT), which is a derivative of brartemicin, a metabolite isolated from actinomycetes, was investigated in an *in vivo* an *in vitro* study was it exhibited an inhibitory effect on VM in MDA-MB-231 xenografts and MDA-MB-231 cells [138], DMBT, exerted its inhibitory effect through inhibiting VM-related proteins such as HIF-1α, VE-cadherin, MMP9 and MMP2 in MDA-MB-231 cells, leading to the suppression of hypoxia-induced VM.

Another compound, Hinokitiol, inhibits VM in breast cancer stem cells by increasing the proteasome-mediated degradation of epidermal growth factor receptor and thus lowering the levels of this protein [139]. Melatonin and entinostat (Histone deacetylase inhibitors) were also found to attenuate VM in a breast cancer preclinical model **(Table 1.5.)**. These compounds inhibit EMT, a factor that contributes to breast cancer stemness [71,140].

Preclinical studies have also focused on the targeting of the PI3K/AKT signalling pathway. MEN-1611, a PI3K inhibitor, in *in vitro* and *in vivo* settings downregulated PI3K and pAKT in breast cancer [147]. Moreover, MEN-1611 had a significant and long-lasting anti-tumour effect reflected by tumour-stasis or tumour regression in trastuzumab-resistant PI3KCA-mutant HER2-positive patient-derived xenograft. Currently, MEN-1611, is a potential VM therapeutic drug that is under investigation in a clinical trial phase I in patients with HER2+/PI3KCA mutant advanced or metastatic breast cancer **(Table 1.6)** [147]. Furthermore, interferon-α binds to its receptor, and subsequent activation of Janus kinase (JAK) 1, phosphorylation of PI3K, AKT, mammalian target of rapamycin (mTOR) promotes HIF-1α mRNA transcription and translation, which ultimately induces EMT and VM. Thus, inhibition of JAK 1, PI3K and mTOR by LY294002, JAK inhibitor I and Rapamycin, respectively, attenuate IFN-induced VM in a preclinical study. JAK1/2 inhibitor, Ruxolitinib, is another compound under clinical development that treats metastatic breast cancer

in a phase I trial [150]. Both MEN-1611 and Ruxolitinib are combined with other drugs, such as trastuzumab and paclitaxel, respectively, for treating breast cancer. Therapeutic combination is advantageous as it increases the therapeutic window and potential to retard VM channel formation in aggressive breast tumors; therefore, more studies aiming at therapeutic solutions in the treatment of breast cancer are needed.

Table 1.5. Therapeutic compounds which inhibit vasculogenic mimicry in breast cancer in preclinical studies

Drug/Compound	**Target**	**Breast cancer Model**	**References**
Liposomes			
Vincristine in combination with Dasatinib	VE cadherin/FAK/PI3K/MMP2/MMP9	MDA-MB-231 breast cancer cells and MDA-MB-231 xenografts in nude mice	[77].
Epirubicin and Celecoxib	MMP/VE cadherin/FAK/EphA2/HIF-1α	MDA-MB-231 xenografts in nude mice	[141]
Natural plant compounds			
Xian-ling-lian-xia-fang	VEGF-A/MMP 2	MDA-MB-231 cells MDA-MB-231 xenografts in nude mice	[142]
Brucine	EpHA2/MMP2/MMP9	Triple-negative breast cancer cell line	[143].
Sinomenine	MiR-340-5p/SIAH2 axis	MDA-MB-231 cells	[144]
Hinokitiol	Epidermal growth factor receptor	Breast cancer stem cells	[139]
Thymoquinone	PI3K/Wnt3a/VE-cadherin	Breast cancer stem cells	[145]

Hormones			
Melatonin	EMT	MDA-MB-231 cells	[71]
Calcitriol	TGF-β/VEGF A/MMP 2 and 9	MDA-MB-231 cells	[146]

VE-vascular endothelial, FAK-focal adhesion kinase, PI3K-phosphoinositide3kinase, MMP-metalloproteinase, EphA-erythropoietin-producing human hepatocellular receptor, HIF-hypoxia inducible factor, VEGF-vascular endothelial growth factor, MiR-microRNA, SIAH-seven *in absentia* Homolog, EMT-epithelial mesenchymal transition, TGF-transforming growth factor.

Table 1.6. Potential drugs targeting vasculogenic mimicry in clinical trials in breast cancer

Drug	Target	Clinical trial ID	Phase	Status	References
MEN-1611	PI3K	NCT03767335	I	Active, not recruiting	[147]
BKM120 (Buparlisib)	PI3K	NCT01790932; NCT01629615	II	Completed (results published)	[148]
OKI-179	HDAC	NCT03931681	I	Completed (results published)	[149]
Ruxolitinib	JAK/STAT	NCT02041429	I	Completed (results published)	[150]
SLC-0111	CA IX	NCT02215850	I	Completed (results published)	[151]

HDAC- histone deacetylase, PI3K-phosphoinositide 3 kinase, JAK- janus kinase, CA- carbonic anhydrase

1.4. Targeted therapy

Targeted therapy is different from traditional chemotherapy (refers to treatment with drugs that have the potential to kill cancer cells) and radiotherapy (refers to the use of high-energy radiation from x-rays, gamma rays, neutrons, protons, and other sources to kill cancer cells and shrink tumours); it involves the use of agents that block the growth and spread of cancer by interfering with specific molecules involved in cell growth and cancer progression [152]. Targeted therapies are often less toxic and better tolerated than chemotherapy and radiotherapy [152]. The two main types of targeted therapy are monoclonal antibodies and small molecule inhibitors.

Monoclonal antibodies are usually water soluble and large, with an approximate molecular weight of 150 000 Da. Due to their large molecular weight and hydrophilic nature, the distribution of monoclonal antibodies is generally limited to the vascular and interstitial spaces [153-154].

1.4.1. Small molecule inhibitors

Small molecule inhibitors have a molecular weight of approximately 500 Da and can enter a cell thereby blocking receptor signalling and interfering with downstream intracellular molecules. These small molecule inhibitors mainly interfere with the intracellular signalling of tyrosine kinases [155]. Tyrosine kinases are enzymes in the kinase family that transfer phosphate groups from one place in the cell to another. Tyrosine kinase initiates a molecular cascade that can lead to cell growth, proliferation, and migration in both normal and malignant tissue [152]. Vascular endothelial growth factor receptor-1 is a tyrosine kinase and is targeted by sunitinib malate and ZM 306416.

1.4.1.1. Sunitinib malate and ZM 306416

Sunitinib malate (Sutent, Pfizer, New York, USA) is an oral small molecule tyrosine kinase inhibitor which inhibits multiple receptor tyrosine kinases, including VEGFR-1–3, platelet-derived growth factor receptor, c-KIT, FLT3 kinase, colony-stimulating factor 1 receptor and RET kinase. Sunitinib is currently approved in the United States and European Union for the treatment of advanced renal cell carcinoma and the treatment of gastrointestinal stromal tumours after disease progression on or intolerance to imatinib mesylate [156-157]. In contrast, ZM 306416, the novel selective vascular endothelial growth factor receptor-1 and epidermal growth factor receptor (EGFR) inhibitor, has not been extensively investigated (**see Figure 1.9.**).

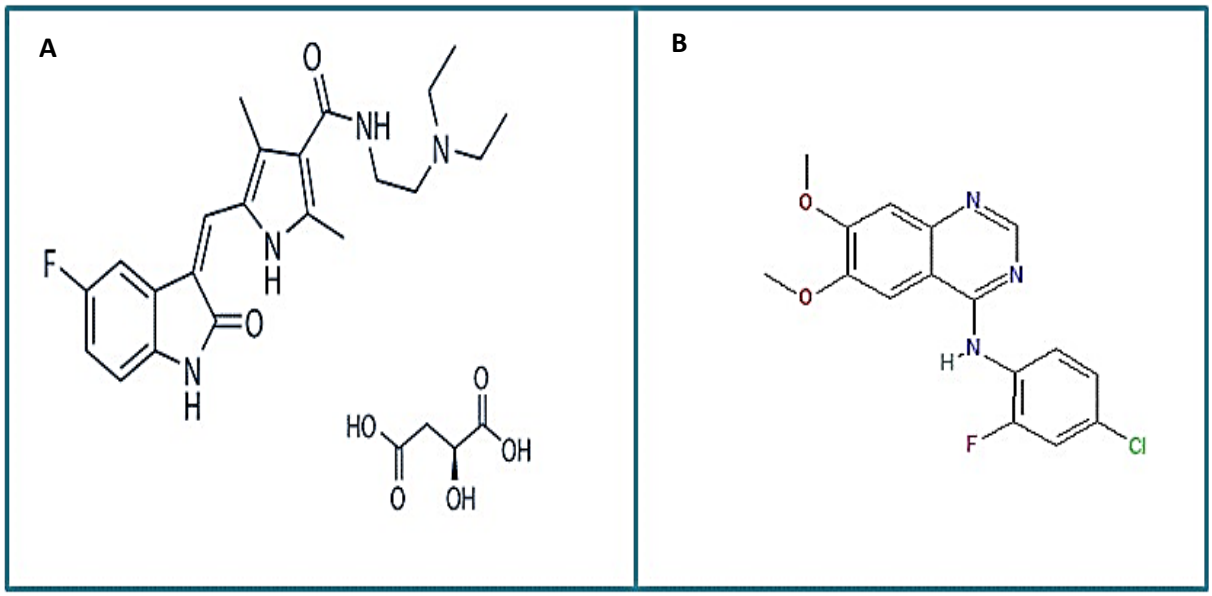

Figure 1.9. Molecular structure of small molecular inhibitors. **A)** sunitinib malate molecular structure. **B)** ZM 306416 molecular structure. *Figure drawn by N.P Sekoba adapted from PubChem* [158-159].

1.5. Problem statement

Breast cancer cells reprogramme their metabolism and induce VM formation with a sole purpose of increasing their chances of survival. Vasculogenic mimicry and metabolic reprogramming support cancer growth and are also drivers of recurrence, therapeutic resistance, and increased mortality rates. Currently, there are drugs undergoing clinical development with the potential to inhibit vasculogenic mimicry and enhanced metabolism in breast cancer. However, exploring various therapeutic options to combat the metabolic shift adapted by tumours and VM in breast tumours is still imperative.

This study evaluated the selective VEGFR-1 inhibitors (sunitinib malate and ZM 306416) in breast cancer cells. Thus, if blocking VEGFR-1 effectively inhibits the steps associated with VM, namely, cell growth, migration, invasion and metabolism, they could have potential benefits in breast cancer treatment.

1.6. Aim

The study aimed to investigate the effects of VEGFR-1 inhibition on the steps associated with VM, namely, cell growth, migration, invasion and metabolism in breast cancer cells *in vitro*.

1.7. Objectives

The following were the objectives of the study:

- To determine the effects of VEGFR-1 inhibition on processes that contribute to vasculogenic mimicry, namely in cell growth, migration and invasion, using the crystal violet assay, the scratch wound assay, and the Boyden chamber.
- To determine the effects of VEGFR-1 inhibition on cell morphology using light microscopy.
- To optimise liquid chromatography with tandem mass spectrometry (LC-MS/MS) method for the simultaneous assay of metabolites in cell culture preparations.

- To determine the effects of treatment on the metabolic profile of breast cells using liquid chromatography with tandem mass spectrometry (LC-MS/MS), ELISA and a pH meter/electrode.

CHAPTER 2: MATERIALS AND METHODS

2.1. Study design

The study design is outlined in the flow diagram (**Figure 2.1.**).

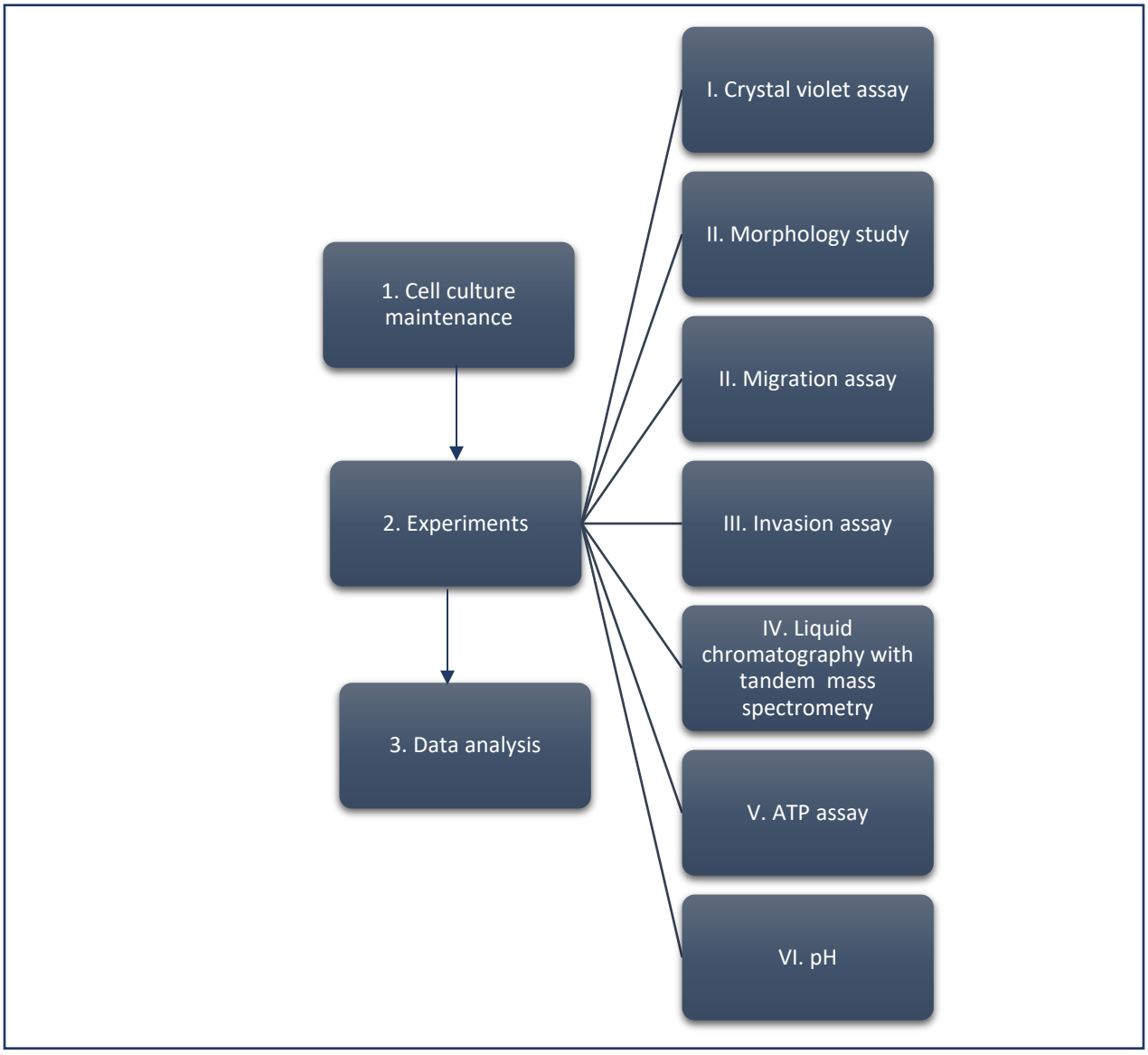

Figure 2.1. Flow diagram illustrating the study design.

2.2. General materials and cell culture maintenance

Cell culture maintenance and experiments were carried out under aseptic conditions in a Type II Biosafety cabinet (Labotec, Midrand, South Africa). The surface of the cabinet was cleaned with 0.1% (m/v) sodium dodecyl sulphate (SDS) and 70% (v/v) ethanol prior to usage. All glassware and non-sterile equipment were sterilised by autoclaving (20 min, 120°C, 15 psi) before use.

2.2.1. Cell lines

2.2.2.1. MCF 7

MCF-7 cell line ((CVCL_0031) serves as a good luminal A model that has been commonly used in preclinical testing of new target therapies [161]. The MCF-7 cell lines were obtained from the American Tissue Culture Collection (ATCC). These breast cancer cells were established from a pleural effusion at the Michigan Cancer Foundation. In microarray profiles, the MCF-7 gene set clusters with the luminal A subtype of breast cancer, displaying an epithelial morphology with adherent growth properties. The cell line is non-invasive and represents a model of early-stage disease due to the high expression of ER-activated genes, low levels of proliferation proliferation-related genes, have low histological grade and a good prognosis.

2.2.2.2. MDA-MB-231

The MDA-MB-231 cell line (CVCL_0062) was obtained from ATCC. This cell line was isolated at MD Anderson from a pleural effusion of a patient with invasive ductal carcinoma and is commonly used to model late-stage breast cancer. MDA-MB-231 cells lack ER, PR, and HER2 receptors and thus are classified as TNBC subtype with a spindle-shaped epithelial morphology and adherent growth. Triple-negative breast cancer has limited and mostly ineffective therapeutic options. As a result, as a good TNBC model, MDA-MB-231 cell line has been widely used in preclinical studies to investigate potential target therapies [160].

2.2.3. Reagents

Dulbecco's modified eagle's medium (DMEM), penicillin, streptomycin, and trypsin were purchased from Whitehead Scientific (Johannesburg, RSA). Phosphate-buffered saline (PBS) was prepared as follows: 80 g/l NaCl (sodium chloride), 2 g/L KH_2PO_4 (monopotassium phosphate) and 11.5 g/L $Na_2HPO_4.2H_2O$ (sodium Phosphate Dibasic Dihydrate) (Sigma-Aldrich Pty Ltd. (Johannesburg, RSA) were dissolved in distilled autoclaved water prepared at pH of 7.4. Foetal bovine serum (FBS) was bought from Scientific Group (Midrand, RSA). Gelatin was bought from Sigma-Aldrich Pty Ltd. (Johannesburg, RSA).

2.2.4. Cell culture maintenance procedure

2.2.4.1. Maintenance and subculturing

Cells were cultured in DMEM supplemented with 10% FBS and 1% penicillin-streptomycin. The cells were maintained in a humidified atmosphere containing 5% CO_2 at a temperature of 37°C. The culture medium was changed every two days. Upon reaching 70-90% confluence, the medium was discarded, and the cells were washed with sterile 1X PBS and trypsinised by adding trypsin to the flasks. To facilitate dissociation, the flask was incubated at 37°C. Cells were observed under an inverted microscope to check for cell rounding, usually, cells would detach after 5 to 10 minutes. Gentle hitting of the flask on the sides was used for cells that did not detach easily. The detached cells were resuspended in fresh medium and were centrifuged and resuspended in 1 mL DMEM. Twenty µL of 0.2% (m/v) trypan blue was added to the total volume of 20 µL of the cell suspension and PBS (only used for dilution if the cell suspension is too concentrated), in order to identify viable cells during the cell counting using a hemocytometer [161]. The dead cells were excluded from the count. The cell density was calculated using the following equation:

$$\text{Cell density (cell/mL)} = \frac{\text{Total number of cells}}{\text{Number of squares (4)}} \times \text{Dilution factor} \times 10^4$$

Appropriate aliquots of the cell suspension were seeded into culture vessels required for experimentation.

2.2.5. Compound preparation

A stock solution of 1 mg/mL sunitinib malate (Sigma-Aldrich Pty (Ltd), Johannesburg, RSA) and ZM 306416 (Cayman Chemical, USA) was prepared in saline. The stock solution was aliquoted into microtubes and stored at -20ºC until use. Drug dilutions were prepared fresh on the day of the experiment using a culture medium.

2.3. Experimental methods

2.3.1. Crystal violet assay

Principle

Crystal violet assay is a quick and versatile assay for screening cell viability under diverse stimulation or inhibition conditions. This assay is based on staining cells that are attached to cell culture plates using the crystal violet dye that binds to protein and DNA. The amount of crystal violet staining in the assay is directly proportional to the cell biomass that is attached to the plate. When cells that undergo cell death lose their adherence and are subsequently lost from the population of cells, reducing the amount of crystal violet staining in a culture, affects the cell biomass which is used to infer the level of cell viability [162]. The absorbance of the dye measured by the spectrophotometry at 570 nm corresponds to cell quantities.

Materials

Glutaraldehyde (1% v/v) in distilled water, crystal violet (1% w/v) in distilled water and Triton X-100 (0.2 % v/v) in distilled water were purchased at Sigma-Aldrich Pty (Ltd). (Johannesburg, RSA).

Methods

MCF-7 cells, MDA-MB-231 cells and MCF-10A were seeded in 96-well culture plates at a density of 5 x 10^3 cells per well and left overnight in a 37ºC incubator with 5% CO_2 for attachment. Phosphate-buffered saline was added in wells that contained no cells as background control. After 24-hour attachment, the medium was aspirated from the culture plate, and the cells were exposed to ZM 306416 and sunitinib malate at a concentration of 0.01 µg/mL; 0.1 µg/mL; 1 µg/ml 10 µg/mL and 20 µg/mL (excluding MCF-10A cell line). Positive control cells were treated with nocodazole, an antineoplastic agent (inhibits maturation and proliferation of malignant cells, and therefore, is used to treat cancer), at a concentration of 0.01 µg/mL; 0.1 µg/mL; 1 µg/mL 10 µg/mL, and 20 µg/mL. Vehicle control cells were treated with 0.05% DMSO, a solvent for Nocodazole and 0.9% saline, a solvent for sunitinib malate and ZM 306416. The culture plates were incubated for 24-, 48- and 72 hours before the assay was performed.

Following incubation, the medium was discarded, and cells were fixed by adding 30 µL glutaraldehyde solution (1% v/v) and left at room temperature for 15 minutes. After 15 minutes, glutaraldehyde was discarded, and cells were stained with the 100 µL crystal violet solution (1% w/v) for 30 minutes. The crystal violet solution was aspirated. The culture plates were rinsed under running tap water and air-dried overnight. To solubilise the stain, 100 µL triton X-100 (0.2% v/v) was added, and the plate was left overnight. Optical density (OD) was then measured by reading the absorbance at 570 nm with an ELx 800 Universal Microplate (BioTek instruments Inc, Weltevreden, South Africa).

To correct for the background average OD_{570} of all drugs was subtracted with the OD_{570} of the background control. Cell number percentage was calculated using the following equation:

$$\text{Cell number \%} = \frac{OD_{570} \text{ of drug treated cells}}{OD_{570} \text{ values vehicle control cells}} \times 100$$

The cell viability percentage was used to plot a scatter plot. The best-fit linear line was inserted along its equation. This equation provided values for a and b from the IC50 equation ($IC50 = 0.5-b/a$).

2.3.2. Morphology study

Principle

Polarisation optical transmitted light differential interference contrast is a polarization-optical transmitted light differential interference contrast method. In contrast to conventional DIC, linearly polarized light is only generated after the objective [163]. The PlasDIC displays the required phase profile, which is relative to the product of the section thickness and the refractive index difference between the environment and the average refractive index of quartz. The PlasDIC provides high-quality imaging of cells to observe their morphological characteristics [164].

Methods

Exponentially growing MDA-MB-231 cells were seeded in 96 well tissue culture plates at a cell density of 5 000 cells per well. Cells were incubated at 37°C for 24 hours to allow for attachment. After 24 hours, the cells were treated for 22 hours with sunitinib malate (10 µg/mL) and nocodazole (3 µg/mL). For this assay and subsequent assays, ZM 306416 was not used dictated by the findings in the cell viability assay (this is elaborated in detail in Chapter 3). The controls were treated with 0.9% saline and 0.05% DMSO. The cells were viewed using a Zeiss Axiovert CFL 40 microscope, and PlasDIC images were captured using a Zeiss Axiovert MRm digital camera (Zeiss, Oberkochen, Germany) at 40× magnification.

2.3.3. Migration assay

Principle

Scratch assay is used to describe and understand cell migration and its many roles in wound healing. Cell migration is defined as the movement of individual cells, cell sheets and clusters from one location to another [165]. Migration assay has been used to successfully demonstrate that certain compounds can accelerate or slow down the rate of migration. This assay requires basic cell culture techniques and supplies, a cell line of choice, and imaging technology to capture movement over time or movement in response to treatments. A pin tool and/or pipette tip is used to scratch and remove cells from a discrete area of the confluent monolayer to form a cell-free zone into which cells at the edges of the wound can migrate (**Figure 2.2.**). Molecules of interest as potential therapeutics are added to the wells/dishes, and images of cell movement are captured at regular intervals within a 24-hour period for data analysis [165].

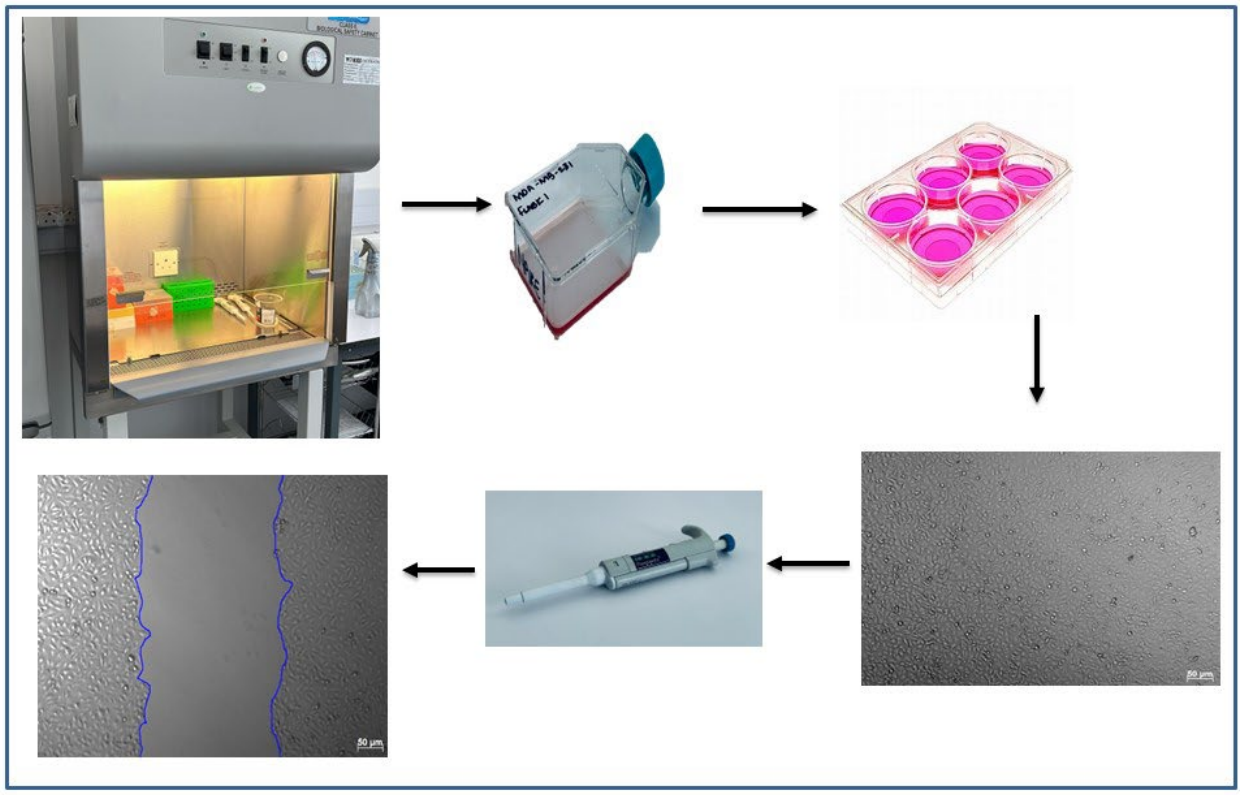

Figure 2.2. Flow diagram of a scratch assay. *Figure drawn by N.P Sekoba using Microsoft PowerPoint adapted from Pinto et al.* [166].

Methods

Cells were seeded into 100 mm x 20 mm gelatin-coated culture dishes at a density of 1.2 x 10^6 and incubated at 37°C for 24 hours to reach 100% confluency. Cells were scratched vertically and horizontally using a 10 µL yellow pipette tip. Cells were washed twice with 1x PBS to remove cells that were detached while scratching. Culture dishes were replenished with fresh medium containing nocodazole (3 µg/mL), sunitinib malate (10 µg/mL) and saline (0.9% v/v). The dishes were incubated at 37°C for 22 hours. The cells were viewed using a Zeiss Axiovert CFL 40 microscope, and polarization-optical differential interference contrast (PlasDIC) images were captured using a Zeiss Axiovert MRm digital camera (Zeiss, Oberkochen, Germany) at 0 hours, 7 hours,14 hours and 22 hours intervals. Images were then analysed using ImageJ software, and the percentage wound closure was calculated as follows:

$$\text{Wound Closure \%} = \frac{\text{the area of the wound measured immediately after scratching}}{\text{the area of the wound measured hours after the scratch is performed}} \times 100$$

2.3.4. Invasion assay

Principle

The transwell invasion assay assesses cell motility and invasiveness in the presence of a chemoattractant gradient. This is accomplished using plastic inserts for multi-well plates with a cell-permeable membrane. When these inserts are placed in the well of a multi-well tissue culture plate, they form a two-chamber system separated by a cell-permeable membrane. To create an invasion assay, the pores in the membrane are blocked with an ECM gel designed to mimic the matrices that tumour cells encounter during the invasion process *in vivo* (**Figure 2.3.**). Invasion

is determined by counting the cells that have traversed the cell-permeable membrane and invaded by placing the cells on one side of the gel and a chemoattractant on the other side of the gel [167-168].

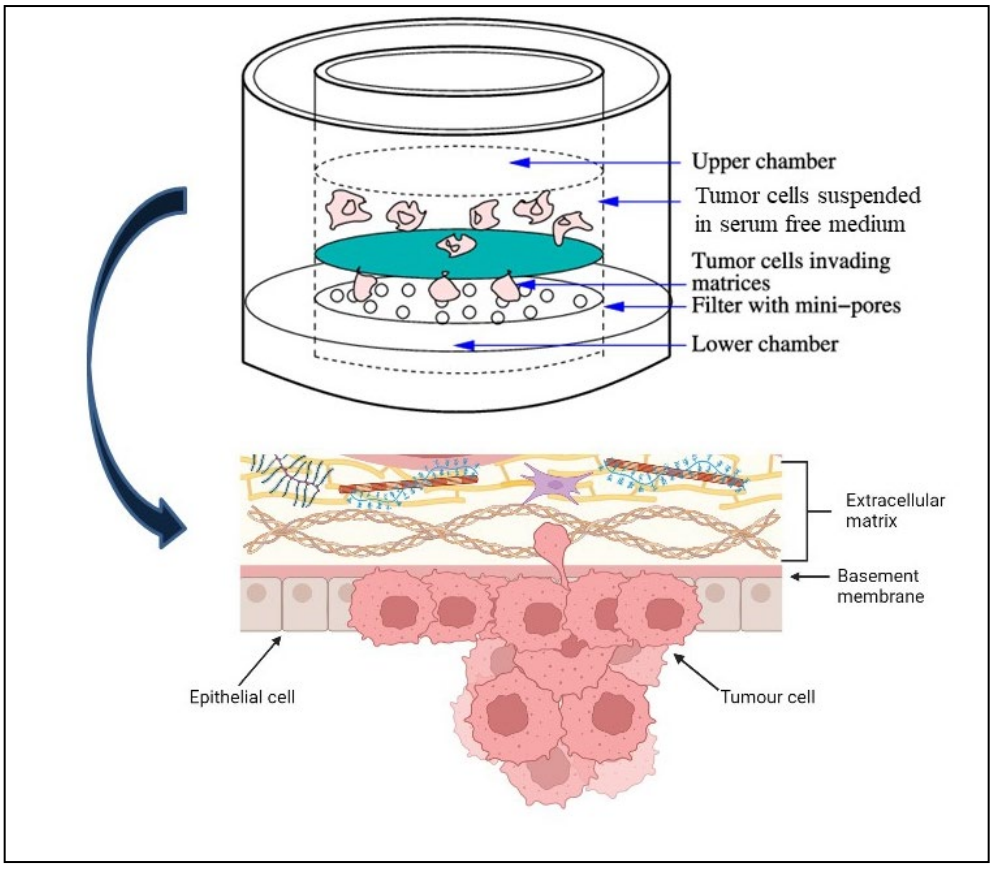

Figure 2.3. The principle of transwell invasion assay is illustrated using Boyden chamber, which mimics invasion *in vivo*. *Figure drawn by N.P Sekoba using Bio render adapted from Kim & Friedman* [169].

Methods

The upper transwell insert was coated with 1.5 % gelatin to form a matrix. Forty µL of DMEM was added into the gelatin-coated upper insert of the 96 well plates. The plate was incubated with the insert for 2 hours at 37°C. Upon reaching confluency, MDA-MB-231 cells grown in DMEM supplemented with 10% FBS, and 1% penicillin-streptomycin, were split. The cells were washed with 1x PBS and then resuspended in serum-free DMEM with treatment of compound (sunitinib malate (10 µg/mL), nocodazole (3 µg/mL), saline (0.9% v/v) and DMSO (0.05% v/v)). Then the

well of the 96-well plate (lower compartment) was subdivided into two settings and filled with 60 µL of DMEM supplemented with 10% FBS, and 1% penicillin-streptomycin and 60 µL of serum-free DMEM which were added as an attractant and control, respectively, in the well labelled as setting 1 and setting 2. The transwell insert was positioned into the well, with the bottom of the insert merged in the medium. Compound treated-MDA-MB-231 cells were seeded into the upper compartment at a density of 1 x $10^{4,}$ and the plate was then incubated for 48 hours at 37 °C. After 48 hours of incubation, the cells on the lower side of the insert membrane were fixed with glutaraldehyde (1% v/v), followed by staining with 1% (w/v) crystal violet. Gelatin and cells that remained in the upper compartment of the insert were gently removed by gently wiping the upper side of the membrane with a cotton swab. Using the inverted microscope, the number of cells in the lower compartment was counted in different fields of view to get an average sum of cells that have migrated through the membrane toward the chemo-attractant and control setting.

2.3.5. Liquid chromatography mass spectrometry

Principle

Liquid chromatography with tandem mass spectrometry (LC-MS/MS) is a technique used to separate a mixture into its individual parts. Components within the mixture are separated in a column based on each component's affinity for the mobile phase. The mixture within the liquid mobile phase will slowly be filtered down through the solid stationary phase, bringing the separated components with it, and the analytes will be detected and identified using the MS [170].

Materials

Reagents

Analytical standards (lactate, pyruvate, glucose-6-phosphate, fructose-6-phosphate and glutamine acid) were purchased from Merk (Pty) Ltd. (Johannesburg, RSA). MS grade (purity

≥99.99%) acetonitrile, methanol; analytical grade (≥98.0%) formic acid and ammonium formate were purchased from Merck (Pty) Ltd. (Darmstadt, Germany).

Instrumentation

Harvard syringe pump with a glass one millilitre Hamilton® GASTIGHT® 4.61 mm ID syringe was purchased from Separations (Randburg, South Africa). Agilent 1260 infinity II high-performance LC system (Agilent technologies, Walbronn, Germany) coupled to an AB Sciex4000 QTrap triple quadrupole tandem mass spectrometer (LC-MS/MS) purchased from Sciex (Toronto, Canada) was used. Analyst software version 1.7 (Sciex, Toronto, Canada) was used to manage the system and optimise analyte detection parameters, data acquisition and analysis.

Methods

2.3.5.1. Sample preparation

Cells were seeded at a density of 1.0 x 10^6 into a T25 and cultivated for 24 hours. After 24 hours, drugs (sunitinib malate, nocodazole, DMSO and saline) were added to the flasks of treatment, and only cultured medium without drugs was added in the no-treatment flasks (incubation period 24 hours). After 24 hours, the medium was aspirated, and flasks were washed with warm PBS first to avoid stressing the cells. Then washed with cold PBS twice to halt metabolism (quenching of metabolism). Flasks were then closed with caps and placed in a container containing cold ethanol, which is a continuous method of quenching the metabolism. The container was then stored at -80°C overnight. The freeze-drying machine was used to dry the samples. Dried samples were then stored in the -80°C freezer.

Extraction of metabolites procedure (methanol and water were used as the extraction solvent as they best suited to extract the metabolites that are under investigation):

The flasks were taken out of the -80°C freezer. Methanol (250 µl) was added into the flasks just to wet the dried surface. Then 500 µl of distilled water was added to the flasks. The flasks were placed into the ultrasonic bath for 15 minutes (this is a form of homogenisation where cells are lysed and the metabolites are released into the solution). The solution from the flask was poured into the eppendorf 1 (the water extraction). Distilled water (500 µl) was again added to the flasks and placed into the ultrasonic bath for 15 minutes. The solution was added to eppendorf 1 (the water extraction). Then 500 µl of methanol was added into the flasks and placed in the ultrasonic bath for 15 minutes. The solution was poured into a separate eppendorf 2 (methanol extraction). The eppendorfs were vacuum dried and stored at -80°C till LC/MS/MS analysis.

2.3.5.2. Preparation of standards

A 1 mg/mL stock solution was prepared for each standard (lactate, pyruvate, glucose-6-phosphate and fructose-6-phosphate) by dissolving it in distilled water. Aliquots were prepared from the stock solution and stored in the -80°C freezer till LC/MS/MS analysis.

2.3.5.3. Mass spectrometry method optimisation

Principle

To be able to identify and differentiate between metabolites, each metabolite must have a unique transition. This is accomplished by determining the precursor and product ions of each metabolite. The first analyser analyses the precursor ion, and the second analyser analyses the production, which is a fragment of the precursor ion.

Method

The direct infusion analysis was performed using the Harvard syringe pump in combination with the AB Sciex 3200 QTrap MS/MS mass spectrometer to identify the product ion mass and the precursor ion mass in each metabolite. An aliquot of the metabolite stock solution (1 mg/mL) was diluted with 20% ammonium formate, 40% methanol and 60% distilled water solution to a detectable concentration. Parameters such as the declustering potential (DP), collision energy (CE), and entrance potential (EP) were optimised for each metabolite to ensure high sensitivity (**see Section 3.5. in Chapter 3**). Other MS parameters, such as the source temperature (TEM), ion spray voltage (ISV), curtain gas (CUR), nebulizing gas (GS1) and drying gas (GS2), were also manually optimised (**see Table 2.1.**).

Table 2.1. Mass spectrometry parameters

Parameter	**Value**
Temperature	500 °C
Ion spray voltage	4500 V
Curtain gas	40 psi
Nebulizing gas	50 psi
Drying gas	50 psi

2.3.5.4. Liquid chromatography method development

The next step in the method development process was to hyphenate the LC module with the MS. Different mobile phases were investigated to get the best peak resolution with acceptable efficiency for the separation of the metabolites under investigation. Mobile phase A contained 10 mM ammonium formate and 0.5% formic acid in distilled water, while mobile phase B contained methanol: acetonitrile (2:8). The final gradient for the chromatographic separation of the mixture of metabolites for MS detection is shown in **Table 2.2.** using the Luna (HILIC) column. However, during the optimisation phase of the chromatography, several different analytical column stationary phases (C18 amide column and IEC QA-825) were investigated. The final gradient was obtained using Luna (HILIC) column (150 x 2mm, 3 µm, 200 Å) (Separations, Johannesburg, RSA) which was also tested to achieve the retention of metabolites.

Table 2.2. Gradient elution method showing the total LC run time vs the % mobile phase B.

Total liquid chromatography run time (mins)	Percentage (%) mobile phase B
0	95
3	95
10	75
11	75
12	95
14	95

2.3.6. Adenosine triphosphate assay

Principle

Adenosine triphosphate is the primary energy unit for cells. Upon cell death, ATP synthesis is arrested, and the ATP levels drop. Increased levels of ATP indicate cell proliferation and signal the presence of metabolically active cells [171-172]. Bioluminiscence ATP assay is one method that is used to determine the concentration of ATP in cells. This assay utilises luciferase to catalyse the formation of light from ATP and luciferin, and the light can be measured using a luminometer. Luminometers are specialised instruments that were first introduced to the market in 1970s. The signal recorded by the luminometer (**Figure 2.4**) is presented in relative luminescence units (RLU) [172].The overall reaction that proceeds in the luciferin–luciferase system of fireflies is as follows:

$$\text{Luciferin} + \text{ATP} + O_2 \xrightarrow[Mg^{2+}]{\text{Luciferase}} \text{Oxyluciferin} + \text{AMP} + \text{Pyrophosphate} + CO_2 + \text{Light}$$

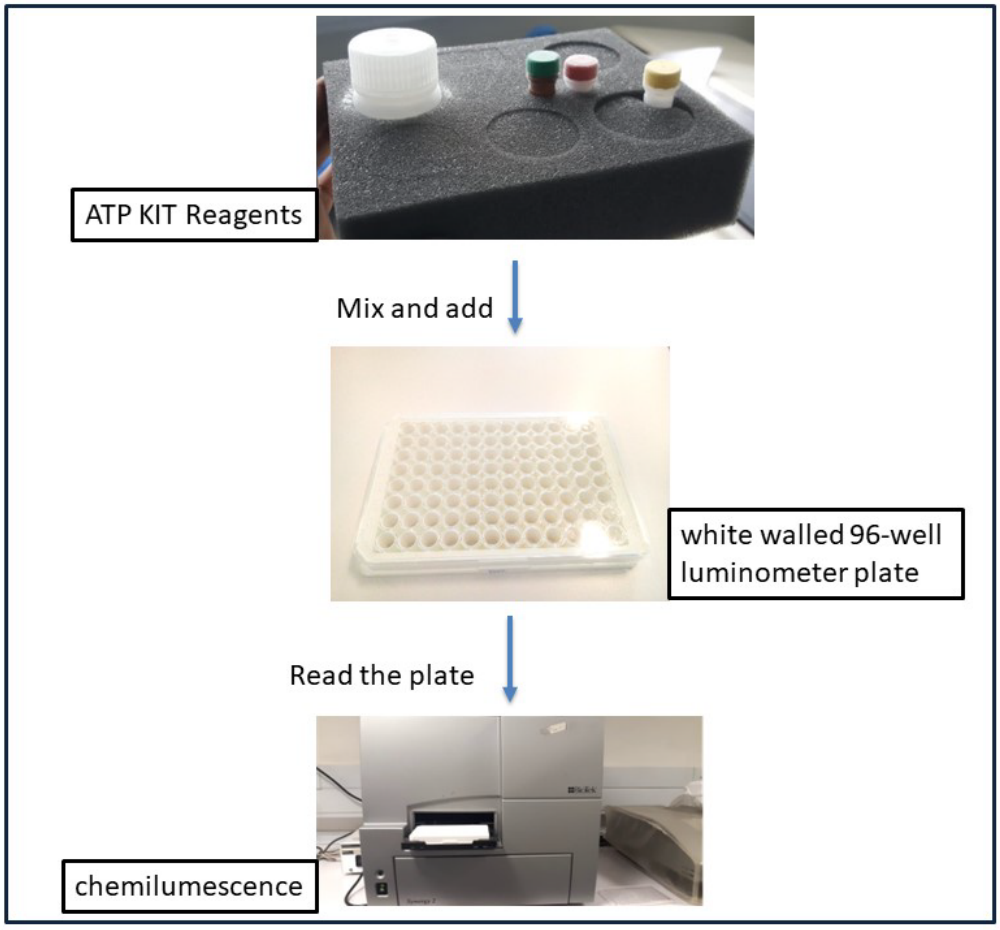

Figure 2.4. Flow diagram depicting the preparation and reading of the ATP assay.

Materials

ATP assay kit 119170 was purchased from Merk Pty (Ltd). (Johannesburg, RSA).

Methods

Cells were seeded at 5 x 10^3 cells in a 96-well luminometer plate, and the plate was incubated for 24 hours to allow cells to attach. Cells were then treated with drugs (0.05% DMSO, sunitinib malate and nocodazole) and incubated for 24 hours. After 24 hours culture medium was aspirated, and cells were treated with 100 µl of nucleotide-releasing buffer for 5 minutes at room temperature. ATP monitoring enzyme was added into the cell lysate (10 µL). Standards were prepared by adding 10 µl of a series of dilutions (1000 µg/mL, 100 µg/mL, 1 µg/mL, 0.1 µg/mL,

0.01 µg/mL, 0.001 µg/mL, 0 µg/mL (serves as a blank)) of ATP standard to the luminometer plate wells. An addition of 100 µl of nucleotide-releasing reagent and 1 µL of ATP monitoring enzyme was also added to the standards. The plate was read using a Biotek Synergy 2 chemiluminescence (Biotek, RSA).

2.3.7. Extracellular pH

Principle

A pH electrode is used to determine the pH of a solution. It consists of a pair of electrodes, a measurement electrode and a reference electrode, both submerged in an unknown pH solution. These two electrodes combine to form two half-cells. The potential developed in the reference cell is constant, whereas the potential developed in the measurement cell is dependent on the concentration of hydrogen ions in the solution and is governed by the Nernst equation [173].

Methods

Culture media was collected from culture plates and transferred to 15-mL tubes after 24 hours of incubation without treatment which serves as a baseline and 24 and 48 hours of incubation with treatment in breast tumour cells and without treatment in media not containing cells. Then the pH was measured with a pH meter.

2.3.8. Statistics

Data analysis was conducted in consultation with a biostatistician (Prof PJ Becker) from the Unit of Biostatistics, Faculty of Health Sciences, University of Pretoria, using Stata Release 17 statistical software. Data summary reported mean and standard error of mean by factors of interest. Viability data were analysed using a two-way analysis of variance (ANOVA) with factors time (24, 48, 72 hours) and concentration (0, 0.01, 0.1, 1, 10 and 20 µg/mL) and interaction. Post-hoc analysis then compared concentrations with 0, by time and drug (sunitinib malate, ZM 306416 and nocodazole). Migration data were analysed using a two-way ANOVA with factors time (0, 7,

14, 22 hours) and drug (sunitinib malate, nocodazole and control) and interaction. Post-hoc analysis then compared drugs with control, by time. Invasion data were analysed by drug (sunitinib malate, nocodazole and control) using one-way ANOVA with factor concentration (0, 0.1, 1, 5 and 10 µg/mL) to compare concentration with 0 µg/mL. ATP data compared drugs (sunitinib malate, nocodazole and control) in a one-way ANOVA. Testing was done at the 0.05 level of significance.

CHAPTER 3: RESULTS

3.1. Cell viability

Cell viability was determined using the crystal violet nuclear staining assay. Cell viability results are expressed as a percentage of surviving cells relative to the vehicle control.

The effects of the VEGFR-1 inhibitors (ZM 306416 and Sunitinib malate) on the viability of three breast cell lines, the non-cancerous MCF-10A cells, and the cancer cell lines MCF-7 and MDA-MB-231 were determined.

3.1.1. Effect of ZM 306416 and Sunitinib malate on the viability of MCF-10A cells

At 0.1 µg/mL ZM 306416 had no effect on MCF-10A at 24, 48 and 72 hours relative to the control vehicle (**Figure 3.1.**). At 1 µg/mL, a decreasing trend of MCF-10A cell viability in a time-dependent manner was observed, although the degree of inhibition on cell growth was not significant. Similarly, at 10 µg/mL, cell viability was decreased to 87.8%, 85.7% and 80.6% in 24, 48 and 72 hours, respectively, although the degree of inhibition was not significant. Therefore, ZM 306416 was not cytotoxic to MCF-10A cells in a dose-dependent and time-dependent manner, similar to the positive control, Nocodazole. Due to the non-significant effect observed on the cell viability of MCF-10A treated at 0.1 µg/ml-10 µg/mL, for subsequent cell lines (MCF-7 and MDA-MB-231 cells), there was a dose increase to 20 µg/mL.

Sunitinib malate treatment at 0.1 µg/mL decreased the viability of MCF-10A cells at 24, 48 and 72 hours, although the degree of inhibition was not significant relative to the vehicle control (**Figure 3.1.**). Similarly, the degree of inhibition was not significant at 1 µg/mL of sunitinib malate treatment, where the cell viability of MCF-10A was reduced to 90.5%, 82.7% and 80.3% at 24, 48 and 72 hours, respectively. At the highest concentration of 10 µg/mL of sunitinib malate treatment, the viability of MCF-10A cells was decreased to 80.7%, 77.5% and 77.4% at 24, 48 and 72 hours,

respectively. However, the degree of inhibition was not significant. The slight cell growth decrease in normal breast cells was also evident when treating with the positive control, Nocodazole.

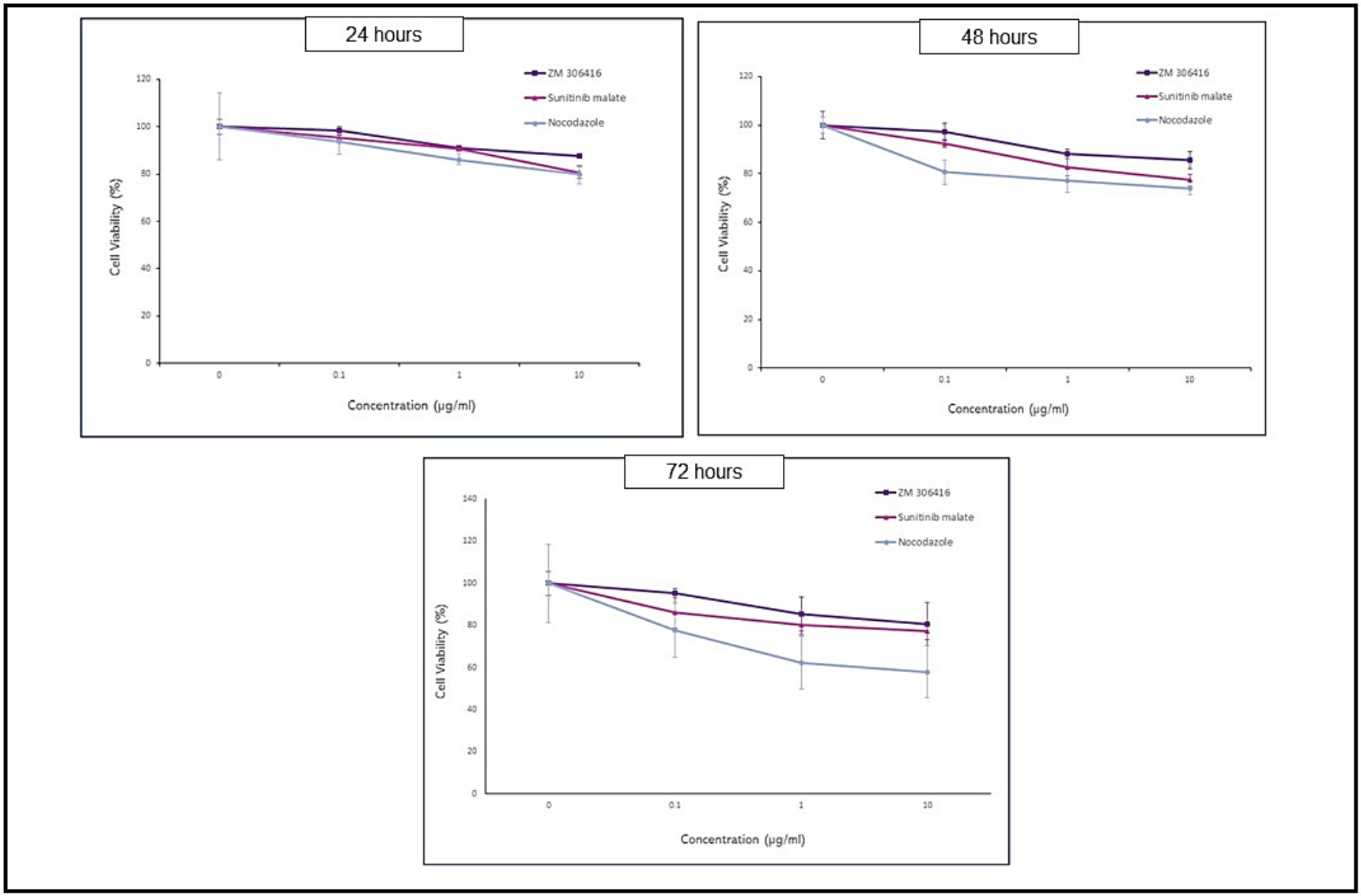

Figure 3.1. Effect of ZM 306416, sunitinib malate and nocodazole on the viability of MCF-10A cells after 24, 48 and 72 hours of treatment. Cell viability is expressed as a percentage relative to the vehicle control. Results represent the mean ± SEM of three independent experiments done in triplicate.

.

3.1.2. Effect of ZM 306416 and Sunitinib malate on the viability of MCF-7 cells

In MCF-7 cells treated with 0.01 µg/mL of ZM 306416 for 24 hours, the degree of inhibition was not significant relative to the vehicle control denoted as 0 µg/ml (**Figure 3.2.**). At 0.1 µg/mL of the drug, tumorigenic MCF-7 cell viability was reduced to 82.1%. At 1 µg/ml and 10 µg/mL, cell viability was decreased to 77.9% and 71.2%, respectively. However, at all concentrations of ZM 306416 treatment (0.01 µg/ml-10 µg/mL), the degree of inhibition was not significant when compared to the control vehicle Saline. The effect exerted by ZM 306416 contrasted with the positive control Nocodazole, which exerted a significant inhibition on growth at all concentrations after 24-hour treatment on MCF-7 cells (0.01 µg/mL (59.3%, $p \leq 0.001$), 0.1 µg/mL (55.3%, $p \leq 0.001$), 1 µg/mL (49.5%, $p \leq 0.001$), 10 (41.4%, $p \leq 0.001$) and 20 (26.0%, $p \leq 0.001$). The significant growth inhibition by the positive control validates the procedure and conditions of the experiment.

Sunitinib malate treated MCF-7 cells at a concentration of 0.01 µg/mL for 24 and 48 hours resulted in minor growth inhibition relative to the vehicle control Saline; however, at 72 hours the degree of inhibition was significant (**Figure 3.2.**). Inhibition of cell growth was also observed at concentrations of 0.1 µg/mL (87.5%), although the degree of inhibition was not significant at 24 hours. However, at 48 (85.4, $p \leq 0.05$) and 72 (59.4, $p \leq 0.001$) hours, the degree of inhibition was significant. At 1 µg/mL after 24 hours, the degree of inhibition of MCF-7 cells was not significant; however, at 48 and 72 hours, a significantly decreasing MCF-7 cell viability trend was observed. After 24, 48 and 72 hours of 10 µg/mL sunitinib malate treatment, cell viability decreased to 51.6% ($p \geq 0.05$), 44.4% ($p \leq 0.001$) and 37.1% ($p \leq 0.001$). At the highest concentration (20 µg/mL), significant inhibition of cell viability was observed in a dose- and time-dependent manner at 24, 48 and 72 hours of treatment relative to the positive control, Nocodazole. Overall, the dose- and time-dependent inhibition of cell growth by sunitinib malate

was lower than the Nocodazole exerted an inhibitory effect on MCF-7 cells at 24-,48- and 72 hours.

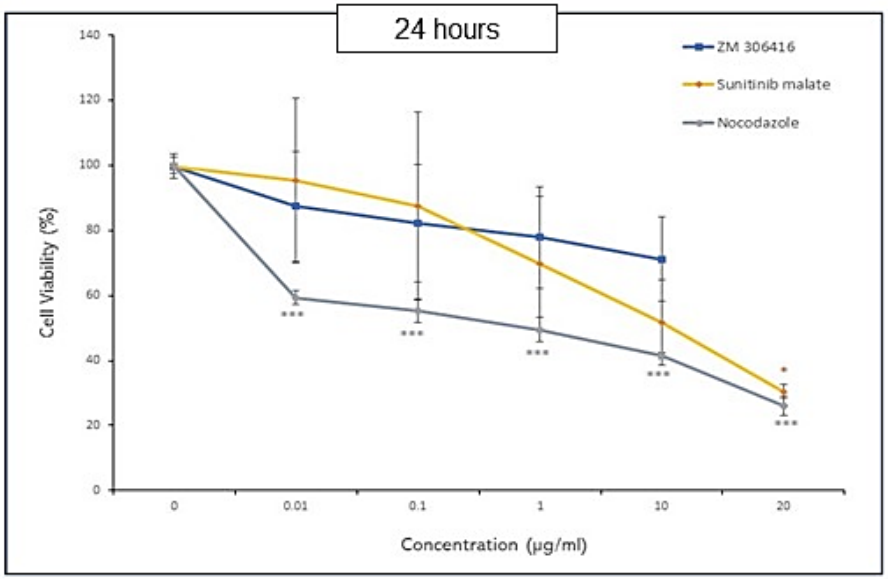

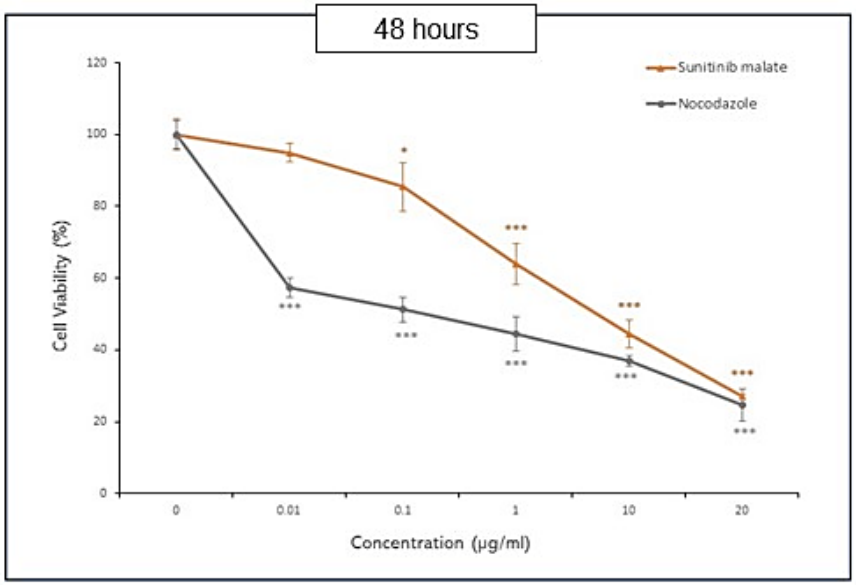

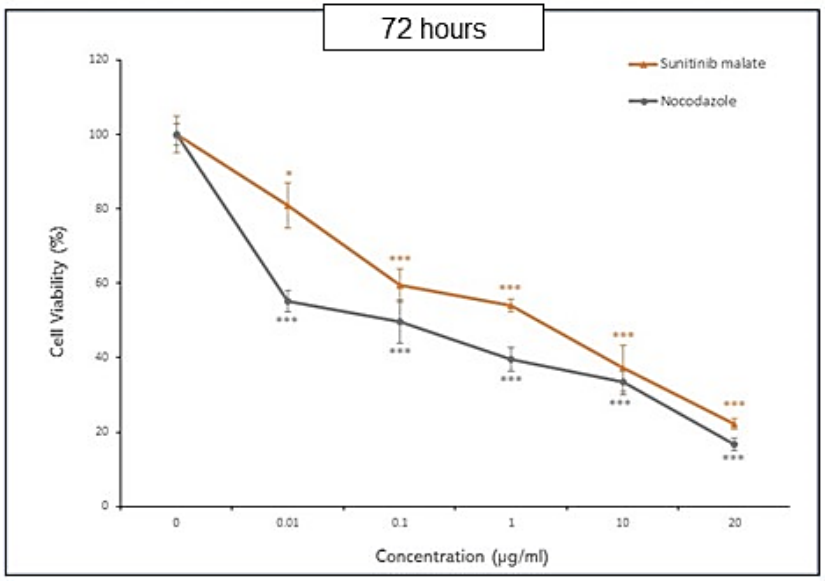

Figure 3.2. Effect of ZM 306416, sunitinib malate and nocodazole on the viability of MCF-7 cells after 24, 48 and 72 hours of treatment. Cell viability is expressed as a percentage relative to the vehicle control. Results represent the mean ± SEM of three independent experiments done in triplicate. * $p \leq 0.05$, *** $p \leq 0.001$.

3.1.3. Effect of ZM 306416 and Sunitinib malate on the viability of MDA-MB-231 cells

After 24-, 48- and 72-hour treatment with 0.01 µg/mL of ZM 306416 on MDA-MB-231 cells, minor growth inhibition was noted relative to the vehicle control (**Figure 3.3.**). However, the growth inhibition degree was insignificant relative to the vehicle control. Similarly, at 0.1 µg/mL of ZM 306416, the degree of inhibition was not significant across all experimental timelines (24, 48 and 72 hours). In contrast, at 72 hours of ZM 306416 treatment at a dose of 1 µg/mL and 10 µg/mL, cell viability was significantly inhibited by 46.1% and 56.4%, respectively. However, at 24 and 48 hours of treatment, the degree of inhibition was not significant at 1 µg/mL and 10 µg/mL concentrations.

Sunitinib malate reduced cell growth of tumorigenic MDA-MB-231 cells after 24 (97%), 48 (94.4%) and 72 (72.6%) hours of exposure at a concentration of 0.01 µg/mL, although the degree of inhibition was not significant (**Figure 3.3.**). Similarly, at 24 and 48 hours of 0.1 µg/mL sunitinib malate treatment of MDA-MB-231 cells, no significant effect was observed. However, at 72-hour treatment, cell viability was significantly reduced in MDA-MB-231 cells (53%, $p \leq 0.01$). The degree of growth inhibition was significant at concentrations of 1 µg/mL, 10 µg/mL and 20 µg/mL after 24-hour exposure. The viability of MDA-MB-231 cells was greatly affected after 48 and 72 hours of sunitinib malate exposure. Sunitinib malate inhibited cell growth to 53.9% ($p \leq 0.01$) at 1 µg/ml, 37.0% ($p \leq 0.001$) at 10 µg/mL and 20.8% ($p \leq 0.001$) at 20 µg/mL compared to vehicle control after 48 hours of exposure. The dose-dependent inhibition of cell growth by sunitinib malate was lower than the nocodazole exerted an inhibitory effect on MDA-MB-231 cells after 48-hour treatment. An increased degree of growth inhibition by sunitinib malate was noted at 72 hours of exposure. A decrease of 51.6% ($p \leq 0.01$) at 1 µg/mL, 32.4% ($p \leq 0.001$) at 10 µg/mL and 17.3% ($p \leq 0.001$) at 20 µg/mL was noted.

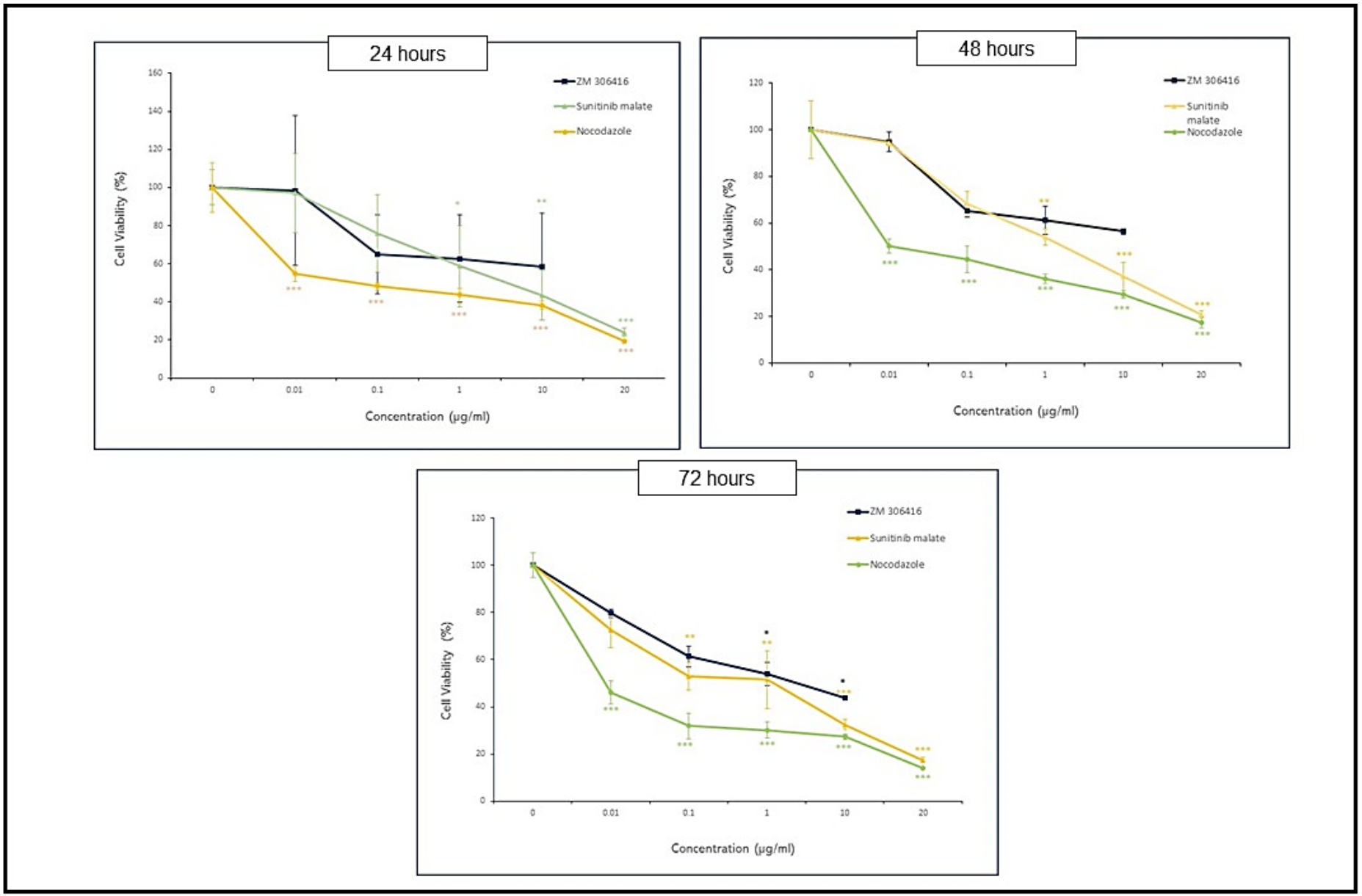

Figure 3.3. Effect of ZM 306416, sunitinib malate and nocodazole on the viability of MCF-7 cells after 24, 48 and 72 hours of treatment. Cell viability is expressed as a percentage relative to the vehicle control. Results represent the mean ± SEM of three independent experiments done in triplicate. * $p \leq 0.05$, ** $p \leq 0.01$, *** $p \leq 0.001$.

In summary, at different concentrations of sunitinib malate (0.1-10 µg/mL) less cytotoxicity was observed in normal breast cells (MCF-10A). In contrast, the tumorigenic cell lines MCF-7 and MDA-MB-231, when exposed to sunitinib malate in various concentrations (0.1-20 µg/mL) resulted in a significant inhibitory effect. The IC50 of the drugs under investigation was calculated using the equation $IC50 = 0.5 - b/a$ as depicted in **Table 3.1.** Therefore, a concentration of 10 µg/mL of sunitinib malate inhibition was determined as the optimal dose for the tumorigenic cell lines. However, the optimal dose of 10 µg/mL of sunitinib malate had a non-significant inhibitory effect on normal breast cells. Hence, all succeeding studies were conducted using 10 µg/mL of sunitinib malate.

Table 3.1. Compound concentrations required for half maximal growth inhibition of MDA-MB-231 and MCF-7 cells.

Compound	**IC50**	
	MCF-7	**MDA-MB-231**
Sunitinib Malate	13 µg/mL	8 µg/mL
ZM 306416	ND	ND
Nocodazole	7 µg/mL	3 µg/mL

Abbreviation: VEGFR-1, vascular endothelial growth factor receptor; ND, not determined. Results represent three independent experiments done in triplicate.

ZM 306416 was not cytotoxic to normal breast cells; however, it was less potent than sunitinib malate when tumorigenic cells were treated. In addition, sunitinib malate displayed higher efficacy than ZM 306416. Therefore, for succeeding studies, sunitinib malate was the compound selected to be investigated further. Moreover, further studies were undertaken using the MDA-MB-231 cell line due to the profound effect (being highly responsive to the drugs of investigation) observed in MDA-MB-231 cells.

3.2. Morphological studies

PlasDIC was used to visualise the effect of sunitinib malate (10 µg/mL) on the morphology of MDA-MB-231 cells after 24 hours (**Figure 3.4.**) and 48 hours (**Figure 3.5.**) of exposure. Following treatment, morphological alterations were identifiable in sunitinib malate-treated cells consistent with the positive control, nocodazole, and in contrast to the vehicle control saline (**Figure 3.4. and Figure 3.5.**).

The cell density was reduced by sunitinib malate treatment in contrast to the vehicle control-treated cells, which did not display a reduced cell density after 24 hours (**Figure 3.4.** (**A**)) and 48 hours (**Figure 3.5.** (**A**)) of exposure.

A characteristic indication of cell death that is rounding of cells, shrinking of cells and membrane blebbing was observed in sunitinib malate-treated cells at 24 hours of exposure (**Figure 3.4.** (**C**)) and 48 hours (**Figure 3.5.** (**C**)) similar to the positive control nocodazole, which displayed decreased cell density and blocked metaphase at 24 hours (**Figure 3.4** (**B**)) and 48 hours of exposure (**Figure 3.5.** (**B**)).

.

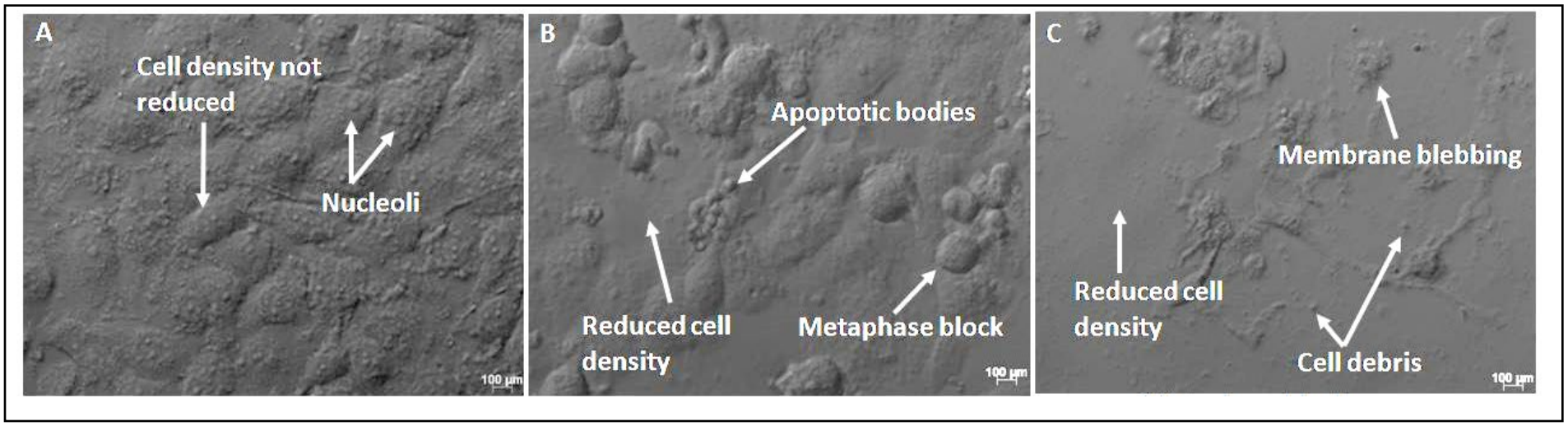

Figure 3.4. Morphological images of MDA-MB-231 cells after 24 hours of treatment. **(A)** untreated cells (control), **(B)** nocodazole treated cells, **(C)** sunitinib malate treated cells. Scale bar =100 µm. Results are representative of three independent experiments.

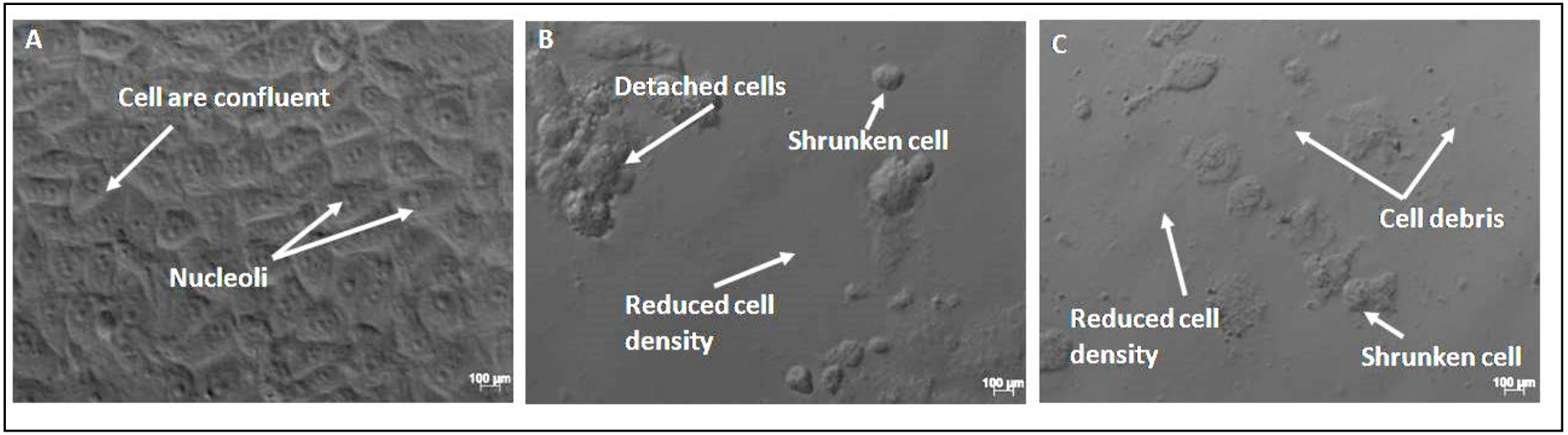

Figure 3.5. Morphological images of MDA-MB-231 cells after 48 hours of treatment. **(A)** untreated cells (control), **(B)** nocodazole treated cells, **(C)** sunitinib malate treated cells. Scale bar =100 µm. Results are representative of three independent experiments.

.

3.3. Cell Migration

To study cell migration, a scratch was created using the 20 µl pipette in a confluent monolayer. The effects of sunitinib malate (10 µg/mL) on cell migration were then measured at 0, 7, 14 and 22 hours (**Figure 3.6.**).

At 0 hours there was no significant difference in the width of the wound area of cultures exposed to the vehicle control (Saline) and that of cultures treated with sunitinib malate. Similarly, sunitinib malate and the positive control, nocodazole had similar widths of wound area at 0 hours (**Figure 3.6.**). At 7 hours, a slight reduction of the wound area in the sunitinib malate-treated culture was observed relative to the vehicle control. After 14 hours of sunitinib malate treatment, the wound width was maintained as cell migration was inhibited by sunitinib malate relative to the vehicle control, where the width of the wound area was greatly reduced due to cells migrating towards the wound area. Similarly, at 22 hours, sunitinib malate inhibited cell migration towards the wound area in comparison with the vehicle control. Moreover, over a 22-hour period, there was no significant difference in the width of the wound area of sunitinib malate and the positive control, Nocodazole. Therefore, similar to the positive control (nocodazole), sunitinib malate inhibited the migration of MDA-MB-231 cells over a period of 22 hours.

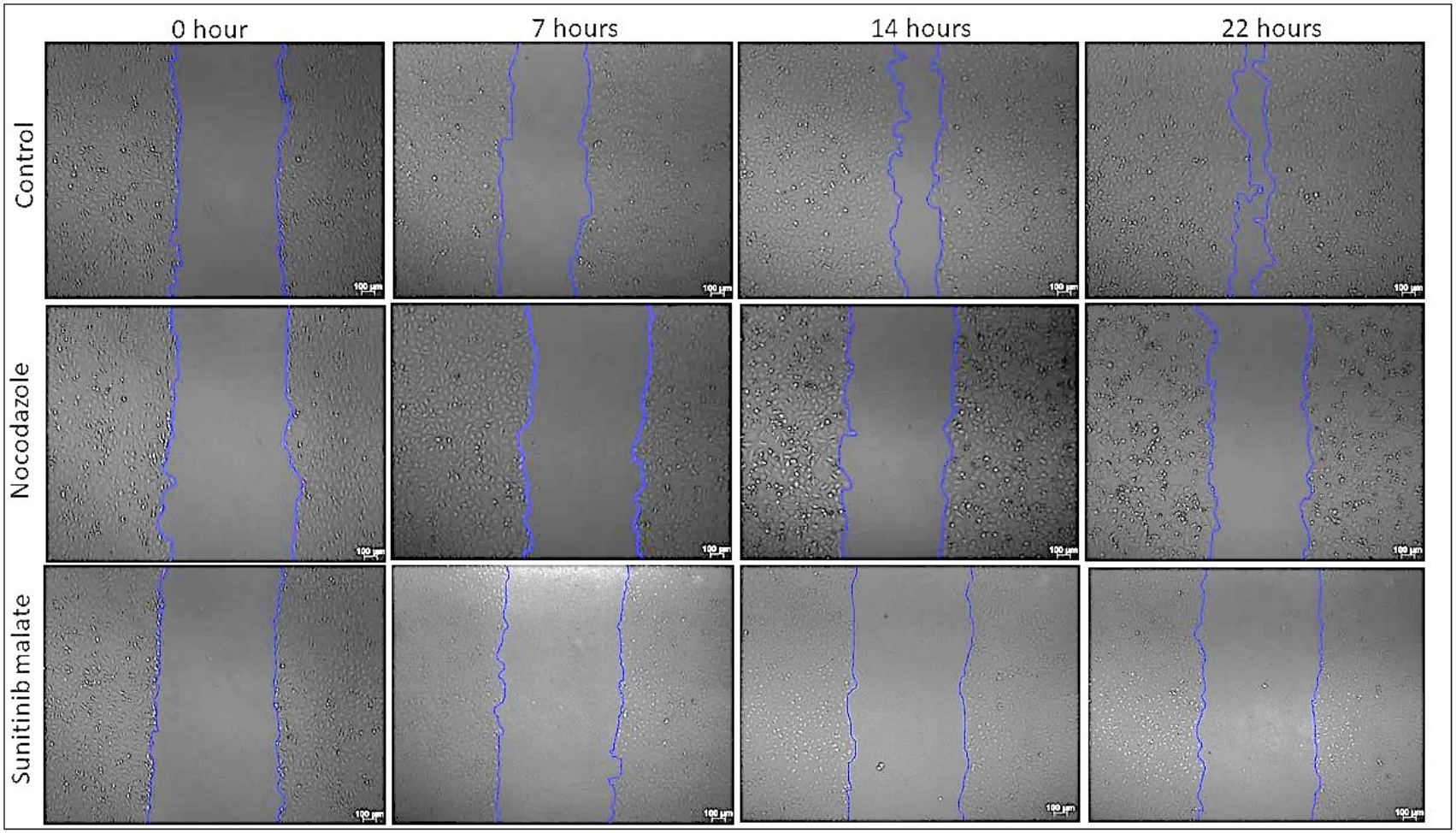

Figure 3.6. Representative scratch assay images over a 22-hour period. MDA-MB-231 cells were plated on gelatin-coated tissue culture dishes. Once confluent, a monolayer was formed after 24 hours, and the monolayer was scratched using a 20 µl pipette tip to create a wound. Wound healing images after the vehicle control (saline), positive control (nocodazole) and sunitinib malate exposure

were captured using Zeiss axiovert microscope (Zeiss, Oberkochen, Germany). The scratch was measured at three different areas, and the calculated average was used. Scale bar at 100 μm.

Figure 3.7. shows the graph wound width analysed using the ImageJ analysis software over a period of 22 hours. At 0 hours, there was no statistical difference between the wound width of sunitinib malate and vehicle control; the same was observed for sunitinib malate and the positive control (Nocodazole), as they had a similar wound width at baseline (**Figure 3.7.**). Minor inhibition of wound closure was detected at 7 hours (196 µm) post-sunitinib malate treatment when compared to the control vehicle. Sunitinib malate exerted a significant reduction of cell migration with wound width of 194 µm and 188 µm at 14 hours ($p \leq 0.01$) and 22 hours ($p \leq 0.001$), respectively, compared to the vehicle control (141 µm, 14 hours and 125 µm, 22 hours).

Thus, over the 22-hour period, sunitinib malate maintained the opening of the wound area similar to a positive control (nocodazole) and inhibited cell migration over time.

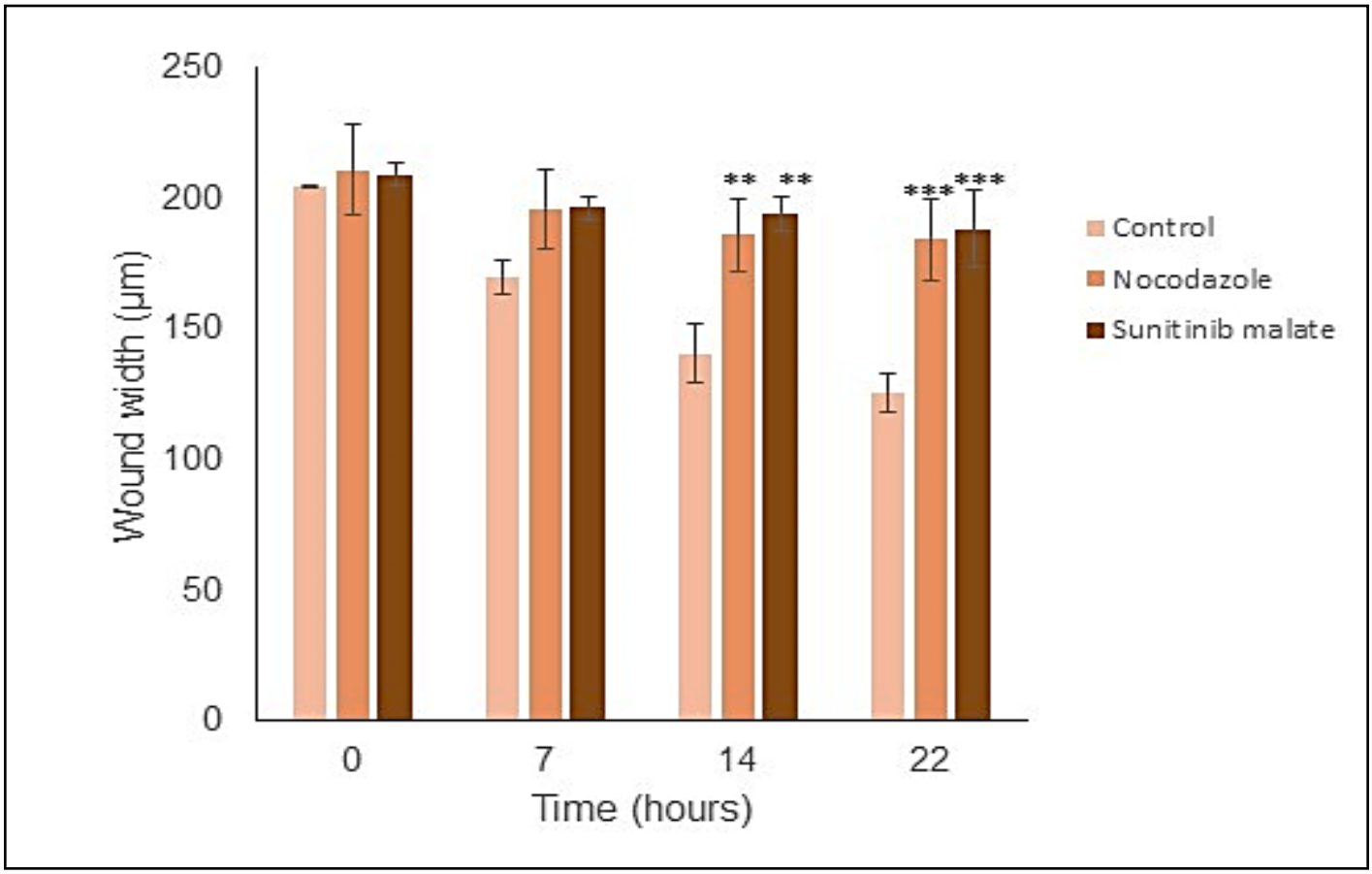

Figure 3.7. Sunitinib malate reduces cellular migration. Quantified rates of wound width were analysed using ImageJ analysis software over a period of 22 hours. Error bars represent the standard error of the mean from three different areas, and the calculated average was used. **p ≤ 0.01, ***p ≤ 0.001.

3.4. Invasion

The effect of sunitinib malate on the invasive capacity of MDA-MB-231 cells in the presence and absence of a chemoattractant (10% FBS) was determined. The total number of cells from the upper compartment that invaded the lower compartment was manually counted using an inverted microscope.

The percentage of invaded cells after 48 hours of vehicle control (Saline) exposure, without the chemoattractant, was 54% and (100 %) in the presence of a chemoattractant (**Figure 3.8.** (**B**)).

Sunitinib malate significantly reduced the percentage of cells invading the lower chamber of the plate to 44% ($p \leq 0.001$) at 0.1 µg/mL in cultures without a chemoattractant. At 1 µg/mL sunitinib malate decreased the percentage of invading cells to 31% ($p \leq 0.001$) relative to the vehicle control. At 10 µg/mL of sunitinib malate treatment, cell invasion was reduced to 18% ($p \leq 0.001$) in comparison to the vehicle control denoted as 0 µg/mL (**Figure 3.8.** (**A**)). The dose-dependent inhibitory effect exerted by sunitinib malate in the absence of a chemoattractant is evident in the positive control nocodazole (**Figure 3.8.** (**C**))**.**

In the presence of a chemoattractant in the lower chamber, sunitinib malate significantly reduced the number of invaded cells to 56% ($p \leq 0.001$) at 0.1 µg/mL. Invasion of cells was decreased to 33% ($p \leq 0.001$) at a dose of 1 µg/mL of sunitinib malate. At the highest dose of 10 µg/mL cell invasion was reduced to 21% ($p \leq 0.001$) relative to the vehicle control. The inhibition of invading MDA-MB-231 cells is dose-dependent and consistent with the positive control nocodazole.

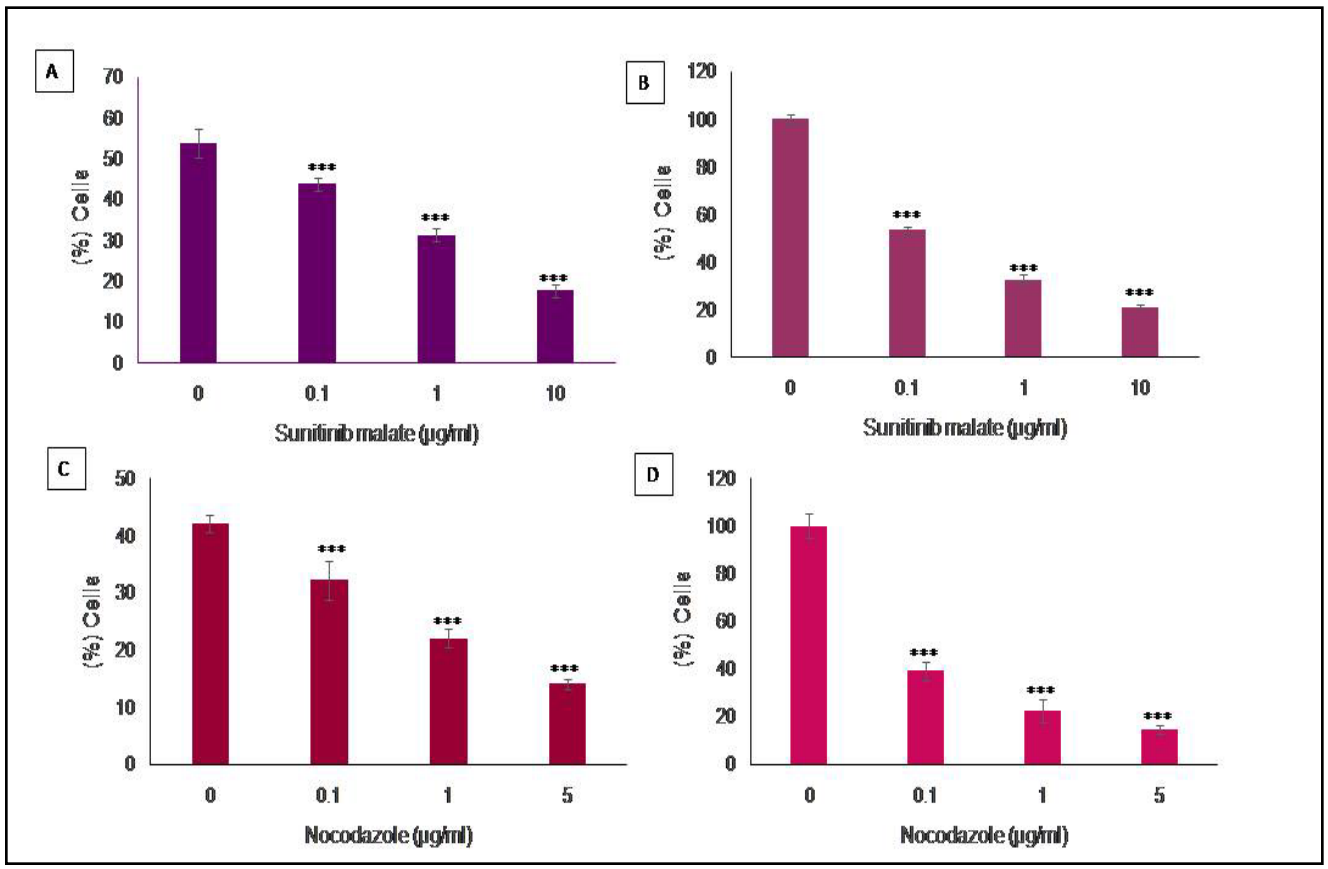

Figure 3.8. Invasion assay of cells after 48 hours of treatment with sunitinib malate. (A) sunitinib malate treated cells without (B) and with chemoattractant in the lower compartment. (C) positive control (nocodazole) treated cells without (C) and with (D) chemoattractant in the lower compartment. Cells were counted from random microscope fields and were represented as a percentage. Error bars represent the standard error of the mean from three experiments. ***p ≤ 0.001.

3.5. Liquid chromatography and mass spectrometry

Liquid chromatography and mass spectrometry are used in metabolic profiling to accurately identify and quantify metabolites. It is a tool used to reveal specific biomarkers for many diseases, including cancer which aids in therapeutic and clinical outcomes.

3.5.1. Mass spectrometry optimisation

Mass spectrometry optimisation was achieved using the tuning method where the DP, CE, EP and ionization mode of each metabolite of interest were determined (**Figure 3.9.** (**A-E**)).

Glucose-6-phosphate	Precursor ion mass	Polarity	DP	EP	CE	Elution time
	259.3	Negative	-35	-10	-24	0.82

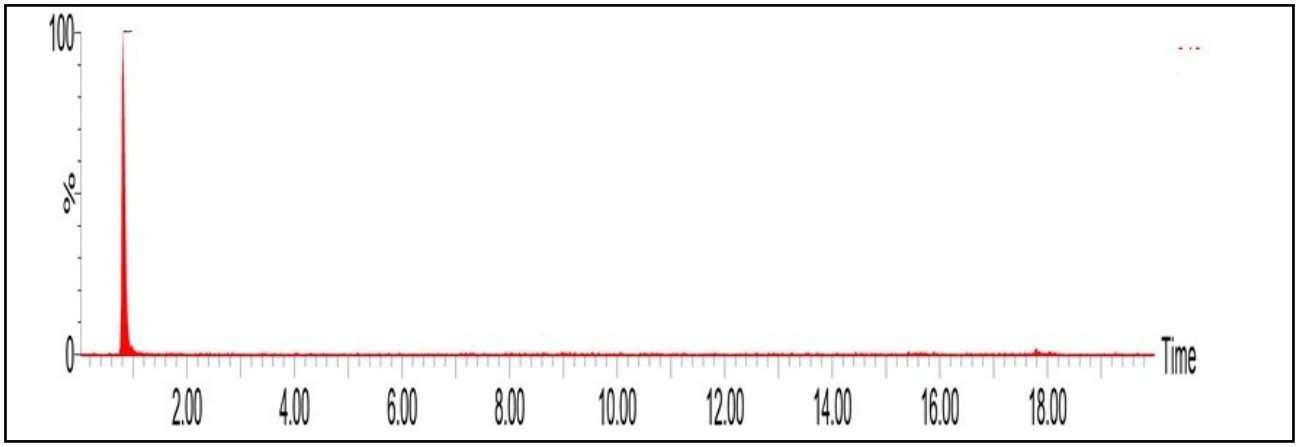

Figure 3.9. (A). LC-MS/MS chromatogram of glucose-6-phosphate.

Fructose-6-phosphate	Precursor ion mass	Polarity	DP	EP	CE	Elution time
	259.2	Negative	-23	-10	-24	0.82

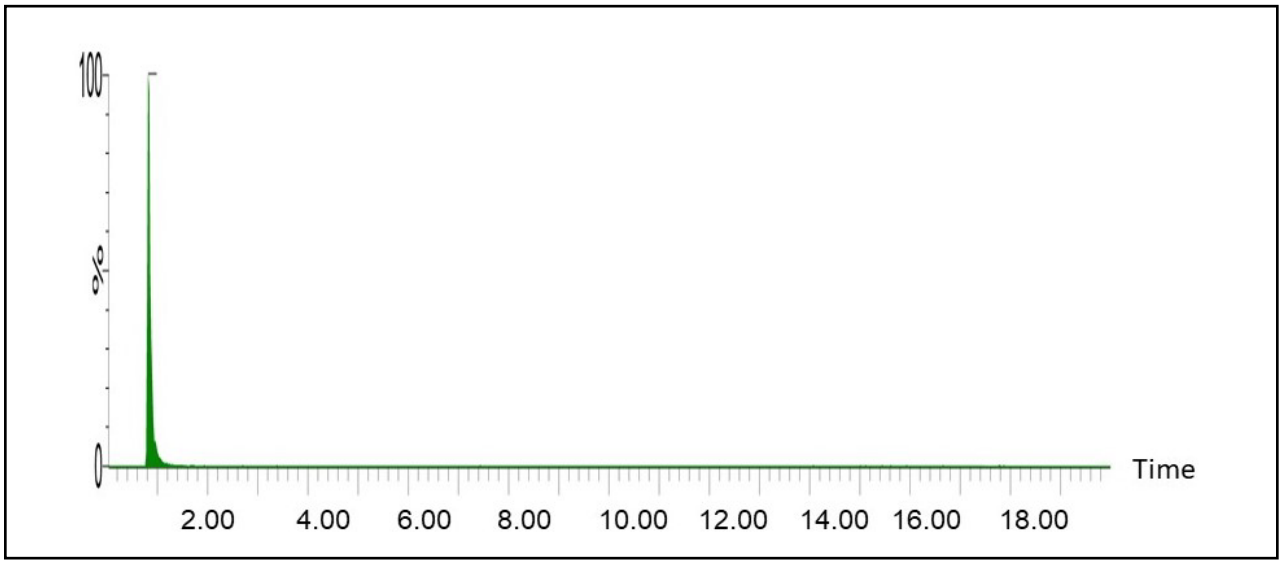

Figure 3.9. (B). LC-MS/MS chromatogram of fructose-6-phosphate.

Pyruvate	Precursor ion mass	Polarity	DP	EP	CE	Elution time
	87	Negative	-27	-10	-18	0.96

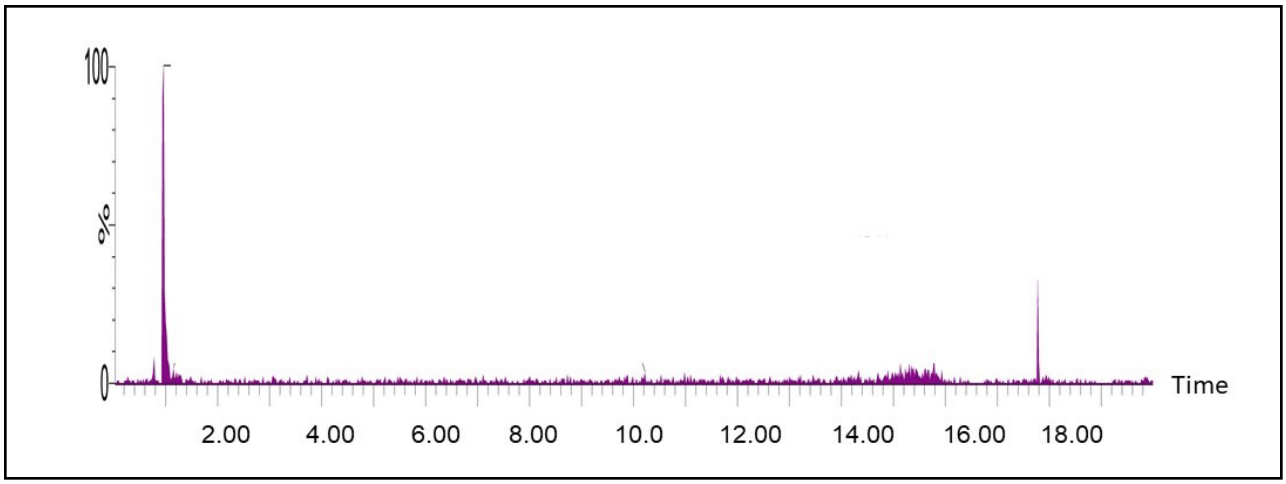

Figure 3.9. (C). LC-MS/MS chromatogram of pyruvate.

Lactate	Precursor ion mass	Polarity	DP	EP	CE	Elution time
	89	Negative	-33	-10	-24	1.07

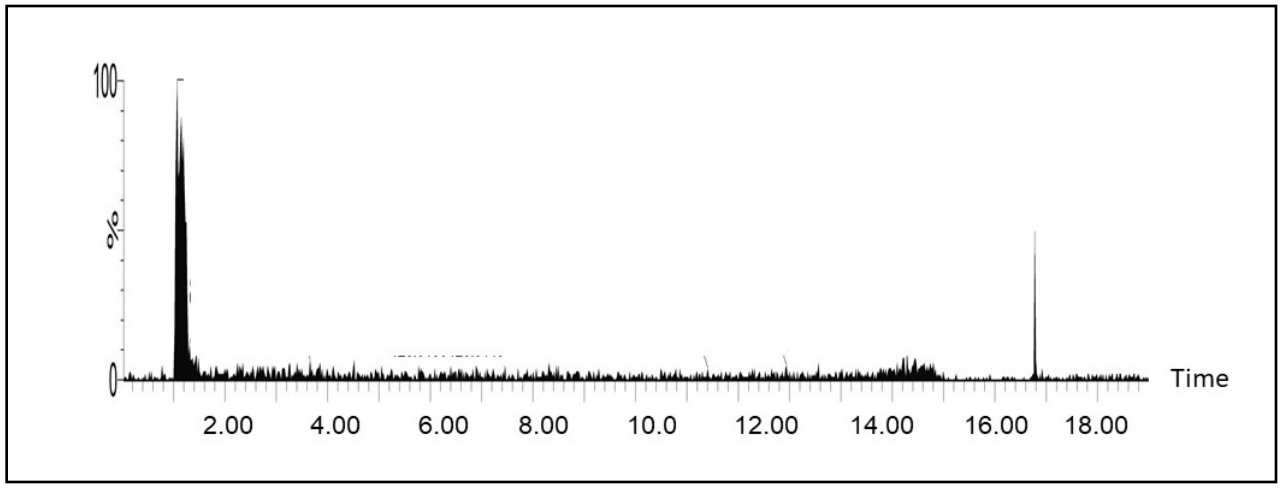

Figure 3.9. (D). LC-MS chromatogram of lactate.

Glutamate	Precursor ion mass	Polarity	DP	EP	CE	Elution time
	147	Positive	80	10	19	0.84

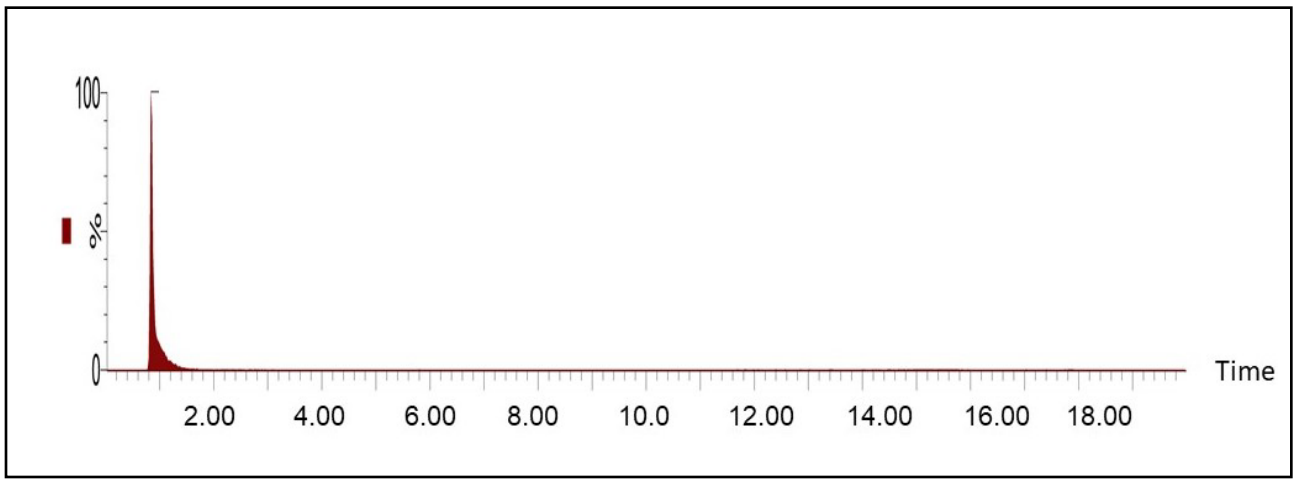

Figure 3.9. (E). LC-MS/MS chromatogram of glutamate.

3.5.2. Liquid chromatography optimisation

3.5.2.1. C18 amide column

The C18 is a reverse column that contains a non-polar stationary phase; however, this column contains the amide stationary phase, making the column hydrophilic. The C18 amide column was first tested to determine if it could separate and retain the polar metabolites of interest. A 7.5-minute method using 15 mM ammonium formate in acetonitrile (solvent A) and 10 mM ammonium formate in water (solvent B) was evaluated at a flow rate of 0.25 µL/min. Standards were used to assess the retention and separation of these polar compounds under the condition mentioned above using the C18-amide column. However, challenges were encountered with the column employed as the retention times for glucose-6-phosphate, fructose-6-phosphate, pyruvate, and glutamate were too short (**Figure 3.9.** (**A-E**) **and Figure 3.10.**). The metabolites of interest were not retained, and therefore, reliable detection was not possible (**Figure 3.10.**)

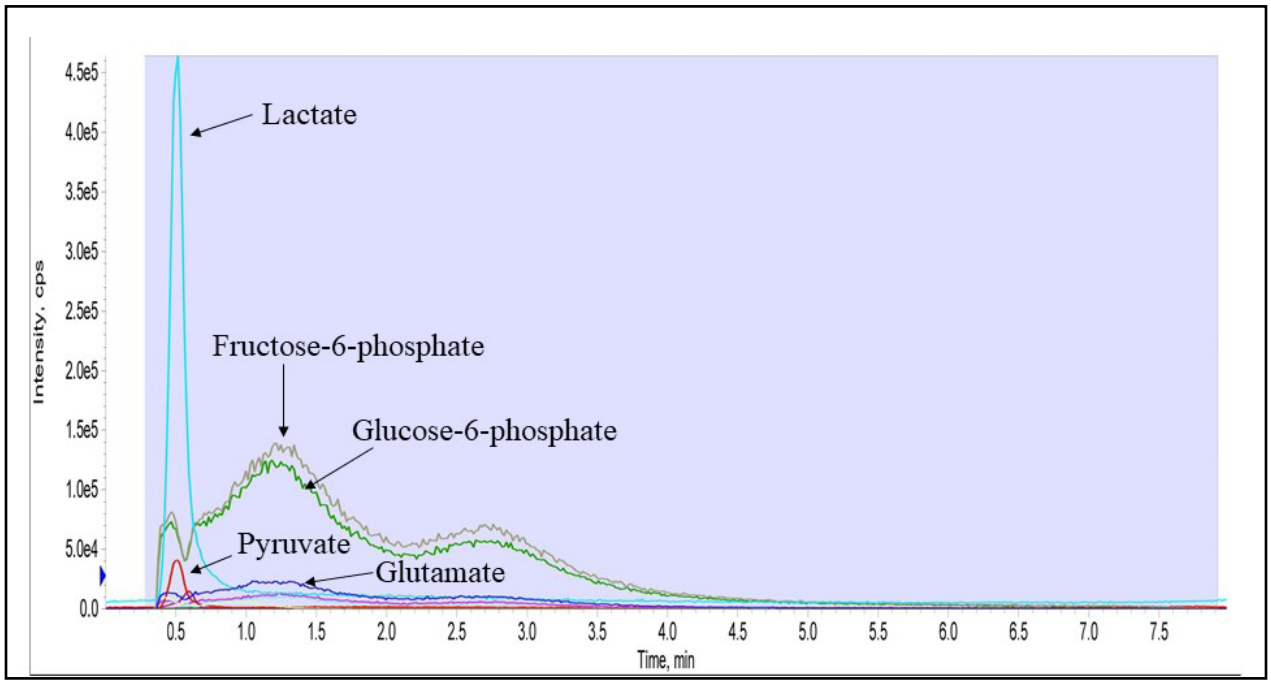

Figure 3.10. C18 amide chromatography of fructose-6-phosphate, glucose-6-phosphate, pyruvate, lactate and glutamate.

3.5.2.2. IEC QA-825 column

IEC QA-825 column is an ion exchange column filled with hydrophilic polymer-based gel modified with a quaternary ammonium group. A 7.5-minute method was used with solvent A containing 20 mM ammonium: 20 mM ammonium hydroxide in water and solvent B containing acetonitrile at a flow rate of 0.25 µL/min. The analytes of interest could be detected under the optimised MS conditions; however, the retention of the metabolites of interest was not achieved, although retained longer than the C18 amide column **see Figure 3.11**.

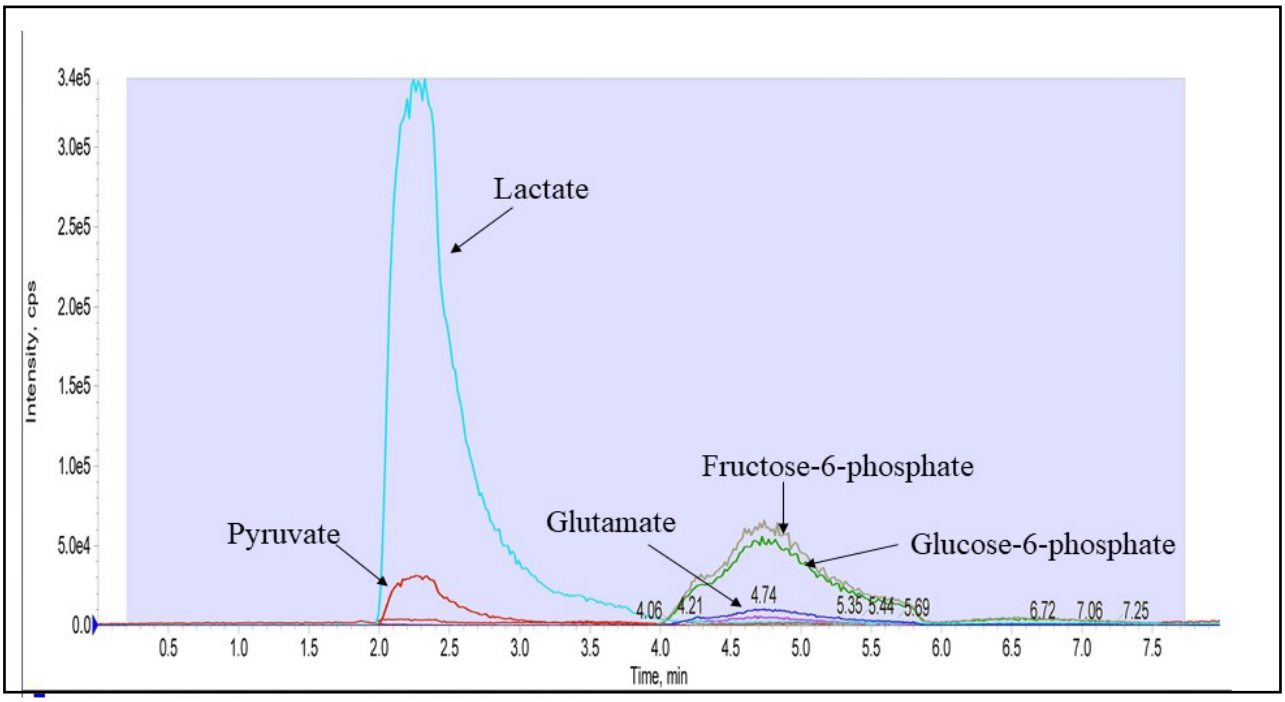

Figure 3.11. IEC QA-825 chromatography of fructose-6-phosphate, glucose-6-phosphate, pyruvate, lactate and glutamate.

3.5.2.3. Luna HILIC column

The third column evaluated in the study was a Luna (HILIC) column (150 x 2mm, 3 µm, 200 Å). Luna HILIC column is a column used to detect and separate hydrophilic metabolites. A water-enriched layer of silica remains on the surface of the Luna HILIC columns. This water layer makes it easier for polar compounds to move onto the stationary phase for improved retention. Several

concentrations of solvents were initially tested to determine the best method to analyse metabolites of interest. The mobile phase used contained 10 mM ammonium formate and 0.5% formic acid in distilled water, and mobile phase B contained methanol: acetonitrile (2:8), at a flow rate of 0.25 µL/min.

Standards were also tested to assess the retention and separation of these polar compounds. The results showed that some of the analytes were retained, such as lactate, fructose-6-phosphate and glucose-6-phosphate. However, glucose-6-phosphate and fructose-6-phosphate were difficult to separate under the various conditions employed as they were isomers and needed to be analysed in negative mode (**Figure 3.12.**). Other analytes, such as glutamate and pyruvate, were not successfully retained. Subsequently, reliable, optimal detection of metabolites of interest was not achieved.

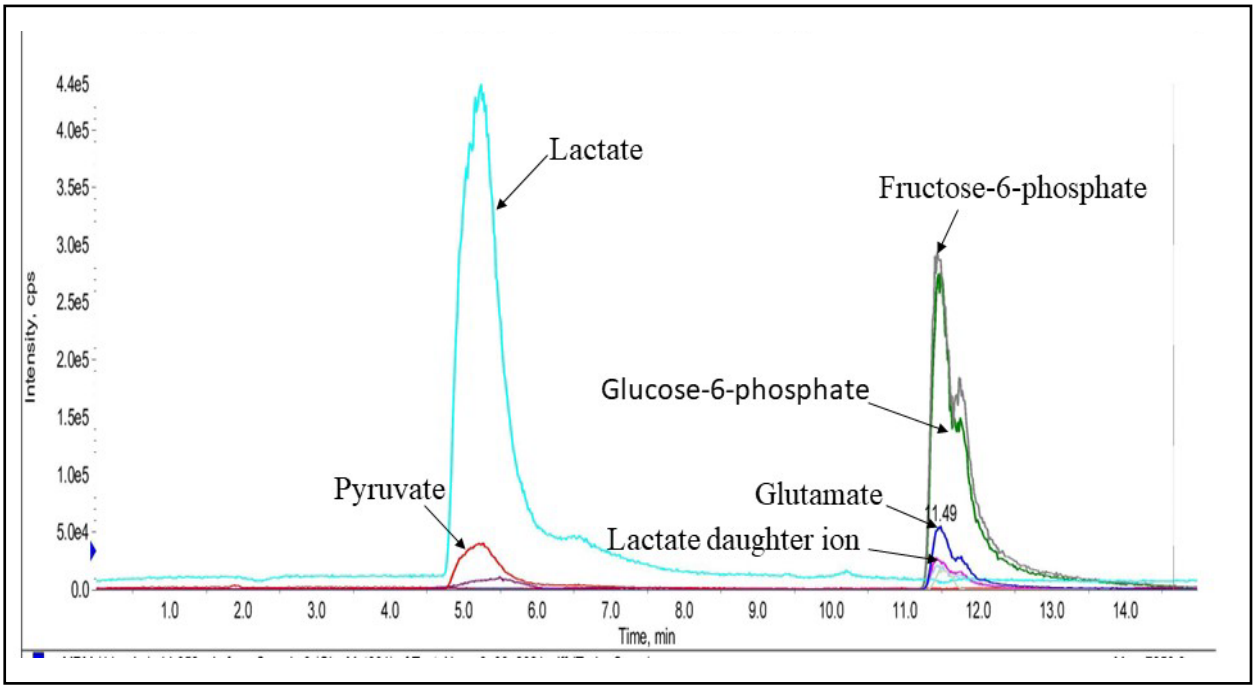

Figure 3.12. Luna HILIC chromatography of fructose-6-phosphate, glucose-6-phosphate, pyruvate, lactate and glutamate.

Overall, the column that can separate the analytes is an amide column, plus glutamine must be analysed in positive mode. Thus, the right column for the analytes, including pyruvate and glutamate, would be the Luna NH2 column. Further analysis in this study has been deferred as the waiting list for this column is almost a year.

However, for each metabolite of interest, successful optimisation of MS parameters was achieved, and this success will serve as a basis for further analysis. ATP and pH were assessed to further investigate the metabolic profile of MDA-MB-231 cells.

3.6. Adenosine triphosphate assay

The ATP levels signal the presence of metabolically active cells. In the presence of luciferase, ATP immediately reacts with the substrate D-luciferin to produce light which is detected through bioluminescence. To generate a standard curve, serial dilution of ATP standards (1000 µg/mL, 100 µg/mL, 10 µg/mL, 1 µg/mL, 0.1 µg/mL) was prepared. The standard curve was used to calculate the ATP levels of MCF-7 cells and MDA-MB-231 cells in treated and untreated groups **(Figure 3.13.)**.

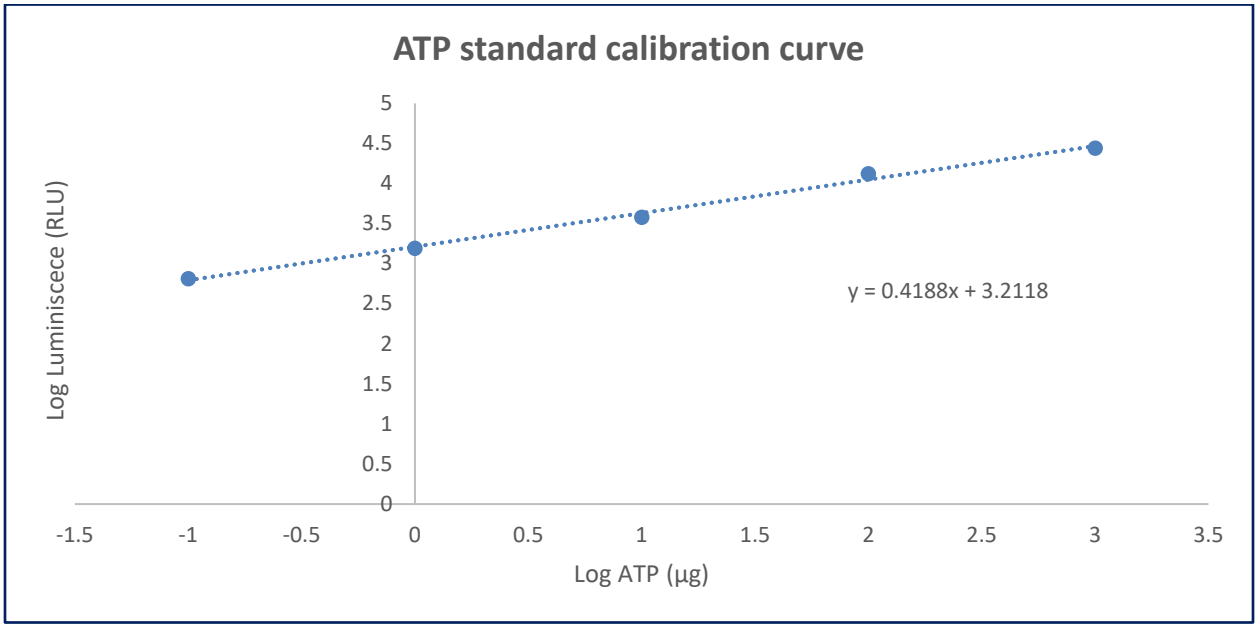

Figure 3.13. ATP Standard curve. The luminescence signal is proportional to the amount of ATP. The RLU values of the standards represent the average of the experiment performed three times, and the data presented are of one representative experiment. ATP, adenosine triphosphate.

MCF-7 cells treated with 10 µg/mL of sunitinib malate did not significantly reduce ATP levels in comparison to the vehicle control; however, a 32% decrease in ATP levels was exerted relative to the control (**Figure 3.14.** (**A**)). The decreased levels of ATP in sunitinib malate-treated MCF-7 cells are consistent with the displayed decreased ATP levels of the positive treated (Nocodazole) MCF-7 cells.

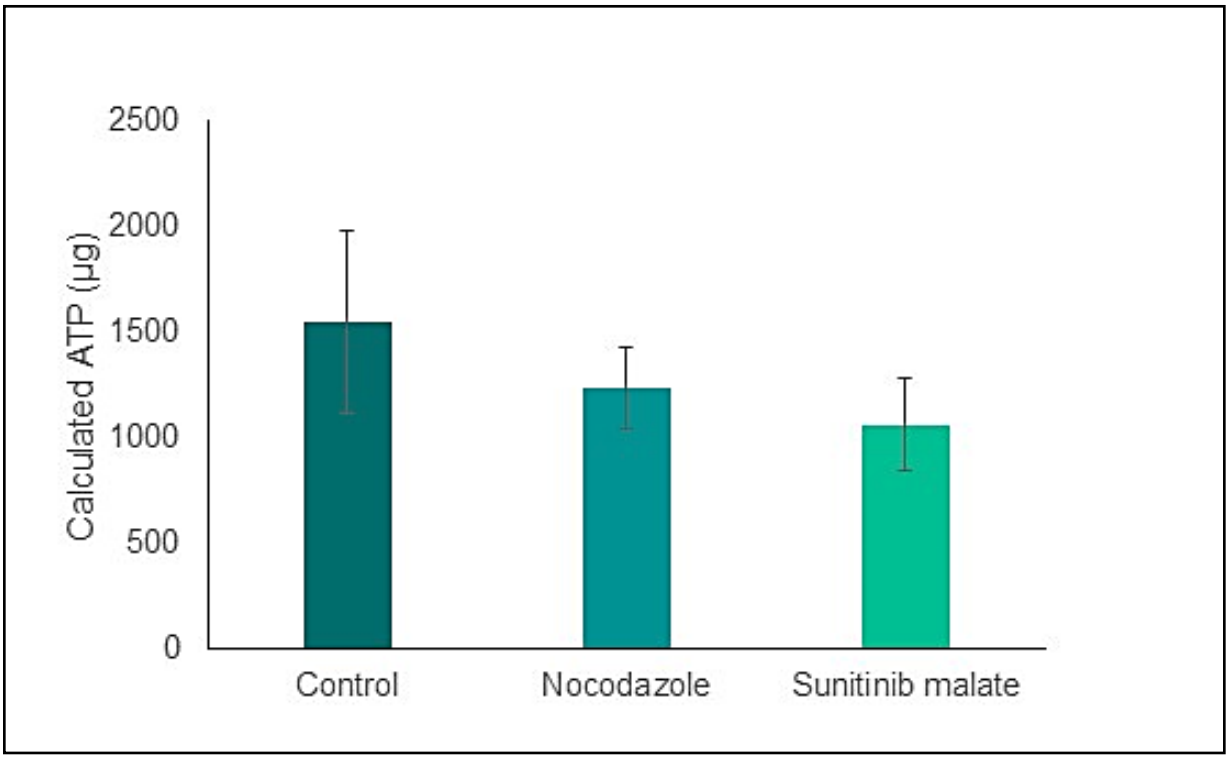

Figure 3.14. (A). The effect of sunitinib malate on the ATP levels in MCF-7 cells. The ATP levels were determined using the ATP assay kit (Sigma). The result represents the calculated ATP (µg) value ± SEM performed in triplicate.

In **Figure 3.14. (B)**, MDA-MB-231 sunitinib malate treated cells had a significant ATP level reduction of 71% ($p \leq 0.001$) as compared to the vehicle control, and a similar decrease trend of ATP levels was noted in Nocodazole treated MDA-MB-231 cells.

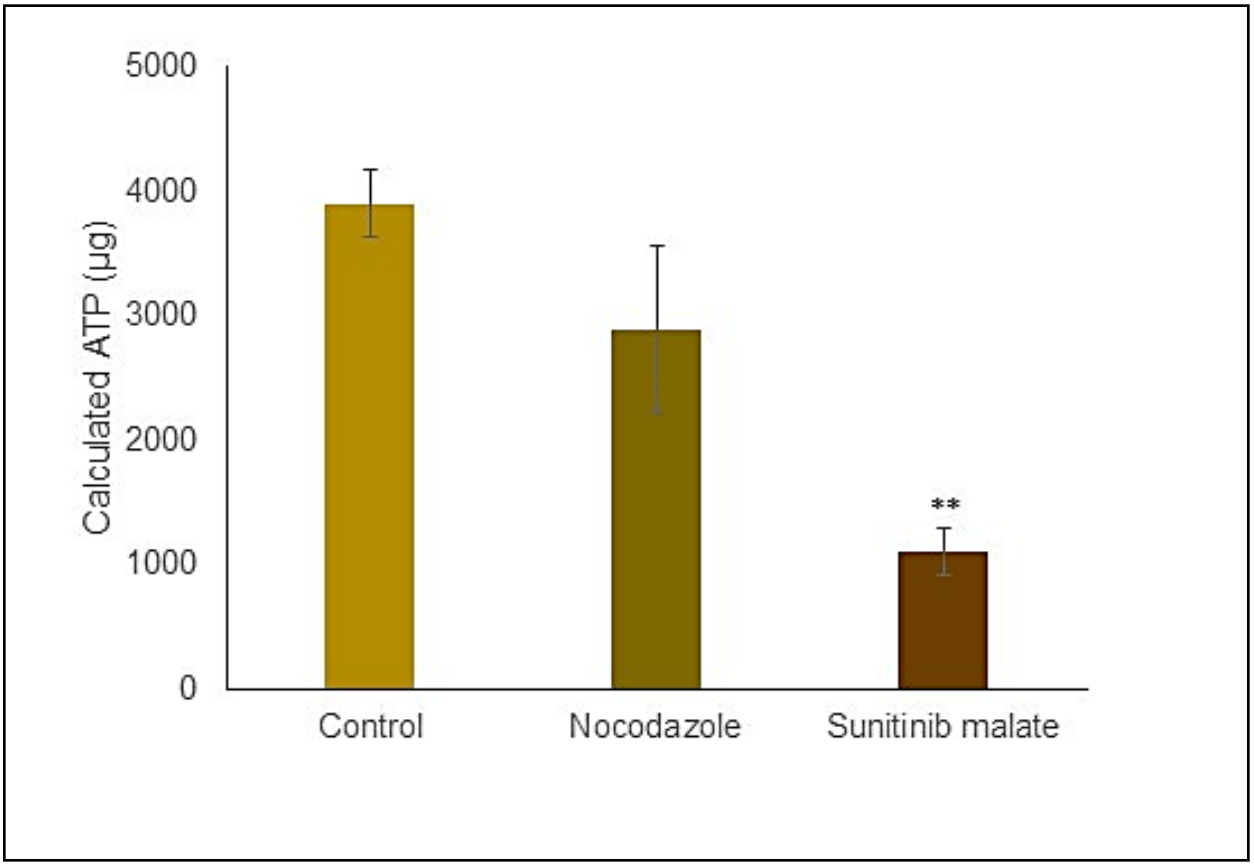

Figure 3.14. (B). The effect of sunitinib malate on the ATP levels in MDA-MB-231 cells. The ATP levels were determined using the ATP assay kit (Sigma). The result represents the calculated ATP(µg) value ± SEM performed in triplicate. ** $p \leq 0.01$.

3.7. Extracellular pH

The pH of MDA-MB-231 cells and MCF-7 cells was measured after 24 hours of incubation before drug exposure and after 24 and 48 hours of treatment using a pH-sensitive electrode (**Table 3.2**).

The culture medium without cells had a stable pH in all the tested time intervals of the experiment, indicating that the cells were grown in a stable pH medium.

After 24 hours of MCF-7 cell incubation without treatment, the pH between the intended MCF-7 cells to be exposed to the control (6.63) and sunitinib malate (6.60) was similar, implying equal cell density. After 24 hours of treatment, sunitinib malate-treated MCF-7 cells had increased the extracellular pH to 6.62 (reduced acidity) in contrast to the decreased pH (increased acidity) of the vehicle control (6.51). However, after 48 hours of treatment in MCF-7 cells, the pH had decreased in both sunitinib malate (6.35), and the vehicle control-treated MCF-7 cells (6.31). Although, sunitinib malate-treated MCF-7 cells had a higher pH when compared to the control group after 48 hours of exposure.

At baseline, without exposure, the cell density in MDA-MB-231 cells to be treated with control (6.60) and sunitinib malate (6.60) was the same. After 24 hours and 48 hours of treatment, sunitinib malate treated cells had an increased extracellular pH in MDA-MB-231 cells (6.75 and 6.34 respectively) in contrast to the vehicle control treated MDA-MB-231 cells (6.53 and 6.20). Therefore, sunitinib malate reduced the number of metabolic active MDA-MB-231 cells after 24 and 48 hours of treatment compared with the vehicle control.

Table 3.2. Comparison of extracellular pH in breast cancer cells

Cell line	Drug treatment	Extracellular pH ± SEM at baseline[a]	Extracellular pH ± SEM after 24 hours[b]	pH unit difference[c]	Extracellular pH ± SEM after 48 hours[d]	pH Unit difference
Culture medium[*]	None	7.2 ± 0.2	7.2 ± 0.2	N/A	7.2 ± 0.2	N/A
MCF-7	Control (Saline)	6.63 ± 0.07	6.51 ± 0.11	0.11	6.31 ± 0.1	0.04
	Sunitinib malate	6.60 ± 0.12	6.62 ± 0.12		6.35 ± 0.21	
MDA-MB-231	Control (Saline)	6.60 ± 0.1	6.53 ± 0.07	0.22	6.20 ± 0.2	0.14
	Sunitinib malate	6.60 ± 0.3	6.75 ± 0.25		6.34 ± 0.06	

[*], Culture medium does not contain breast cancer cells, [a]; pH measured after 24-hour incubation before treatment, [b], pH measured after 24 hours of drug exposure, [c], pH difference between sunitinib malate and control in each cell line separately, [d], pH measured after 48 hours of drug exposure. Results represent the mean ± SEM of two independent experiments. SEM, standard error of the mean. N/A, not applicable.

CHAPTER 4: DISCUSSION

Vascular endothelial growth factor receptor-1 is a tyrosine kinase receptor for VEGF A, VEGF B and placental growth factor (PIGF) ligands, with VEGF B and PIGF exclusively binding to VEGFR-1 [174-175]. Vascular endothelial growth factor A binds to both VEGFR-1 and VEGFR 2; however, VEGFR-1 has low kinase activity and high binding affinity to VEGF A when compared to VEGFR 2 [176]. The VEGF A/VEGFR-1 axis induces proliferation, migration, and extracellular invasion in tumour cells [174-175]. Moreover, VEGFR-1 is implicated with the induction of tumour-cell lined vessels and enhanced metabolism of cancer cells [174,177]. In this study, two major hallmarks contributing to breast cancer recurrence and poor prognosis were investigated: the alteration of breast cancer metabolism and the contributors of VM (cell growth, migration, and invasion). The capability of cancerous cells to enhance their metabolic activity and invade the ECM potentiate cell growth, distant metastasis, and sustainability by providing sufficient energy and augmenting the aggressive phenotype of breast cancer cells.

Vascular endothelial growth factor receptor-1 is highly expressed in tumorous breast tissues and correlates with poor prognosis [178-179]. In contrast, VEGFR-1 expression in normal breast tissue is absent or undetectable [176]. Moreover, VEGFR-1 plays no physiological role in adult angiogenesis functions such as tissue repair [178]. Thus, targeting VEGFR-1 might provide therapeutic benefits as it is anticipated to result in fewer adverse effects [174].

In this study, two compounds were investigated, namely ZM 306416 and sunitinib malate. ZM 306416, is a potent VEGFR-1 and EGFR inhibitor. Research on the anti-tumour effect of ZM 306416 in breast cancer cells is scarce. Sunitinib malate is an orally bio-available, multi-targeting tyrosine kinase inhibitor with a high binding affinity for VEGFR-1 and has shown anti-tumour activities. In this study, the *in vitro* effects of VEGFR-1 inhibitors on cell proliferation, metabolic profile, and VM channel formation were evaluated.

4.1. Growth Studies

Vascular endothelial growth factor receptor-1 expressed by breast cancer cells has been associated with tumour growth and survival through the VEGF A/VEGFR-1 and/or PIGF/VEGFR-1 axis [175,180]. In patients with breast cancer, high VEGFR-1 expression levels are associated with metastasis and recurrence risk [181-182]. Therefore, the anti-growth effect of VEGFR-1 inhibitors (ZM 306416 and sunitinib malate) on MDA-MB-231 and MCF-7 cells were investigated.

ZM 306416 exerted a growth inhibition effect on MDA-MB-231 cells after 72 hours of treatment, possibly through the inhibition of VEGFR-1 and EGFR, as MDA-MB-231 cells overexpress EGFR [183]. The overexpression of EGFR in breast cancer cells has been associated with increased tumour growth and poor clinical outcome [184]. Therefore, activated VEGFR-1 also increases proliferation in an autocrine endothelial growth factor (EGF)/EGFR–dependent manner [185]. Specifically, VEGFR-1 interacts with stabilised EGFR leading to an increased EGFR-dependent proliferative activity of cancer cells. The expression of EGFR is inversely proportional to the estrogen status [184]. In addition, both VEGFR-1 and EGFR have been associated with the aggressive phenotype and metastatic potential of breast cancer cells [175,186].

On the other hand, ZM 306416 did not inhibit the growth of MCF-7 cells after 24 hours of treatment. The lack of growth inhibition on MCF-7 cells by ZM 306416 might be attributed to the ER-positive status of MCF-7 cells. Firstly, ER signalling pathway drives tumour growth through the EGFR-dependent pathway, as there is a cross-link between the two pathways [187]. That is, plasma membrane-associated ER alpha can utilise the EGFR cascade for its signal transduction, and activation of the EGFR tyrosine kinase can phosphorylate and activate the nuclear estrogen receptor and its coregulator proteins. Thus, treated MCF-7 cells with acquired tamoxifen (a selective estrogen receptor modulator used to treat hormone-receptor breast cancer) show increased EGFR compared to the parent cell-line [187-188]. Therefore, the cross-link from the two pathways provides an escape from a single-targeted pathway treatment, as it is evident in our

study where EGFR was the only targeted pathway between the two pathways (EGFR and ER signalling pathway) by ZM 306416. Secondly, MCF-7 cells are estrogen-dependent for their proliferation; that is, estrogen signalling increases VEGF A expression in MCF-7 cells through an estrogen-responsive element within the VEGF A promoter which in turn promotes growth [184]. Hence, inhibition of VEGFR-1 and EGFR after 24-hour treatment with ZM 306416 did not yield any significant growth inhibition. Therefore, exploring combination/multi-targeting therapies might improve breast cancer treatment.

Multi-kinase inhibitor, sunitinib malate inhibited the growth of MCF-7 cells at 24, 48 and 72 hours of treatment. The observation of this study is in alignment with other studies where sunitinib malate was found to exert anti-growth effects on MCF-7 cells [189-190]. In our study, profound growth inhibition could be noted at 48 and 72 hours. These observations are similar to a study conducted by the Ghimirey *et al*. [190] where inhibition of MCF-7 cell growth treated with sunitinib malate after 72 hours was noted. Moreover, MCF-7 cells express low levels of VEGFR-1 and VEGF A when compared to MDA-MB-231 cells [191-192]. Thus, it is postulated that the MCF-7 cells are sensitive to VEGFR-1 inhibitors, as evident in sunitinib malate MCF-7 treated cells. However, MCF-7 cells are not solely dependent on VEGFR-1 signalling for growth but are also estrogen-dependent, which affects treatment efficacy, as observed with ZM 306416.

On the other hand, sunitinib malate decreased the growth of MDA-MB-231 cells in a time-dependent and dose-dependent manner. The growth inhibition could be through inhibiting the autocrine VEGF A/VEGFR-1 pathway as it regulates proliferation and growth in breast cancer **(Figure 4.1)** [175,185]. Our results agree with other studies, where the anti-growth effect of sunitinib malate was evident in MDA-MB-231 cells [189,193]. At the highest concentrations of sunitinib malate treatment, a significant decrease in growth was observed in MDA-MB-231 cells (it should be noted that sunitinib malate is only approved by FDA for treatment of renal cell carcinoma and it is still in clinical trials for breast cancer treatment) ; this might be attributed to the highest levels of VEGFR-

1 expressed by MDA-MB-231 cells, which is postulated to render these cells resistant to VEGFR-1 inhibition; thus higher concentrations would be required to competitively block VEGFR-1 signalling.

In addition, sunitinib malate had higher potency and efficacy in contrast to ZM 306416. This could be due to the advantage that sunitinib malate is a multi-kinase inhibitor, which targets more than one kinase increasing its potency [194]. Sunitinib malate also targets VEGFR 2 (a membrane-bound tyrosine kinase receptor that plays a role in breast tumour proliferation and metastasis) and platelet growth factor receptor α and -β (are receptors with intrinsic tyrosine kinase activity which binds platelet growth factors and play a role in cell proliferation and migration in malignancies such as breast cancer) [195-197]. Hence, combination studies of drugs are being mostly investigated as multi-target agents may reduce drug resistance development.

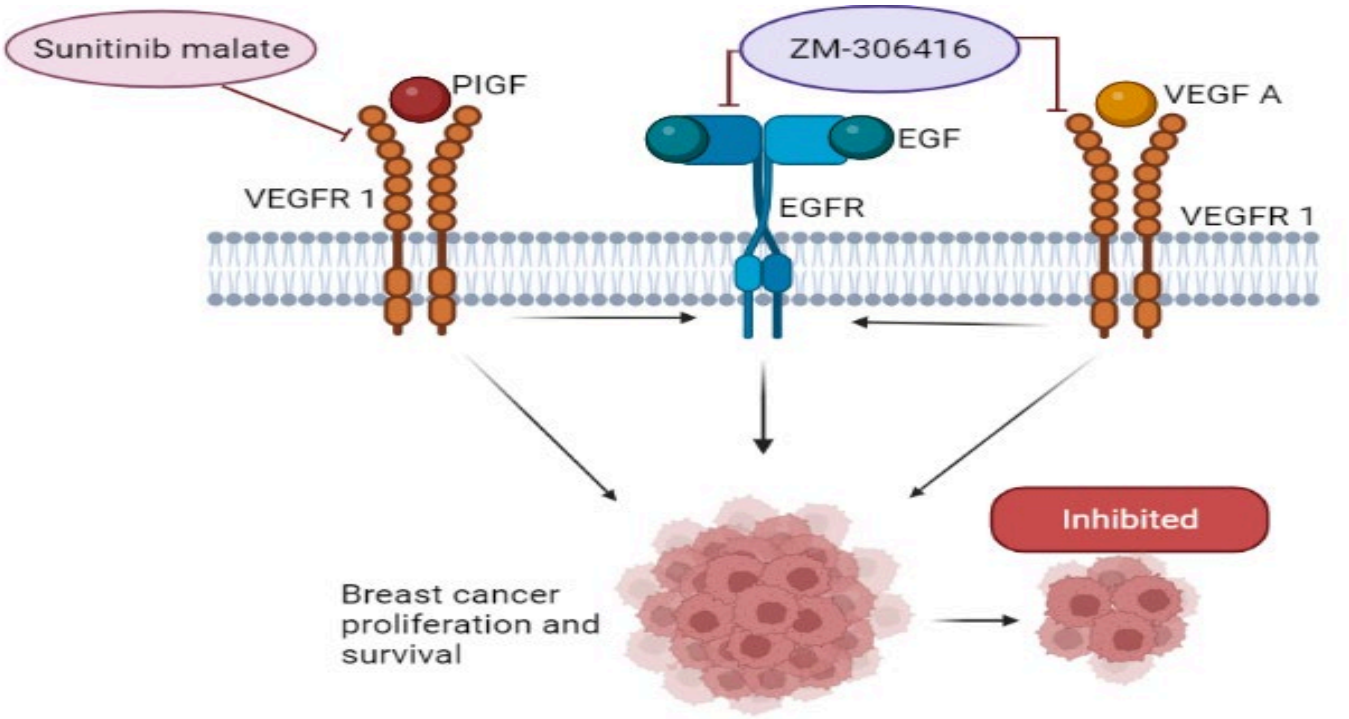

Figure 4.1. Postulated mechanism of ZM 306416 and sunitinib malate in inhibiting breast cancer cell growth. ZM 306416 inhibits tumour growth by inhibiting the VEGFR1-EGFR axis. Sunitinib malate inhibits VEGFR-1 to affect tumour growth in breast cancer cells. *Figure drawn by N.P Sekoba using Biorender.*

4.2. Morphological studies

Cell death (apoptosis) is characterised by structural changes such as cell rounding, cell shrinkage, apoptotic bodies, and membrane blebbing [198-199]. When MDA-MB-231 cells were treated with sunitinib malate, the above characteristics were observed. These morphological observations suggest that treated MDA-MB-231 cells undergo cell death (apoptosis), possibly through the inhibition of multi-kinase receptors such as VEGFR 2, platelet growth factor receptors and VEGFR-1 signalling pathway, as their inhibition is associated with cell cycle arrest or apoptosis in breast cancer [197,200]. Therefore, targeting multiple kinases instigate cancer cell death, and warrants further investigation as it provides a potential curative solution.

4.3. Vasculogenic mimicry - migration and Invasion

Metastasis is a multistage process that entails tumour migration and invasion to distant organs [180]. However, migration and invasion are not sufficient to produce distant metastasis, VM serves as a transport for malignant cells to disseminate and invade distant organs [201]. Subsequently, VM is one of the hallmarks of cancer. Successful invasion entails the detachment of malignant cells from the tumour cells due to the reduction or loss of intercellular adhesion molecules [202]. Thus, obtaining high motility capabilities that enable migration through the ECM, resulting in intravasation into the vasculature and extravasation into the surrounding tissue [201,203]. Malignant tumour cells use collective and single-cell migration as a migratory mechanism to invade, grow and metastasise [202]. Most breast cancer-related deaths result from metastasis [204]. In TNBC, early disease progression and metastasis often occur within the first 5 years after diagnosis. It is imperative to research drugs that interfere with the metastasis of tumours and VM [116,205].

In this present study, the *in vitro* inhibition of sunitinib malate on TNBC (MDA-MB-231) migration was observed at different time intervals. Thus, sunitinib malate displayed anti-growth and anti-migratory properties in MDA-MB-231 cells [206]. These findings are supported by a study conducted by Sommer *et al*. [207], where they demonstrated reduced migratory capabilities of sunitinib malate-treated breast cancer cells. The postulated mechanism that drives tumour proliferation, migration and invasion are through the autocrine effects of VEGF A/VEGFR-1. Autocrine VEGF A/VEGFR-1 trigger cellular signalling that promotes proliferation, migration, and apoptosis resistance. In contrast with the latter mechanism, a study conducted by Ning *et al*. [175] found that autocrine PIGF /VEGFR1 signalling activates migration and invasion of breast cancer cells; however, VEGF A does not. Nonetheless, inhibiting VEGFR-1 in MDA-MB-231 xenografts result in the suppression of tumour growth and metastasis capacity in athymic nude mice, which is consistent with the findings of the study. Moreover, the binding of VEGF A/VEGFR-1 has been associated with VM formation in aggressive and highly invasive breast cancer cells. This was observed in Interleukin-1β treated MCF-7 and MDA-MB-231 cells, which exhibited VM channel forming capability by upregulating biomarkers associated with VM such as VEGFR-1 through the activation of p38/MAPK and PI3K/AKT signaling pathways [208]. Azad *et al*. [209] confirmed that VEGF A/VEGFR-1/PI3K/MAPK axis promotes VM in MDA-MB-231 cells. Activated PI3K has been correlated with the promotion of metalloproteinase, which degrades and remodels the ECM, promoting VM formation and invasion of tumour cells. In this present study, sunitinib malate attenuated invasion capabilities of aggressive and highly metastatic MDA-MB-231 cells through the 3D ECM by possibly targeting the VEGFR-1/PI3K/MMP axis.

Epithelial cells such as MDA-MB-231 cells undergo a transition to a mesenchymal state to adopt the migratory phenotype. VEGFR-1 triggers EMT in breast cancer cells, increasing the potential for motility, invasiveness, and metastasis of breast cancer cells [175,203]. Vascular endothelial growth factor receptor-1 expression is correlated with low expression of E-cadherin (epithelial marker)

and high N-cadherin (mesenchymal marker) in breast cancer cells [175]. Thus, low E-cadherin expression results in loss of cell-to-cell adhesion, inducing migration and invasion. On the other hand, EMT is associated with elevated VEGF A levels, which play a role in VM formation and apoptosis suppression. In breast cancer cells, EMT process is triggered by VEGFR-1 through the MAPK/ERK 1/2 and PI3K/AKT signalling [203,210]. The PI3K and AKT regulate NF-kβ; this pathway is responsible for the activation of MMP-9. Subsequently, MMP-9 is responsible for cleaving cells adhesion molecules such as E-cadherin and degradation of ECM, promoting invasiveness and VM [210]. Therefore, targeting VEGFR-1 inhibits MAPK/ERK 1/2- and PI3K/AKT/NF-kβ signalling pathways, which exerts an anti-growth effect and abrogates metastasis in breast cancer cells. The decreased migration, invasion and VM capabilities is executed through stabilisation of adherence junction by promoting mesenchymal to epithelial transition (low levels of N-cadherin and high levels of E-cadherin) and downregulation of MMPs [175,210]. This might also be employed by sunitinib malate to inhibit migration and invasion of breast cancer cells in the 3D ECM.

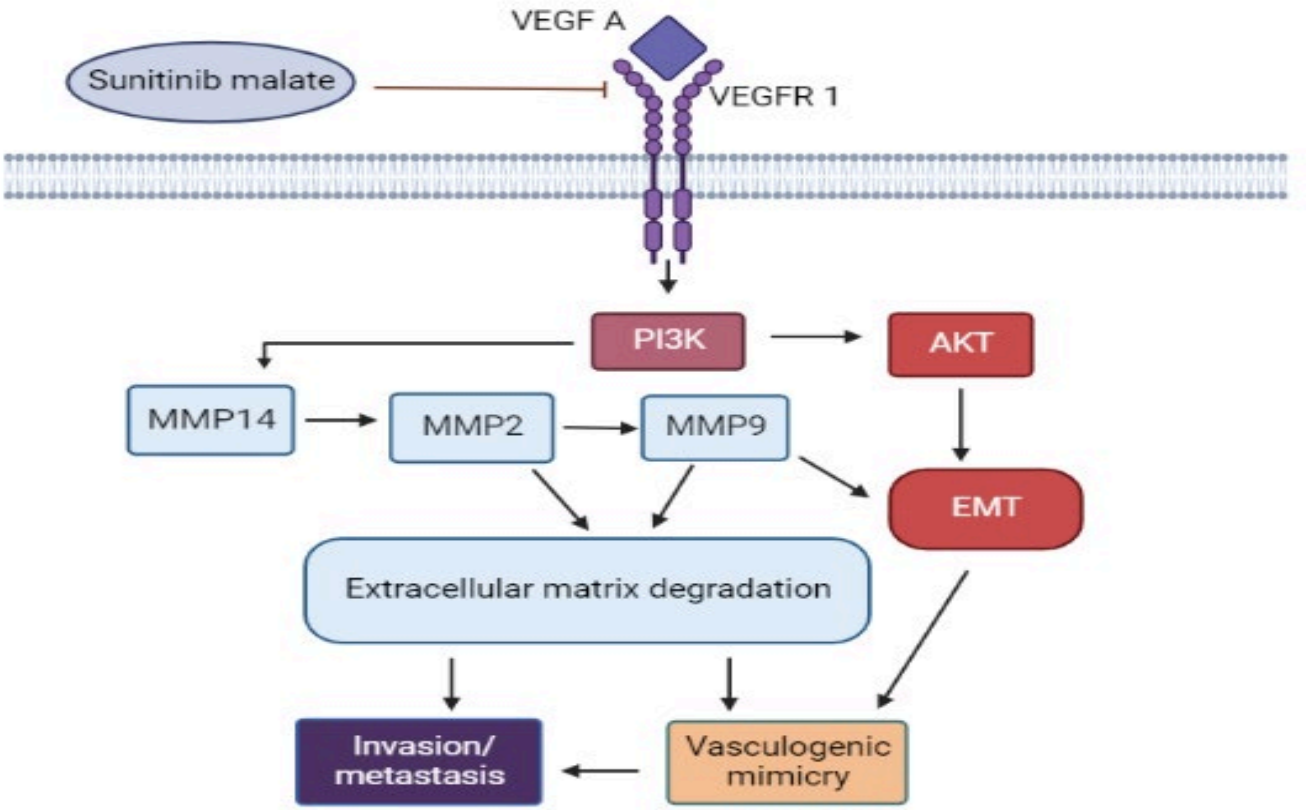

Figure 4.2. Anti-migratory, -invasive and -vasculogenic mimicry properties of sunitinib malate. Binding of vascular endothelial growth factor A (VEGF A) with Vascular endothelial growth factor receptor-1 (VEGFR1), activates the phosphoinositide 3-kinase (PI3K)/ metalloproteinase pathway, which results in the degradation of matrix and induction of epithelial-mesenchymal transition. The former and the latter promote vasculogenic mimicry formation and invasiveness of breast tumours. *Figure drawn by N.P Sekoba using Biorender.*

4.4. Liquid chromatography-mass spectrometry

Metabolomics is a powerful tool used to accurately identify and quantify as many compounds as possible utilising reference standards to achieve the highest level of annotation confidence [211]. However, metabolite quantification and identification are highly challenging due to the varying physical and chemical properties such as polarity, hydrophobicity and solubility [211-212]. Another challenge faced is the lack of a standardised sample preparation and metabolite extraction

protocol, which are imperative for reproducible and comparability of results [213]. In this study, a targeted metabolic profiling method, together with sample preparation and metabolite extraction procedure used for the establishment of the metabolic profile of MDA-MB-231 cells, was partially established. Metabolic profiling of cancer cells is utilised to understand the complex and diverse biology of cancer cells. Different pathways are affected during cancer development, which alters cancer cells' metabolism compared to normal cells. Therefore, metabolic mapping of tumour cells is considered a promising tool in cancer diagnostics [214].

Method development entails the optimisation of the parameters needed for successful identification and chromatography separation [211]. It is imperative to optimise the analytical aspects of the method, the sample preparation and metabolite extraction procedures to ensure the best recovery of the metabolites of interest. The metabolite of interest for this study was glucose-6-phosphate, fructose-6-phosphate, pyruvate, lactate and glutamine, which are intermediates and products of glycolysis and the TCA cycle. To establish identification and determine the retention times of each metabolite, the standards of these metabolites were analysed. Tuning was performed to standardise the MS parameters for each metabolite of interest. Therefore, tuning is done to determine ionisation mode, positive or negative, and identify the precursor and product ion of each metabolite with its corresponding DP and CE value. Each metabolite is tuned separately to ensure the correct production is identified. Therefore, for each metabolite of interest, successful optimisation of MS parameters was achieved in this study.

Liquid chromatography method development entails several factors that have to be optimised to achieve the best separation of the metabolites. Factors include a selection of a column, mobile phase, buffer, pH, gradient slope, flow rate and injection volume. The selection of a column can depend on the polarity of the metabolites [215]. Hydrophobic metabolites are usually separated on a reverse phase column, such as the C18 and hydrophilic metabolites are usually separated on a normal phase column (HILIC column) [216]. In this study, the metabolites of interest are polar

molecules detected in negative ionization mode except for glutamine, which is detected in the positive mode. Therefore, for this study, different columns (C18 amide, IEC QA-825 and Luna HILIC column) were tested to find an appropriate column to separate all the metabolites of interest. The first column tested, a C18 amide column, a reverse column that is highly suited to separate hydrophobic metabolites also hydrophilic metabolites (because of its amide component), resulted in all the metabolites of interest not being retained on the column; therefore, reliable detection was not evident, possibly due to the difference in the ionisation charge of metabolites. As the column is not suitable to separate ionized molecules. Therefore, an ion exchange column (IEC QA-825) was next tested as it uses charge to separate molecules that can be easily ionised. However, the retention of metabolites was not achieved. Lastly, a Luna HILIC column was tested, a column designed to retain and separate polar-ionic compounds from each other. Although retention of metabolites was possible with this column, the retention was not optimal since the elution time was early for some metabolites and separation of isomers of glucose-6-phosphate and fructose-6-phosphate was not achieved. The HILIC column in comparison with the reverse phase column and IEC QA-825 column, achieved retention; therefore it is postulated that a Luna NH2 column which has been shown to produce high peak separation in cancer metabolism, might have the potential to achieve retention and best separation time [217].

Optimisation of the LC/MS/MS method is crucial to enable the detection and measurement of metabolites in breast cancer. Moreover, metabolic profiling comparing conditions such as treated breast tumours and untreated tumours can predict changes in substrate-product flux and possible changes in specific enzyme activity, providing a curative window to the metabolic shift employed by tumours to proliferate.

4.5. ATP and pH

Energy harvested through metabolism sponsors the growth and metastasis of tumours, thus enabling adaptation to change microenvironment for survival purposes [218-219]. The proliferation

rate of breast tumour cells is faster than that of normal cells; therefore not only energy is required but also metabolic intermediates for the biosynthesis of macromolecules [220]. These intermediates are from glycolysis and the truncated TCA cycle, used to synthesise nucleic acids, lipids and proteins, which are vital for tumour growth and proliferation [221]. The rapid proliferation of breast tumours is accompanied by more usage of glycolysis than OXPHOS, as glycolysis generates ATP at a faster rate than OXPHOS, matching the proliferation demands of breast tumours [221-222]. One of the end products of glycolysis is lactate, which is released in the extracellular space contributing to the acidic microenvironment. The acidic extracellular microenvironment is advantageous to tumour cells as it aids in breast tumours' proliferation, invasion and metastasis.

In this study MDA-MB-231 cells utilised an increased amount of ATP compared to MCF-7 cells, due to the high proliferative rate incurred by MDA-MB-231 cells. MCF-7 cells are luminal A subtype which has a slow proliferative rate and are less aggressive. Luminal A exerts a Pasteur and reverses warburg phenotype that does not promote an acidic extracellular environment which was evident in our study where the extracellular pH of MCF-7 cells was higher than that of the MDA-MB-231 cells. This might also contribute to the non-invasive characteristic of MCF-7 cells and the inability to form VM channel formation. Inhibiting VEGFR-1 in MCF-7 cells did not significantly reduce the ATP levels of MCF-7 cells. The VEGF A/VEGFR-1 pathway promotes the Warburg phenotype, thus enhancing glycolysis and favouring lactate production. In MCF-7 cells, estrogen stimulates the TCA cycle and suppresses glycolysis under normal physiological glucose level. Thus, inhibition of enhanced glycolysis through VEGFR-1 does not significantly affect the ATP levels of MCF-7 cells; in addition, MCF-7 cells energy production does not rely on adapting to the Warburg phenotype. Hence, the observed less inhibitory effect by sunitinib malate in MCF-7 cells.

In contrast, MDA-MB-231 cells have high expression of VEGFA/VEGFR1, which correlates to disease aggressiveness [178-179]. The aggressive phenotype of MDA-MB-231 cells is accompanied

by a high glycolytic phenotype, which is associated with extracellular acidosis [116,122,131]. Moreover, the Warburg phenotype is crucial for rapid ATP production, which contributes to the survival of MDA-MB-231 cells. In this present study, sunitinib malate reduced ATP levels in MDA-MB-231 cells, which might be through the inhibition of multi-targeting VEGFRs as VEGF A has been correlated with enhanced glycolytic activity as it upregulates some of the glycolytic enzymes [93,101-102]. Thus, the energy reduction by sunitinib malate in MDA-MB-231 might be through the inhibition of the VEGF A/VEGFR-1 pathway.

Increased glycolysis results in increased lactate production. This decreases the intracellular pH, which is detrimental to cell viability. Thus, to continue proliferating and surviving against decreased intracellular pH, lactate and other end products that contribute to decreased intracellular pH are exported from the tumour cell to maintain the intracellular pH while the extracellular pH becomes acidic. This results in chemoresistance and causes apoptosis in normal cells [122,223]. Therefore, increased proliferation is correlated with increased metabolic activity and decreased extracellular pH [224-225]. In this present study, sunitinib malate-treated MDA-MB-231 cells had minor unit increase in the extracellular pH relative to the untreated cells. The pH increase is postulated to be due to decreased cell proliferation and decreased metabolic activity due to the deprivation of nutrients such as glucose by inhibiting VEGF A/VEGFR-1 pathway. As VEGF A upregulates GLUT 1 transporter and glucose uptake [114]. VEGF A/VEGFR-1 also upregulate lactate fermentation which results in an acidic extracellular environment. Our findings are aligned with other studies, where apoptosis results in increased extracellular pH (reduced acidity) and decreased invasiveness of cancer cells [225-227].

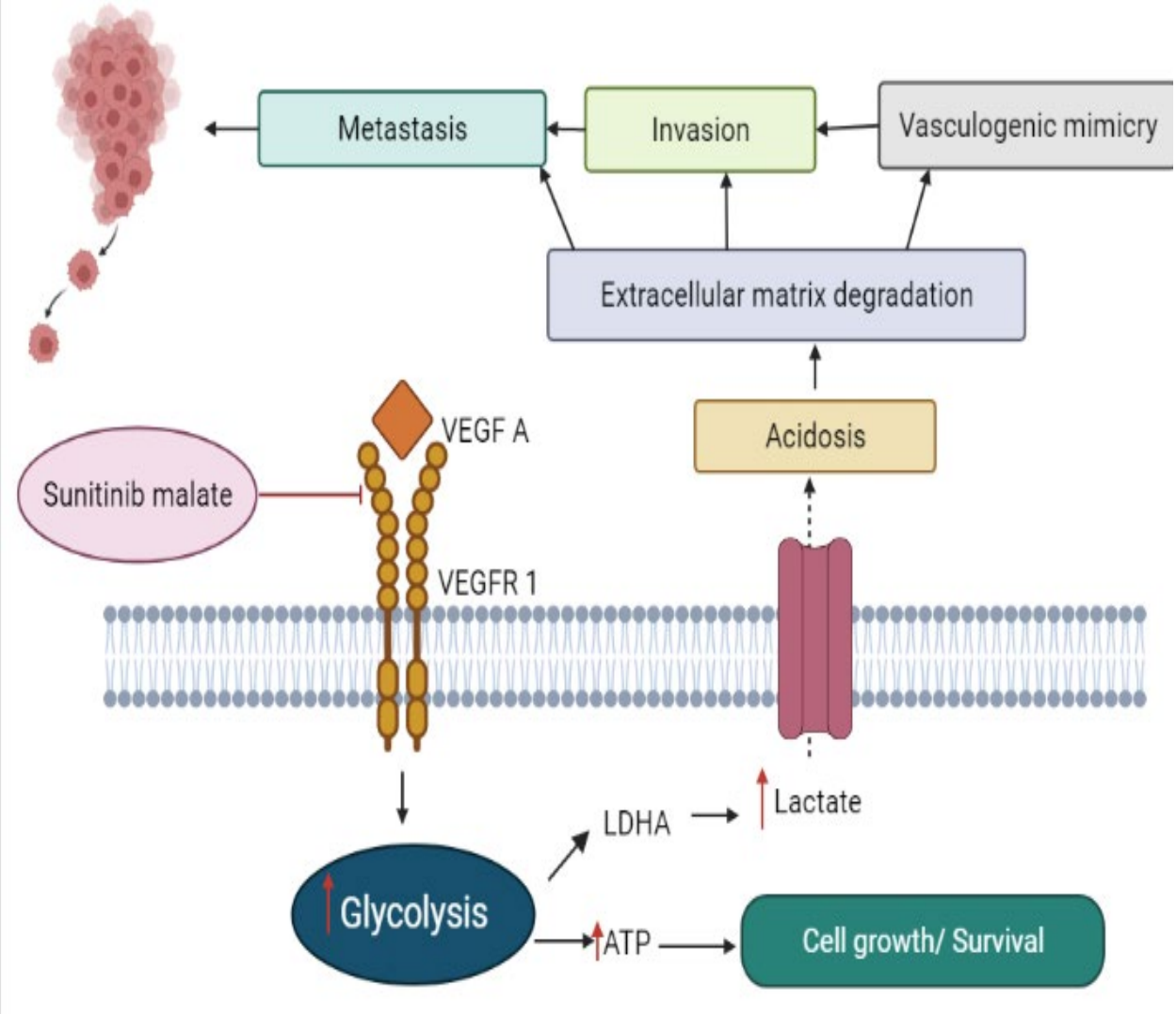

Figure 4.3. Effect of sunitinib malate on the metabolic patterns of MDA-MB-231 cells. Inhibition of the VEGFR-1 signalling pathway attenuates proliferation, migration, and invasion in breast cancer cells by reducing the enhanced glycolytic pathway and the acidity of the extracellular environment. *Figure drawn by N.P Sekoba using Biorender.*

CHAPTER 5: CONCLUSION

This study explored the cytotoxic effect of VEGFR-1 inhibitors on breast cancer cells with the purpose of inhibiting steps associated with VM such as proliferation and migration of cancer cells, their invasion of the extracellular matrix and enhanced metabolism.

The anti-growth effects of VEGFR-1 inhibitors (ZM 306416 and sunitinib malate) on MCF-7 cells and MDA-MB 231 cells were determined using crystal violet assay. Cell viability decrement was noted in MCF-7 cells significantly in a time-dependent manner when treated with sunitinib malate and a decreasing cell viability trend was observed in ZM 306416 treated MCF-7 cells. ZM 306416 reduced MDA-MB-231 cell growth after 72 hours of treatment. On the other hand, sunitinib malate inhibited cell viability to varying degrees, with higher concentrations being more potent in MDA-MB- 231 cells in a dose- and time-dependent manner. ZM 306416 exerts its anti-growth effect by inhibiting the VEGER 1- EGFR synergistic axis while the multi-targeting kinase, sunitinib malate, also targets the VEGFR-1 signalling pathway to exerts its growth inhibitory effect. Therefore, this study highlights the role played by VEGFR-1 in breast tumour growth.

PlasDIC light microscopy was used to examine the morphological alteration in sunitinib malate-treated MDA-MB-231 cells. Sunitinib malate induced morphological features of cell death (apoptosis). Therefore, inhibiting VEGFR-1 pathway provides a potential clinical benefit in the treatment of breast cancer due to the anti-tumour effect associated with VEGFR-1 inhibition.

In this study, inhibiting VEGFR-1 signalling pathway by sunitinib malate attenuated migration and 3D extracellular invasion of breast cancer cells assessed using the scratch wound assay and Boyden chamber assay, respectively. It is postulated that through inhibiting the VEGFR-1/PI3K/MMP axis, sunitinib malate abrogates invasion capabilities of highly metastatic MDA-MB-231 cells through the 3D ECM. Furthermore, inhibiting VEGFR-1 attenuates VEGFR-1-induced EMT in breast cancer cells, promoting migration, invasion and VM. It is postulated that sunitinib

malate, through inhibiting VEGFR-1/MAPK/ERK 1/2 and/or VEGFR-1/ PI3K/ AKT/NF-kβ EMT promoting signalling axis, reduces migration, invasion which are steps that are associated with VM in breast cancer cells. Subsequently, this study highlights the curative potential of inhibiting VEGFR-1 in breast cancer.

Optimisation of MS was achieved (only in terms of its mass ratio) during method development in this study. The ionisation mode of the analytes of interest was determined (glucose-6-phosphate, fructose-6-phosphate, pyruvate, lactate–negative mode and glutamate–positive mode). The DP and CE values of each analyte of interest were also determined. Liquid chromatography optimisation was challenging, although it was noted that analytes of interest in this study should be analysed using the Luna NH2 column to achieve retention and high separation. Overall, it is imperative to optimise LC/MS/MS method to aid in the detection and analysis of metabolites.

To further understand the metabolic energy of breast cancer cells, ATP assay and pH meter were employed to assess ATP and pH levels of breast cancer cells, respectively. In this study, MDA-MB-231 cells had higher levels of ATP than MCF-7 cells due to the aggressive rapid proliferative nature of MDA-MB-231 cells compared to the non-invasive MCF-7 cells. Sunitinib malate treatment did not significantly reduce ATP levels of MCF-7 cells due to the non-dependence of these cells to glycolysis, as VEGFR-1 signalling is associated with the glycolytic phenotype. In contrast, sunitinib malate treatment reduced ATP levels of the glycolysis-addicted MDA-MB-231 cells, possibly by inhibiting the glycolysis-promoting pathway VEGFR-1 signalling pathway. The glycolytic phenotype is associated with an acidic extracellular environment. In this study, treating MCF-7 and MDA-MB-231 cells with sunitinib malate might have reduced the acidic extracellular environment, possibly by inhibiting the VEGFR-1 signalling pathway as it enhances lactate fermentation and increases the acidic extracellular environment.

Overall, inhibition of the VEGFR-1 signalling pathway attenuates cell growth and changes the morphology of breast cancer cells. In addition, inhibiting VEGFR-1 signalling reduces migration

and the 3D-matrix extracellular invasion in breast cancer cells by possibly reducing ATP formation and the acidity of the extracellular environment (**Figure 5.1.**). Therefore, this study has formed the basis for further investigation of VEGFR-1 targeting in reducing VM and altering metabolic patterns in breast cancer to improve the treatment of this disease.

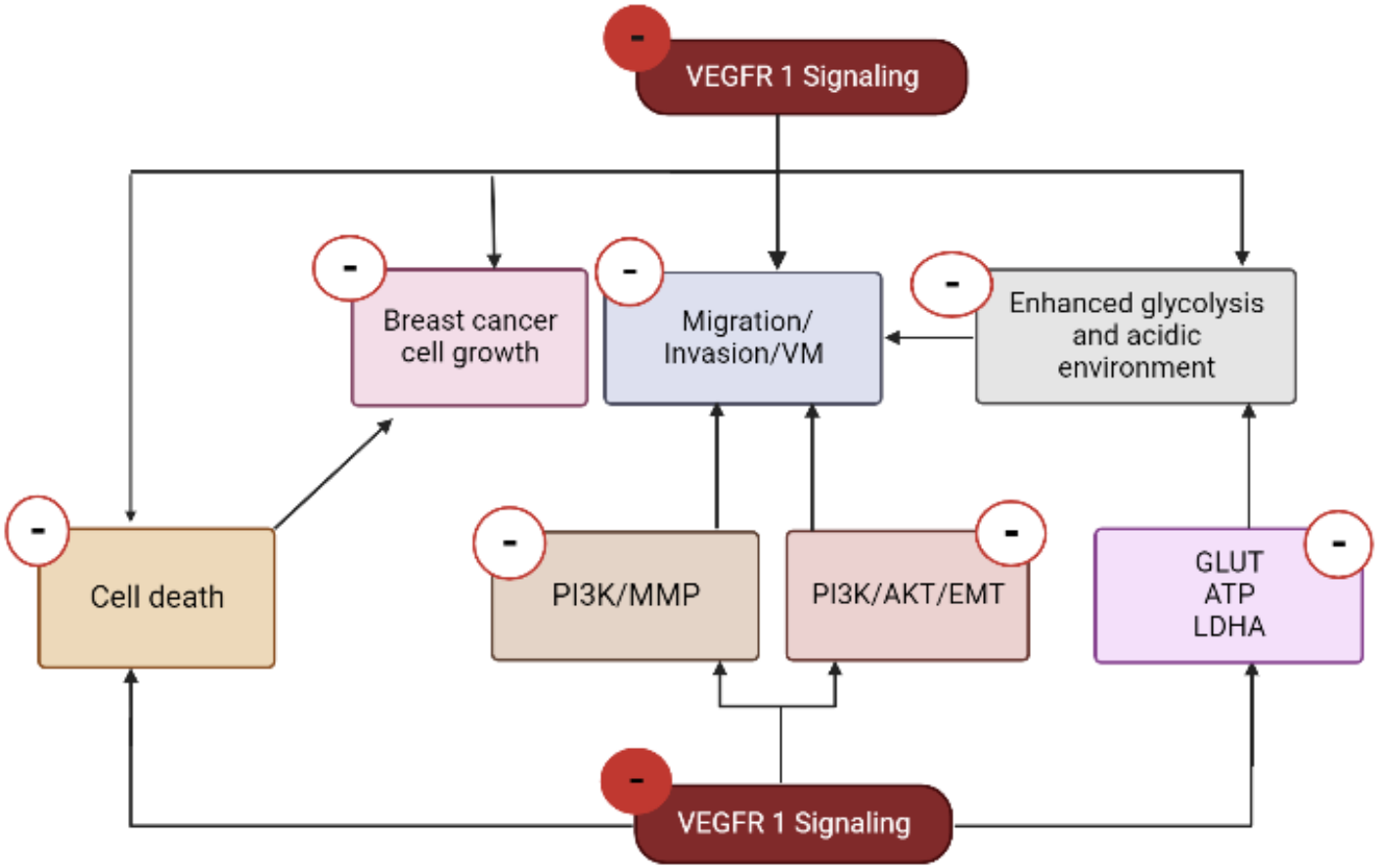

Figure 5.1. The integrative mechanism of inhibiting VEGFR-1 and its effects on the steps that constitute vasculogenic mimicry (growth, migration and invasion) in breast cancer cells. *Figure drawn by N.P Sekoba using Biorender.*

5.1. Future Studies

For future studies it is recommended that cell migration be tested at broad range of concentrations (e.g., 0.1 – 20 µg/mL) to observe the effect of various concentrations including lower concentrations on migration. In this study only the optimal dose was used to investigate the anti-migratory effect of the drug following similar studies.

Further studies are required to detect and analyse metabolites of interest in breast cancer cells using LC-MS/MS. As LC optimisation for the simultaneous detection of the various metabolites was not achieved in this study due to the close elution times, the column (Luna NH_2) may overcome the limitations of this study. Due to time constraints required to acquire the rightful column and the pandemic, further analysis could not be done.

In this study, steps involved in VM were investigated; thus, tube formation, which is the final step in VM, should be investigated to further validate the observed effects. In addition, the western blot should be employed to determine the expression of proteins that regulate these steps, such as VEGF-A, VEGFR-1, PI3K, MMP 14, MMP 2, and MMP 9.

Western blot should also be employed to determine the VEGFR 1 expression before and after treatment. To help support the anti-growth, -migratory and – invasive role it plays in breast cancer cells.

REFERENCES

1. Ferlay J, Shin HR, Bray F, Forman D, Mathers C, Parkin DM. Estimates of worldwide burden of cancer in 2008: Globocan 2008. *International Journal of Cancer*. 2010; 127(12):2893-2917.

2. Sung H, Ferlay J, Siegel RL, Laversanne M, Soerjomataram I, Jemal A, Bray F. Global cancer statistics 2020: Globocan estimates of incidence and mortality worldwide for 36 cancers in 185 countries. CA: A Cancer Journal for Clinicians. doi:https://doi.org/10.3322/caac.21660.

3. Forouzanfar MH, Foreman KJ, Delossantos AM, Lozano R, Lopez AD, Murray CJ, Naghavi M. Breast and cervical cancer in 187 countries between 1980 and 2010: A systematic analysis. *The Lancet*. 2011; 378(9801):1461-1484.

4. Youlden DR, Cramb SM, Dunn NA, Muller JM, Pyke CM, Baade PD. The descriptive epidemiology of female breast cancer: An international comparison of screening, incidence, survival and mortality. *Cancer Epidemiology*. 2012; 36(3):237-248.

5. Azubuike SO, Muirhead C, Hayes L, McNally R. Rising global burden of breast cancer: The case of sub-Saharan Africa (with emphasis on Nigeria) and implications for regional development: A review. *World Journal of Surgical Oncology*. 2018; 16(1):63. doi: https://doi.org/10.1186/s12957-018-1345-2.

6. Rayne S, Schnippel K, Kruger D, Benn C, Firnhaber C. Delay to diagnosis and breast cancer stage in an urban South African breast clinic. *South African Medical Journal*. 2019; 109(3):159-163.

7. Brinton L, Figueroa J, Adjei E, Ansong D, Biritwum R, Edusei L, Nyarko KM, Wiafe S, Yarney J, Addai BW, Awuah B, Clegg-Lamptey JN. Factors contributing to delays in diagnosis of breast cancers in Ghana, West Africa. *Breast Cancer Research and Treatment*. 2017; 162(1):105-114.

8. Bray F, Ferlay J, Soerjomataram I, Siegel RL, Torre LA, Jemal A. Global cancer statistics 2018: Globocan estimates of incidence and mortality worldwide for 36 cancers in 185 countries. *CA: a Cancer Journal for Clinicians*. 2018; 68(6):394-424.

9. Organization WHO. International agency for research on cancer Globocan 2012: Estimated cancer incidence, mortality and prevalence worldwide in 2012. *Lung Cancer*. 2012.

10. Adeloye D, Sowunmi OY, Jacobs W, David RA, Adeosun AA, Amuta AO, Misra S, Gadanya M, Auta A, Harhay MO, Chan KY. Estimating the incidence of breast cancer in Africa: A systematic review and meta-analysis. *Journal of Global Health*. 2018; 8(1). doi:https://doi.org/10.7189%2Fjogh.08.010419.

11. Islam RA, Hossain S, Chowdhury EH. Potential therapeutic targets in energy metabolism pathways of breast cancer. *Current Cancer Drug Targets*. 2017; 17(8):707-721.

12. Place AE, Huh SJ, Polyak K. The microenvironment in breast cancer progression: Biology and implications for treatment. *Breast Cancer Research*. 2011; 13(6):227. doi:https://doi.org/10.1186/bcr2912.

13. Kabel AM, Baali FH. Breast cancer: Insights into risk factors, pathogenesis, diagnosis and management. *Journal of Cancer Research and Treatment.* 2015; 3(2):28-33.

14. Parks R, Derks M, Bastiaannet E, Cheung K. Breast cancer epidemiology. Breast cancer management for surgeons: *Springer*; 2018. p. 19-29.

15. Buckley E, Sullivan T, Farshid G, Hiller J, Roder D. Risk profile of breast cancer following atypical hyperplasia detected through organized screening. *The Breast*. 2015; 24(3):208-212.

16. Hertz-Picciotto I, Adams-Campbell L, Devine P, Eaton D, Hammond S, Helzlsouer K, Hiatt R, Hughes-Halbert C, Hunter D, Kramer B. Breast cancer and the environment: A life course approach: *National Academies. Press Washington, DC*; 2012. doi:https://doi.org/10.17226/13263.

17. Hiatt RA, Brody JG. Environmental determinants of breast cancer. A*nnual Review of Public Health*. 2018; 39:113-133.

18. Petridou ET, Georgakis MK, Antonopoulos CN. Effect of oestrogen exposure, obesity, exercise and diet on breast cancer risk. Breast cancer management for surgeons: *Springer*; 2018. p. 31-42.

19. Khalis M, Charbotel B, Chajes V, Rinaldi S, Moskal A, Biessy C, . Menstrual and reproductive factors and risk of breast cancer: A case-control study in the Fez region, Morocco. *PloS One*. 2018; 13(1). doi:https://doi.org/10.1371/journal.pone.0191333.

20. Ellingjord-Dale M, Vos L, Tretli S, Hofvind S, dos-Santos-Silva I, Ursin G. Parity, hormones and breast cancer subtypes-results from a large nested case-control study in a national screening program. *Breast Cancer Research*. 2017; 19(1):10. doi:https://doi.org/10.1186/s13058-016-0798-x.

21. Soini T, Hurskainen R, Grénman S, Mäenpää J, Paavonen J, Joensuu H, Pukkala E. Levonorgestrel-releasing intrauterine system and the risk of breast cancer: A nationwide cohort study. *Acta Oncologica*. 2016; 55(2):188-192.

22. Jung S, Wang M, Anderson K, Baglietto L, Bergkvist L, Bernstein L, van den Brandt P, Brinton L, Buring JE, Eliassen AH, Falk R, Gapstur SM, Giles GG, Goodman G, Hoffman-Bolten J, Horn-Ross PL, Inoue M, Kolonel LN, Krogh V, Lof M, Maas P, Miller AB, Neuhouser ML, Park Y, Robien K, Rohan TE, Scarmo S, Schouten LJ, Sieri S, Stevens VL, Tsugane S, Visvanathan K, Wilkens LR, Wolk A, Weiderpass E, Willett WC, Zeleniuch-Jacquotte A, Zhang SM, Zhang X, Zeigler RG, Smith-Warner SA. Alcohol consumption and breast cancer risk by estrogen receptor status: In a pooled analysis of 20 studies. *International Journal of Epidemiology*. 2016; 45(3):916-928.

23. Dam MK, Hvidtfeldt UA, Tjønneland A, Overvad K, Grønbæk M, Tolstrup JS. Five year change in alcohol intake and risk of breast cancer and coronary heart disease among postmenopausal women: Prospective cohort study. BMJ. 2016; 353:i2314. doi:https://doi.org/10.1136/bmj.i2314.

24. Turashvili G, Brogi E. Tumor heterogeneity in breast cancer. *Frontiers in Medicine*. 2017; 4:227. doi:https://doi.org/10.3389/fmed.2017.00227.

25. Tang Y, Wang Y, Kiani MF, Wang B. Classification, treatment strategy, and associated drug resistance in breast cancer. *Clinical Breast Cancer*. 2016; 16(5):335-343.

26. Aftimos P, Azim Jr HA, Sotiriou C. Molecular biology of breast cancer. Molecular Pathology: *Elsevier*; 2018. p. 569-588.

27. Bertos NR, Park M. Breast cancer—one term, many entities? *The Journal of Clinical Investigation*. 2011; 121(10):3789-3796.

28. WHO [Internet]. 2021 [cited 2022 July 08]. Available from: https://www.who.int/news-room/fact-sheets/detail/breast-cancer.

29. van Seijen M, Lips EH, Thompson AM, Nik-Zainal S, Futreal A, Hwang ES, Verschuur E, Lane J, Jonkers J, Rea DW, Wesseling J. Ductal carcinoma in situ: To treat or not to treat, that is the question. *British Journal of Cancer*. 2019:1. doi:https://doi.org/10.1038/s41416-019-0478-6.

30. Weigelt B, Geyer FC, Reis-Filho JS. Histological types of breast cancer: How special are they? *Molecular Oncology*. 2010; 4(3):192-208.

31. Lakhani S, Ellis I, Schnitt S, Tan P, van de Vijver M. World Health Organization classification of tumours. WHO classification of tumours of the breast. 2012.

32. Zhang Y, Lv F, Yang Y, Qian X, Lang R, Fan Y, Liu F, Li Y, Li S, Shen B, Pringle GA, Zhang X, Fu L, Guo X. Clinicopathological features and prognosis of metaplastic breast carcinoma: Experience of a major chinese cancer center. *PloS One*. 2015; 10(6):e0131409. doi:https://doi.org/10.1371/journal.pone.0131409.

33. Pradhan A, Paudyal P, Sinha A, Agrawal C. Grading, staging and nottingham prognostic index scoring of breast carcinoma. *Journal of Pathology of Nepal*. 2017; 7(1):1078-1083.

34. Perou CM, Sørlie T, Eisen MB, Van De Rijn M, Jeffrey SS, Rees CA, Pollack JR, Ross DT, Johnsen H, Akslen LA, Øystein F, Pergamenschikov A, Williams C, Zhu SX, Lønning PE, Børresen-Dale A-L, Brown PO, Botstein D. Molecular portraits of human breast tumours. *Nature*. 2000; 406(6797):747-752.

35. Dai X, Cheng H, Bai Z, Li J. Breast cancer cell line classification and its relevance with breast tumor subtyping. *Journal of Cancer*. 2017; 8(16):3131-3141.

36. Hashmi AA, Aijaz S, Khan SM, Mahboob R, Irfan M, Zafar NI, Nisar M, Siddiqui M, Edhi MM, Faridi N, Khan A. Prognostic parameters of luminal A and luminal B intrinsic breast cancer

subtypes of Pakistani patients. *World Journal of Surgical Oncology*. 2018; 16(1):1. doi:https://doi.org/10.1186/s12957-017-1299-9.

37. Soule H, Vazquez J, Long A, Albert S, Brennan M. A human cell line from a pleural effusion derived from a breast carcinoma. Journal of the National Cancer Institute. 1973; 51(5):1409-1416.

38. Li Z-H, Hu P-H, Tu J-H, Yu N-S. Luminal B breast cancer: Patterns of recurrence and clinical outcome. *Oncotarget*. 2016; 7(40):65024-65033.

39. Cheng SH-C, Yu B-L, Horng C-F, Tsai SY, Chen C-M, Chu N-M, Tsou M-H, Lin CKJ, Shih L-S, Liu M-C, . Long-term survival and stage I breast cancer subtypes. *Journal of Cancer Research and Practice*. 2016; 3(1):1-8.

40. Chavez KJ, Garimella SV, Lipkowitz S. Triple negative breast cancer cell lines: One tool in the search for better treatment of triple negative breast cancer. *Breast Disease*. 2010; 32(1-2):35-48.

41. Prat A, Parker JS, Karginova O, Fan C, Livasy C, Herschkowitz JI, He X, Perou CM. Phenotypic and molecular characterization of the claudin-low intrinsic subtype of breast cancer. *Breast Cancer Research*. 2010; 12(5):R68. doi:https://doi.org/10.1186/bcr2635.

42. Welch DR, Hurst DR. Defining the hallmarks of metastasis. *Cancer Research*. 2019; 79(12):3011-3027.

43. Jin K, Li T, van Dam H, Zhou F, Zhang L. Molecular insights into tumour metastasis: Tracing the dominant events. *The Journal of Pathology*. 2017; 241(5):567-577.

44. Meirson T, Genna A, Lukic N, Makhnii T, Alter J, Sharma VP, Wang Y, Samson AO, Condeelis JS, Gil-Henn H. Targeting invadopodia-mediated breast cancer metastasis by using ABL kinase inhibitors. *Oncotarget*. 2018; 9(31):22158-22183.

45. Chung HJ, Mahalingam M. Angiogenesis, vasculogenic mimicry and vascular invasion in cutaneous malignant melanoma–implications for therapeutic strategies and targeted therapies. *Expert Review of Anticancer Therapy*. 2014; 14(5):621-639.

46. Maniotis AJ, Folberg R, Hess A, Seftor EA, Gardner LM, Pe'er J, Trent JM, Meltzer PS, Hendrix MJC. Vascular channel formation by human melanoma cells *in vivo* and *in vitro*: Vasculogenic mimicry. *The American Journal of Pathology*. 1999; 155(3):739-752.

47. Wagenblast E, Soto M, Gutiérrez-Ángel S, Hartl CA, Gable AL, Maceli AR, Erard N, Williams AM, Kim SY, Dickopf S, Harrell JC, Smith AD, Perou CM, Wilkinson JE, Hannon GJ, Knott SRV. A model of breast cancer heterogeneity reveals vascular mimicry as a driver of metastasis. *Nature*. 2015; 520(7547):358-362.

48. Morales-Guadarrama G, García-Becerra R, Méndez-Pérez EA, García-Quiroz J, Avila E, Díaz L. Vasculogenic mimicry in breast cancer: Clinical relevance and drivers. *Cells*. 2021; 10(7):1758. doi:https://doi.org/10.3390/cells10071758.

49. Folberg R, Pe'er J, Gruman LM, Woolson RF, Jeng G, Montague PR, Moninger TO, Yi H, Moore KC. The morphologic characteristics of tumor blood vessels as a marker of tumor progression in primary human uveal melanoma: A matched case-control study. *Human Pathology*. 1992; 23(11):1298-1305.

50. Maniotis AJ, Chen X, Garcia C, DeChristopher PJ, Wu D, Pe'er J, Folberg R. Control of melanoma morphogenesis, endothelial survival, and perfusion by extracellular matrix. L*aboratory Investigation*. 2002; 82(8):1031-1043.

51. Folberg R, Maniotis AJ. Vasculogenic mimicry. *Apmis*. 2004; 112(7-8):508-525.

52. Bissell MJ. Tumor plasticity allows vasculogenic mimicry, a novel form of angiogenic switch: A rose by any other name? *The American Journal of Pathology*. 1999; 155(3):675-679.

53. Barinaga M. New type of blood vessel found in tumors. American Association for the Advancement of Science; 1999. doi:https://doi.org/10.1126/science.285.5433.1475.

54. McDonald DM, Munn L, Jain RK. Vasculogenic mimicry: How convincing, how novel, and how significant? *The American Journal of Pathology*. 2000; 156(2):383-388.

55. Willis RA. Pathology of tumours. Pathology of tumours. 1948-1992.

56. Pötgens A, van Altena MC, Lubsen NH, Ruiter DJ, De Waal R. Analysis of the tumor vasculature and metastatic behavior of xenografts of human melanoma cell lines transfected with vascular permeability factor. *The American Journal of Pathology*. 1996; 148(4):1203-1217.

57. Clarijs R, Otte-Höller I, Ruiter DJ, de Waal RM. Presence of a fluid-conducting meshwork in xenografted cutaneous and primary human uveal melanoma. *Investigative Ophthalmology & Visual Science*. 2002; 43(4):912-918.

58. Ruf W, Seftor EA, Petrovan RJ, Weiss RM, Gruman LM, Margaryan NV, Seftor REB, Miyagi Y, Hendrix MJC. Differential role of tissue factor pathway inhibitors 1 and 2 in melanoma vasculogenic mimicry. *Cancer research*. 2003; 63(17):5381-5389.

59. Tímár J, Tóth J. Tumor sinuses-vascular channels. *Pathology & Oncology Research.* 2000; 6(2):83-86.

60. Shirakawa K, Tsuda H, Heike Y, Kato K, Asada R, Inomata M, Saskai H, Kasumi F, Yoshimoto M, Iwannaga T, Konishi F, Terada M, Wakasugi H. Absence of endothelial cells, central necrosis, and fibrosis are associated with aggressive inflammatory breast cancer. *Cancer Research.* 2001; 61(2):445-451.

61. Shirakawa K, Kobayashi H, Heike Y, Kawamoto S, Brechbiel MW, Kasumi F, Iwanaga T, Konishi F, Terada M, Wakasugi H. Hemodynamics in vasculogenic mimicry and angiogenesis of inflammatory breast cancer xenograft. *Cancer research*. 2002; 62(2):560-566.

62. Ge H, Luo H. Overview of advances in vasculogenic mimicry–a potential target for tumor therapy. *Cancer Management and Research*. 2018; 10:2429-2437.

63. Wagenblast E, Soto M, Gutiérrez-Ángel S, Hartl CA, Gable AL, Maceli AR, Erard N, Williams AM, Kim SY, Dickopf S, Harrell JC, Smith AD, Perou CM, Williknson JE, Hannon GJ, Knott SRV. A model of breast cancer heterogeneity reveals vascular mimicry as a driver of metastasis. *Nature*. 2015; 520(7547):358-362.

64. Sarnella A, D'Avino G, Hill BS, Alterio V, Winum J-Y, Supuran CT, De Simone G, Zannetti A. A novel inhibitor of carbonic anhydrases prevents hypoxia-induced TNBC cell plasticity.

International *Journal of Molecular Sciences.* 2020; 21(21):8405. doi:https://doi.org/10.3390/ijms21218405.

65. Liu T, Sun B, Zhao X, Zhao X, Sun T, Gu Q, Yao Z, Dong XY, Zhao N, Liu N. CD133+ cells with cancer stem cell characteristics associates with vasculogenic mimicry in triple-negative breast cancer. *Oncogene*. 2013; 32(5):544-553.

66. Zhang J-G, Zhou H-M, Zhang X, Mu W, Hu J-N, Liu G-L, Li Q. Hypoxic induction of vasculogenic mimicry in hepatocellular carcinoma: Role of HIF-1 α, Rhoa/ROCK and Rac1/PAK signaling. *BioMed Central Cancer*. 2020; 20(1):1-13.

67. Campbell EJ, Dachs GU, Morrin HR, Davey VC, Robinson BA, Vissers MC. Activation of the hypoxia pathway in breast cancer tissue and patient survival are inversely associated with tumor ascorbate levels. *BioMed Central Cancer*. 2019; 19(1):307. doi:https://doi.org/10.1186/s12885-019-5503-x.

68. Gielata M, Karpińska K, Gwiazdowska A, Boryń Ł, Kobielak A. Catulin reporter marks a heterogeneous population of invasive breast cancer cells with some demonstrating plasticity and participating in vascular mimicry. *Scientific Reports*. 2022; 12(1):1-19.

69. Morales-Guadarrama G, Méndez-Pérez EA, García-Quiroz J, Avila E, García-Becerra R, Zentella-Dehesa A, Larrea F, Diaz L. Endothelium-dependent induction of vasculogenic mimicry in human triple-negative breast cancer cells is inhibited by calcitriol and curcumin. *International Journal of Molecular Sciences*. 2022; 23(14):7659. doi:https://doi.org/10.3390/ijms23147659.

70. Guo Q, Pei X-H, Chu A-J, Guo Y-B, Fan Y-Y, Wang C-H, Zhang S-J, Sun Y-F Wang X. The mechanism of action of Fangji Huangqi Decoction on epithelial-mesenchymal transition in breast cancer using high-throughput next-generation sequencing and network pharmacology. J*ournal of Ethnopharmacology*. 2022; 284:114793. doi:https://doi.org/10.1016/j.jep.2021.114793.

71. Maroufi NF, Amiri M, Dizaji BF, Vahedian V, Akbarzadeh M, Roshanravan N, Haiaty S, Nouri M, Rashidi M-R. Inhibitory effect of melatonin on hypoxia-induced vasculogenic mimicry via

suppressing epithelial-mesenchymal transition (EMT) in breast cancer stem cells. European Journal of Pharmacology. 2020; 881:173282. doi:https://doi.org/10.1016/j.ejphar.2020.173282.

72. Shirakawa K, Wakasugi H, Heike Y, Watanabe I, Yamada S, Saito K, Konishi F. Vasculogenic mimicry and pseudo-comedo formation in breast cancer. *International Journal of Cancer*. 2002; 99(6):821-828.

73. Kirschmann DA, Seftor EA, Hardy KM, Seftor RE, Hendrix MJ. Molecular pathways: Vasculogenic mimicry in tumor cells: Diagnostic and therapeutic implications. *Clinical Cancer Research*. 2012; 18(10):2726-2732.

74. Sun H, Zhang D, Yao Z, Lin X, Liu J, Gu Q, Dong X, Liu F, Wang Y, Yao N, Cheng S, Li L, Sun S. Anti-angiogenic treatment promotes triple-negative breast cancer invasion via vasculogenic mimicry. *Cancer Biology & Therapy*. 2017; 18(4):205-213.

75. Andonegui-Elguera MA, Alfaro-Mora Y, Cáceres-Gutiérrez R, Caro-Sánchez CHS, Herrera LA, Díaz-Chávez J. An overview of vasculogenic mimicry in breast cancer. *Frontiers in Oncology*. 2020; 10:220. doi:https://doi.org/10.3389/fonc.2020.00220.

76. Mitra D, Bhattacharyya S, Alam N, Sen S, Mitra S, Mandal S, Vignesh S, Majumder B, Murmu N. Phosphorylation of EphA2 receptor and vasculogenic mimicry is an indicator of poor prognosis in invasive carcinoma of the breast. *Breast Cancer Research and Treatment*. 2020; 179(2):359-370.

77. Zeng F, Ju R-J, Liu L, Xie H-J, Mu L-M, Zhao Y, Yan Y, Hu Y-J, Wu J-S, Lu W-L. Application of functional vincristine plus dasatinib liposomes to deletion of vasculogenic mimicry channels in triple-negative breast cancer. *Oncotarget*. 2015; 6(34):36625-36642.

78. Zhang X, Zhang J, Zhou H, Fan G, Li Q. Molecular mechanisms and anticancer therapeutic strategies in vasculogenic mimicry. *Journal of Cancer*. 2019; 10(25):6327-6340.

79. Itzhaki O, Greenberg E, Shalmon B, Kubi A, Treves AJ, Shapira-Frommer R, . Nicotinamide inhibits vasculogenic mimicry, an alternative vascularization pathway observed in highly

aggressive melanoma. *Plos One*. 2013; 8(2):e57160. doi:https://doi.org/10.1371/journal.pone.0057160.

80. Xing P, Dong H, Liu Q, Zhao T, Yao F, Xu Y, Chen B, Zheng X, Wu Y, Jin F, Li J. ALDH1 expression and vasculogenic mimicry are positively associated with poor prognosis in patients with breast cancer. *Cellular Physiology and Biochemistry*. 2018; 49(3):961-970.

81. Luo Q, Wang J, Zhao W, Peng Z, Liu X, Li B, Zhang H, Shan B, Zhang C, Duan C. Vasculogenic mimicry in carcinogenesis and clinical applications. J*ournal of Hematology & Oncology*. 2020; 13(1):1-15.

82. Frenkel S, Barzel I, Levy J, Lin A, Bartsch D, Majumdar D, Folberg R, Pe'er J. Demonstrating circulation in vasculogenic mimicry patterns of uveal melanoma by confocal indocyanine green angiography. *Eye*. 2008; 22(7):948-952.

83. Sun H, Yao N, Cheng S, Li L, Liu S, Yang Z, Shang G, Zhang D, Yao Z. Cancer stem-like cells directly participate in vasculogenic mimicry channels in triple-negative breast cancer. *Cancer Biology & Medicine*. 2019; 16(2):299-311.

84. Shen Y, Quan J, Wang M, Li S, Yang J, Lv M, Chen Z, Zhang L, Zhao X, Yang J. Tumor vasculogenic mimicry formation as an unfavorable prognostic indicator in patients with breast cancer. *Oncotarget*. 2017; 8(34):56408-56416.

85. Cao Z, Bao M, Miele L, Sarkar FH, Wang Z, Zhou Q. Tumour vasculogenic mimicry is associated with poor prognosis of human cancer patients: A systemic review and meta-analysis. *European Journal of Cancer*. 2013; 49(18):3914-3923.

86. Liu T, Sun B, Zhao X, Li Y, Gu Q, Dong X, Liu F. OCT4 expression and vasculogenic mimicry formation positively correlate with poor prognosis in human breast cancer. I*nternational Journal of Molecular Sciences*. 2014; 15(11):19634-19649.

87. Hori A, Shimoda M, Naoi Y, Kagara N, Tanei T, Miyake T, Shimazu K, Kim SJ, Noguchi S. Vasculogenic mimicry is associated with trastuzumab resistance of HER2-positive breast cancer. Breast *Cancer Research*. 2019; 21(1):1-18.

88. Andonegui-Elguera MA, Alfaro-Mora Y, Cáceres-Gutiérrez R, Caro-Sánchez CHS, Herrera LA, Díaz-Chávez J. An overview of vasculogenic mimicry in breast cancer. *Frontiers in Oncology*. 2020; 10. doi:https://doi.org/10.3389/fonc.2020.00220.

89. Boroughs LK, DeBerardinis RJ. Metabolic pathways promoting cancer cell survival and growth. *Nature Cell Biology*. 2015; 17(4):351-359.

90. Feichtinger RG, Lang R, Geilberger R, Rathje F, Mayr JA, Sperl W, Bauer JW, Hauser-Krounberger C, Kofler B, Emberger M. Melanoma tumors exhibit a variable but distinct metabolic signature. *Experimental Dermatology*. 2018; 27(2):204-207.

91. Long J-P, Li X-N, Zhang F. Targeting metabolism in breast cancer: How far we can go? World *Journal of Clinical Oncology*. 2016; 7(1):122-130.

92. Kalyanaraman B. Teaching the basics of cancer metabolism: Developing antitumor strategies by exploiting the differences between normal and cancer cell metabolism. *Redox Biology*. 2017; 12:833-842.

93. Yeh W-L, Lin C-J, Fu W-M. Enhancement of glucose transporter expression of brain endothelial cells by vascular endothelial growth factor derived from glioma exposed to hypoxia. *Molecular Pharmacology*. 2008; 73(1):170-177.

94. Penkert J, Ripperger T, Schieck M, Schlegelberger B, Steinemann D, Illig T. On metabolic reprogramming and tumor biology: A comprehensive survey of metabolism in breast cancer. *Oncotarget*. 2016; 7(41):67626-67649.

95. Kharitonov S, Zikiriahodzhaev A, Ermoshchenkova M, Sukhot'ko A, Fedorova M, Pudova E, Alekseev B, Kaprin A, Kudryavtseva A. Hexokinases in breast cancer. *International Journal of Biosciences and Biotechnology*. 2017; 4(2):110-116.

96. Yang T, Ren C, Qiao P, Han X, Wang L, Lv S, Sun Y, Liu Z, Du Y, Yu Z. PIM2-mediated phosphorylation of hexokinase 2 is critical for tumor growth and paclitaxel resistance in breast cancer. *Oncogene*. 2018; 37(45):5997-6009.

97. Sakharkar MK, Shashni B, Sharma K, Dhillon SK, Ranjekar PR, Sakharkar KR. Therapeutic implications of targeting energy metabolism in breast cancer. *PPAR Research*. 2013; 2013. doi:https://doi.org/10.1155/2013/109285.

98. Zhao F, Ming J, Zhou Y, Fan L. Inhibition of Glut1 by WZB117 sensitizes radioresistant breast cancer cells to irradiation. *Cancer Chemotherapy and Pharmacology*. 2016; 77(5):963-972.

99. Peng F, Li Q, Sun J-Y, Luo Y, Chen M, Bao Y. PFKFB3 is involved in breast cancer proliferation, migration, invasion and angiogenesis. *International Journal of Oncology*. 2018; 52(3):945-554.

100. O'Neal J, Clem A, Reynolds L, Dougherty S, Imbert-Fernandez Y, Telang S, Chesney J, Clem BF. Inhibition of 6-phosphofructo-2-kinase (PFKFB3) suppresses glucose metabolism and the growth of HER2+ breast cancer. Breast *Cancer research* and Treatment. 2016; 160(1):29-40.

101. Eelen G, de Zeeuw P, Simons M, Carmeliet P. Endothelial cell metabolism in normal and diseased vasculature. *Circulation Research*. 2015; 116(7):1231-1244.

102. Ronca R, Benkheil M, Mitola S, Struyf S, Liekens S. Tumor angiogenesis revisited: Regulators and clinical implications. Medicinal Research Reviews. 2017; 37(6):1231-1274.

103. Moon J-S, Kim HE, Koh E, Park SH, Jin W-J, Park B-W, Kim K-S. Krüppel-like factor 4 (KLF4) activates the transcription of the gene for the platelet isoform of phosphofructokinase (PFKP) in breast cancer. *Journal of Biological Chemistry.* 2011; 286(27):23808-23816.

104. Huang L, Yu Z, Zhang Z, Ma W, Song S, Huang G. Interaction with pyruvate kinase M2 destabilizes tristetraprolin by proteasome degradation and regulates cell proliferation in breast cancer. *Scientific Reports*. 2016; 6:22449. doi:https://doi.org/10.1038/srep22449.

105. Hsu M-C, Hung W-C, Yamaguchi H, Lim S-O, Liao H-W, Tsai C-H, Hung M-C. Extracellular PKM2 induces cancer proliferation by activating the EGFR signaling pathway. *American Journal of Cancer research*. 2016; 6(3):628-638.

106. Jin L, Zhou Y. Crucial role of the pentose phosphate pathway in malignant tumors. *Oncology Letters*. 2019; 17(5):4213-4221.

107. Choi J, Kim E-S, Koo JS. Expression of pentose phosphate pathway-related proteins in breast cancer. Disease Markers. 2018; 2018. doi:https://doi.org/10.1155/2018/9369358.

108. Meadows AL, Kong B, Berdichevsky M, Roy S, Rosiva R, Blanch HW, Clark DS. Metabolic and morphological differences between rapidly proliferating cancerous and normal breast epithelial cells. *Biotechnology Progress*. 2008; 24(2):334-341.

109. Chen EI, Hewel J, Krueger JS, Tiraby C, Weber MR, Kralli A, Becker K, Yates JR, Felding-Habermann B. Adaptation of energy metabolism in breast cancer brain metastases. *Cancer research*. 2007; 67(4):1472-1486.

110. Golias T, Kery M, Radenkovic S, Papandreou I. Microenvironmental control of glucose metabolism in tumors by regulation of pyruvate dehydrogenase. *International Journal of Cancer*. 2019; 144(4):674-686.

111. Lu H, Forbes RA, Verma A. Hypoxia-inducible factor 1 activation by aerobic glycolysis implicates the warburg effect in carcinogenesis. J*ournal of Biological Chemistry*. 2002; 277(26):23111-23115.

112. Hirschhaeuser F, Sattler UG, Mueller-Klieser W. Lactate: A metabolic key player in cancer. *Cancer research*. 2011; 71(22):6921-5692.

113. Mishra P, Ambs S. Metabolic sig*nature*s of human breast cancer. *Molecular & Cellular Oncology*. 2015; 2(3):e992217. doi:https://doi.org/10.4161/23723556.2014.992217.

114. Azuma M, Shi M, Danenberg KD, Gardner H, Barrett C, Jacques CJ, Sherod A, Iqbal S, El-Khoueiry A, Yang D, Zhang W, Danenberg PV, Lenz H-J. Serum lactate dehydrogenase levels and glycolysis significantly correlate with tumor VEGFA and VEGFR expression in metastatic CRC patients. 2007. doi:https://doi.org/10.2217/14622416.8.12.1705.

115. Lin J, Xia L, Liang J, Han Y, Wang H, Oyang L, Tan S, Tian Y, Rao S, Chen X, Tang Y, Su M, Luo X, Wang Y, Wang H, Zhou Y, Liao Q. The roles of glucose metabolic reprogramming in chemo-and radio-resistance. *Journal of Experimental & Clinical Cancer research.* 2019; 38(1):1-13.

116. Ogrodzinski MP, Bernard JJ, Lunt SY. Deciphering metabolic rewiring in breast cancer subtypes. *Translational Research*. 2017; 189:105-122.

117. Mayers JR, Vander Heiden MG. Famine versus feast: Understanding the metabolism of tumors *in vivo*. *Trends in Biochemical Sciences*. 2015; 40(3):130-140.

118. Corbet C, Feron O. Metabolic and mind shifts: From glucose to glutamine and acetate addictions in cancer. *Current Opinion in Clinical Nutrition & Metabolic Care*. 2015; 18(4):346-353.

119. Gandhi N, Das GM. Metabolic reprogramming in breast cancer and its therapeutic implications. *Cells*. 2019; 8(2):89. doi:https://doi.org/10.3390/cells8020089.

120. Wang L, Zhang S, Wang X. The metabolic mechanisms of breast cancer metastasis. *Frontiers in Oncology*. 2021; 10:2942. doi:https://doi.org/10.3389/fonc.2020.602416.

121. O'Mahony F, Razandi M, Pedram A, Harvey BJ, Levin ER. Estrogen modulates metabolic pathway adaptation to available glucose in breast cancer cells. *Molecular Endocrinology*. 2012; 26(12):2058-5270.

122. Tan J, Le A. The heterogeneity of breast cancer metabolism. The heterogeneity of cancer metabolism: *Springer*, Cham; 2021. p. 89-101.

123. Theodossiou TA, Ali M, Grigalavicius M, Grallert B, Dillard P, Schink KO, Olsen CE, Wȁlchli S, Indernerg EM, Kubin A, Peng Q, Berg K. Simultaneous defeat of MCF7 and MDA-MB-231 resistances by a hypericin PDT–tamoxifen hybrid therapy. *NPJ Breast Cancer*. 2019; 5(1):1-10.

124. Elia I, Schmieder R, Christen S, Fendt S-M. Organ-specific cancer metabolism and its potential for therapy. *Metabolic Control*. 2015:321-353.

125. Martinez-Outschoorn UE, Lin Z, Trimmer C, Flomenberg N, Wang C, Pavlides S, Pestell RG, Howell A, Sotgia F, Lisanti MP. Cancer cells metabolically" fertilize" the tumor microenvironment with hydrogen peroxide, driving the warburg effect: Implications for PET imaging of human tumors. *Cell Cycle*. 2011; 10(15):2504-2520.

126. Martinez-Outschoorn UE, Pavlides S, Whitaker-Menezes D, Daumer KM, Milliman JN, Chiavarina B, Migneco G, Witkiewicz AK, Martinez-Cantarin MP, Flomenberg N, Howell A, Pestell

RG, Lisanti MP, Sotgia F. Tumor cells induce the cancer associated fibroblast phenotype via caveolin-1 degradation: Implications for breast cancer and DCIS therapy with autophagy inhibitors. *Cell Cycle*. 2010; 9(12):2423-2433.

127. Wilde L, Roche M, Domingo-Vidal M, Tanson K, Philp N, Curry J, Martinez-Outschoorn U. Metabolic coupling and the reverse warburg effect in cancer: Implications for novel biomarker and anticancer agent development. *Seminars in Oncology*; 2017; 44(3):198-203.

128. Lunetti P, Di Giacomo M, Vergara D, De Domenico S, Maffia M, Zara V, Capobianco L, Ferramosca A. Metabolic reprogramming in breast cancer results in distinct mitochondrial bioenergetics between luminal and basal subtypes. T*he FEBS journal*. 2019; 286(4):688-709.

129. Choi J, Jung W-H, Koo JS. Metabolism-related proteins are differentially expressed according to the molecular subtype of invasive breast cancer defined by surrogate immunohistochemistry. *Pathobiology*. 2013; 80(1):41-52.

130. Doyen J, Trastour C, Ettore F, Peyrottes I, Toussant N, Gal J, Ilc K, Roux D, Parks SK, Ferrero JM, Pouyssègur J. Expression of the hypoxia-inducible monocarboxylate transporter MCT4 is increased in triple negative breast cancer and correlates independently with clinical outcome. *Biochemical and Biophysical Research Communications*. 2014; 451(1):54-61.

131. Wang Z, Jiang Q, Dong C. Metabolic reprogramming in triple-negative breast cancer. *Cancer Biology & Medicine*. 2020; 17(1):44-59.

132. Sun X, Wang M, Wang M, Yu X, Guo J, Sun T,Li X, Yao L, Dong H, Xu Y . Metabolic reprogramming in triple-negative breast cancer. *Frontiers in oncology*. 2020; 10:428. doi:https://doi.org/10.3389/fonc.2020.00428.

133. Santidrian AF, Matsuno-Yagi A, Ritland M, Seo BB, LeBoeuf SE, Gay LJ, Yagi T, Felding-Habermann B. Mitochondrial complex I activity and NAD+/NADH balance regulate breast cancer progression. *The Journal of Clinical Investigation*. 2013; 123(3):1068-1081.

134. Kim J-W, Tchernyshyov I, Semenza GL, Dang CV. HIF-1-mediated expression of pyruvate dehydrogenase kinase: A metabolic switch required for cellular adaptation to hypoxia. *Cell Metabolism.* 2006; 3(3):177-185.

135. Bhutia YD, Babu E, Ramachandran S, Ganapathy V. Amino acid transporters in cancer and their relevance to “glutamine addiction”: Novel targets for the design of a new class of anticancer drugs. *Cancer research*. 2015; 75(9):1782-1788.

136. Van Geldermalsen M, Wang Q, Nagarajah R, Marshall A, Thoeng A, Gao D, Ritchie W, Feng Y, Bailey CG, Deng N, Harvey K, Beith JM, Selinger CI, O'Toole SA, Rasko JEJ, Holst J. ASCT2/SLC1A5 controls glutamine uptake and tumour growth in triple-negative basal-like breast cancer. *Oncogene*. 2016; 35(24):3201-3208.

137. Yu P, Zhu X, Zhu J-L, Han Y-B, Zhang H, Zhou X, Yang L,Xia Y-Z, Zhang C, Kong L-Y. The Chk2-PKM2 axis promotes metabolic control of vasculogenic mimicry formation in p53-mutated triple-negative breast cancer. *Oncogene*. 2021; 40(34):5262-5274.

138. Li S, Zhang Q, Zhou L, Guan Y, Chen S, Zhang Y, Han X. Inhibitory effects of compound dmbt on hypoxia-induced vasculogenic mimicry in human breast cancer. *Biomedicine & Pharmacotherapy*. 2017; 96:982-992.

139. Tu DG, Yu Y, Lee CH, Kuo YL, Lu YC, Tu CW, Chang W-W. Hinokitiol inhibits vasculogenic mimicry activity of breast cancer stem/progenitor cells through proteasome-mediated degradation of epidermal growth factor receptor. *Oncology Letters*. 2016; 11(4):2934-2940.

140. Maiti A, Qi Q, Peng X, Yan L, Takabe K, Hait NC. Class I histone deacetylase inhibitor suppresses vasculogenic mimicry by enhancing the expression of tumor suppressor and anti-angiogenesis genes in aggressive human TNBC cells. *International Journal of Oncology*. 2019; 55(1):116-130.

141. Ju R-J, Li X-T, Shi J-F, Li X-Y, Sun M-G, Zeng F, Zhou J, Liu L, Zhang C-X, Zhao W-Y, Lu W-L. Liposomes, modified with PTD_{HIV-1} peptide, containing epirubicin and celecoxib, to target vasculogenic mimicry channels in invasive breast cancer. *Biomaterials*. 2014; 35(26):7610-7621.

142. Li F, Shi Y, Zhang Y, Yang X, Wang Y, Jiang K, Hua C, Wu C, Sun C, Qin Y, Liu S. Investigating the mechanism of Xian-ling-lian-xia-fang for inhibiting vasculogenic mimicry in triple negative breast cancer via blocking VEGF/MMPS pathway. *Chinese Medicine*. 2022; 17(1):1-20.

143. Xu M-R, Wei P-F, Suo M-Z, Hu Y, Ding W, Su L, Zhu Y-D, Song W-J, Tang G-H, Zhang M, Li P. Brucine suppresses vasculogenic mimicry in human triple-negative breast cancer cell line MDA-MB-231. BioMedicinal Research International. 2019; 2019. doi:https://doi.org/10.1155/2019/6543230.

144. Song L, Tang L, Lu D, Hu M, Liu C, Zhang H, Zhao Y, Liu D, Zhang S. Sinomenine inhibits vasculogenic mimicry and migration of breast cancer side population cells via regulating miR-340-5p/SIAH2 axis. *BioMedicinal Research International*. 2022; 2022. doi:https://doi.org/10.1155/2022/4914005.

145. Haiaty S, Rashidi M-R, Akbarzadeh M, Bazmani A, Mostafazadeh M, Nikanfar S, Zibaei Z, Rahbarghazi R, Nouri M. Thymoquinone inhibited vasculogenic capacity and promoted mesenchymal-epithelial transition of human breast cancer stem cells. *BioMed Central Complementary Medicine and Therapies*. 2021; 21(1):1-12.

146. Bajbouj K, Al-Ali A, Shafarin J, Sahnoon L, Sawan A, Shehada A, Elkhalifa W, Saber-Ayad M, Muhammed JS, Elmosehli AB, Guraya SY, Hamad M. Vitamin D exerts significant antitumor effects by suppressing vasculogenic mimicry in breast cancer cells. *Frontiers in Oncology*. 2022; 12. doi:https://doi.org/10.3389%2Ffonc.2022.918340.

147. [Internet]. Men1611 with trastuzumab (+/- fulvestrant) in metastatic breast cancer (B-precise-01). 2018. Available from: https://clinicaltrials.gov/ct2/show/NCT03767335.

148. Garrido-Castro AC, Saura C, Barroso-Sousa R, Guo H, Ciruelos E, Bermejo B, Gavilà J, Serra V, Prat A, Parè L, Cèliz P, Villagrasa P, Li Y, Savoie J, Xu Z, Arteaga CL, Krop IE, Solit DB, Mills GB, Cantley LC, Winer EP, Lin NU, Rodon J. Phase 2 study of buparlisib (BKM120), a pan-class I PI3K inhibitor, in patients with metastatic triple-negative breast cancer. *Breast Cancer Research*. 2020; 22(1):1-13.

149. Kagihara JA, Corr B, Pacheco JM, Davis SL, Lieu CH, Kim SS, Jimeno A, Hiem AM, DeMattei JA, Gordon G, Triplett TA, Eckhardt G, WInkler JD, Piscopio AD, Diamond JR. Phase 1 study of OKI-179, an oral class 1-selective depsipeptide HDAC inhibitor, in patients with advanced solid tumors: Final results. *Wolters Kluwer Health*; 2021. doi:10.1200/JCO.2021.39.15_suppl.3075.

150. Lynce F, Williams JT, Regan MM, Bunnell CA, Freedman RA, Tolaney SM, Chen WY, Mayer EL, Partridge AH, Winer EP, Overmoyer B. Phase I study of JAK1/2 inhibitor ruxolitinib with weekly paclitaxel for the treatment of HER2-negative metastatic breast cancer. *Cancer Chemotherapy and Pharmacology*. 2021; 87(5):673-679.

151. McDonald PC, Chia S, Bedard PL, Chu Q, Lyle M, Tang L, Singh M, Zhang Z, Supuran CT, Renouf DJ, Dedhar S. A phase 1 study of SLC-0111, a novel inhibitor of carbonic anhydrase IX, in patients with advanced solid tumors. *American Journal of Clinical Oncology*. 2020; 43(7):484-490.

152. Gerber DE. Targeted therapies: A new generation of cancer treatments. *American Family Physician*. 2008; 77(3) :311-319.

153. Ryman JT, Meibohm B. Pharmacokinetics of monoclonal antibodies. CPT: *Pharmacometrics & Systems Pharmacology*. 2017; 6(9):576-588.

154. Kamath AV. Translational pharmacokinetics and pharmacodynamics of monoclonal antibodies. Drug Discovery Today: *Technologies.* 2016; 21:75-83.

155. Xue C, Gudkov A, Haber M, Norris MD. Small molecule drugs and targeted therapies for neuroblastoma. *Neuroblastoma: Present and Future*. 2012:299.

156. Chow LQ, Eckhardt SG. Sunitinib: From rational design to clinical efficacy. J*ournal of Clinical Oncology*. 2007; 25(7):884-896.

157. Telli M, Witteles R, Fisher G, Srinivas S. Cardiotoxicity associated with the cancer therapeutic agent sunitinib malate. *Annals of Oncology*. 2008; 19(9):1613-1618.

158. Kim A, Balis FM, Widemann BC. Sorafenib and sunitinib. *The Oncologist*. 2009; 14(8):800-805.

159. Kim S, Chen J, Cheng T, Gindulyte A, He J, He S, Li Q, Shoemaker B, Theissen PA, Yu B, Zaslavsky L, Zhang J, Bolten EE. Pubchem in 2021: New data content and improved web interfaces. *Nucleic Acids Research*. 2021; 49(D1):D1388-D1395.

160. Welsh J. Animal models for studying prevention and treatment of breast cancer. Animal models for the study of human disease: *Elsevier*; 2013. p. 997-1018.

161. Piccinini F, Tesei A, Arienti C, Bevilacqua A. Cell counting and viability assessment of 2D and 3D cell cultures: Expected reliability of the trypan blue assay. Biological procedures online. 2017; 19(1):1-12.

162. Feoktistova M, Geserick P, Leverkus M. Crystal violet assay for determining viability of cultured cells. *Cold Spring Harbor Protocols*. 2016; 2016(4):pdb. prot087379.

163. Danz R, Vogelgsang A, Käthner R. PLASDIC–a useful modification of the differential interference contrast according to Smith/Nomarski in transmitted light arrangement. *Photonik*. 2004; 1:42.

164. Rathi S, Zoubek N, Zagarese VJ, Johnson DS. Differential interference contrast microscopy with adjustable plastic sanderson prisms. *Applied Optics*. 2020; 59(11):3404-3410.

165. Hulkower KI, Herber RL. Cell migration and invasion assays as tools for drug discovery. *Pharmaceutics*. 2011; 3(1):107-124.

166. Pinto BI, Cruz ND, Lujan OR, Propper CR, Kellar RS. *In vitro* scratch assay to demonstrate effects of arsenic on skin cell migration. *Journal of Visualised Experiments*. 2019; (144):e58838. doi:10.3791/58838.

167. Justus CR, Leffler N, Ruiz-Echevarria M, Yang LV. *In vitro* cell migration and invasion assays. *Journal of Visualized Experiments*. 2014; (88):e51046. doi:https://dx.doi.org/10.3791/51046.

168. Marshall J. Transwell® invasion assays. *Cell migration: Springer*; 2011. p. 97-110.

169. Kim Y, Friedman A. Interaction of tumor with its micro-environment: A mathematical model. Bulletin of Mathematical Biology. 2010; 72(5):1029-1068.

170. Pitt JJ. Principles and applications of liquid chromatography-mass spectrometry in clinical biochemistry. *The Clinical Biochemist Reviews*. 2009; 30(1):19-34.

171. Hannah R, Beck M, Moravec R, Riss T. Celltiter-glo™ luminescent cell viability assay: A sensitive and rapid method for determining cell viability. *Promega Cell Notes*. 2001; 2:11-13.

172. Lomakina GY, Modestova YA, Ugarova N. Bioluminescence assay for cell viability. Biochemistry (Moscow). 2015; 80(6):701-713.

173. Karastogianni S, Girousi S, Sotiropoulos S. Ph: Principles and measurement. T*he Encyclopedia of Food and Health*. 2016; 4:333-338.

174. Lacal PM, Graziani G. Therapeutic implication of vascular endothelial growth factor receptor-1 (VEGFR-1) targeting in cancer cells and tumor microenvironment by competitive and non-competitive inhibitors. *Pharmacological Research*. 2018; 136:97-107.

175. Ning Q, Liu C, Hou L, Meng M, Zhang X, Luo M, Shao S, Zuo X, Zhao X. Vascular endothelial growth factor receptor-1 activation promotes migration and invasion of breast cancer cells through epithelial-mesenchymal transition. *Plos One*. 2013; 8(6):e65217. doi:https://doi.org/10.1371/journal.pone.0065217.

176. Srabovic N, Mujagic Z, Mujanovic-Mustedanagic J, Softic A, Muminovic Z, Rifatbegovic A, Begic L. Vascular endothelial growth factor receptor-1 expression in breast cancer and its correlation to vascular endothelial growth factor A. *International Journal of Breast Cancer*. 2013; 2013. doi:https://doi.org/10.1155/2013/746749.

177. Seki T, Hosaka K, Fischer C, Lim S, Andersson P, Abe M, Iwamoto H, Gao Y, Wang X, Fong G-H, Cao Y. Ablation of endothelial VEGFR1 improves metabolic dysfunction by inducing adipose tissue browning. *Journal of Experimental Medicine*. 2018; 215(2):611-626.

178. Ceci C, Atzori MG, Lacal PM, Graziani G. Role of VEGFS/VEGFR-1 signaling and its inhibition in modulating tumor invasion: Experimental evidence in different metastatic cancer

models. *International Journal of Molecular Sciences*. 2020; 21(4):1388. doi:https://doi.org/10.3390/ijms21041388.

179. Weigand M, Hantel P, Kreienberg R, Waltenberger J. Autocrine vascular endothelial growth factor signalling in breast cancer. Evidence from cell lines and primary breast cancer cultures *in vitro*. *Angiogenesis*. 2005; 8(3):197-204.

180. Perrot-Applanat M, Di Benedetto M. Autocrine functions of VEGF in breast tumor cells: Adhesion, survival, migration and invasion. *Cell Adhesion & Migration*. 2012; 6(6):547-553.

181. Linardou H, Kalogeras KT, Kronenwett R, Alexopoulou Z, Wirtz RM, Zagouri F, Scopa CD, Gogas H, Petraki K, Christodoulou C, Pavlakis K, Koutras AK, Samantas E, Patsea H, Pectasides D, Bafaloukos D, Fountzilas G. Prognostic significance of VEGFC and VEGFR1 mRNA expression according to HER2 status in breast cancer: A study of primary tumors from patients with high-risk early breast cancer participating in a randomized hellenic cooperative oncology group trial. Anti*cancer research*. 2015; 35(7):4023-4036.

182. Bando H, Weich H, Brokelmann M, Horiguchi S, Funata N, Ogawa T, Toi M. Association between intratumoral free and total VEGF, soluble VEGFR-1, VEGFR-2 and prognosis in breast cancer. *British Journal of Cancer.* 2005; 92(3):553-561.

183. Hossein-Nejad-Ariani H, Althagafi E, Kaur K. Small peptide ligands for targeting EGFR in triple negative breast cancer cells. *Scientific Reports*. 2019; 9(1):1-10.

184. Masuda H, Zhang D, Bartholomeusz C, Doihara H, Hortobagyi GN, Ueno NT. Role of epidermal growth factor receptor in breast cancer. *Breast Cancer research and Treatment*. 2012; 136(2):331-345.

185. Nagano H, Tomida C, Yamagishi N, Teshima-Kondo S. VEGFR-1 regulates EGF-R to promote proliferation in colon cancer cells. *International Journal of Molecular Sciences*. 2019; 20(22):5608. doi:https://doi.org/10.3390/ijms20225608.

186. Oshi M, Gandhi S, Tokumaru Y, Yan L, Yamada A, Matsuyama R, Ishikawa T, Endo I, Tabake K. Conflicting roles of egfr expression by subtypes in breast cancer. *American Journal of Cancer Research*. 2021; 11(10):5094-5110.

187. Chan SK, Hill ME, Gullick WJ. The role of the epidermal growth factor receptor in breast cancer. J*ournal of Mammary Gland Biology and Neoplasia*. 2006; 11(1):3-11.

188. Knowlden JM, Hutcheson IR, Jones HE, Madden T, Gee JM, Harper ME, Barrow D, Wakeling AE, Nicholson RI. Elevated levels of epidermal growth factor receptor/c-erbB2 heterodimers mediate an autocrine growth regulatory pathway in tamoxifen-resistant MCF-7 cells. *Endocrinology*. 2003; 144(3):1032-1044.

189. Young E, Miele L, Tucker KB, Huang M, Wells J, Gu J-W. SU11248, a selective tyrosine kinases inhibitor suppresses breast tumor angiogenesis and growth via targeting both tumor vasculature and breast cancer cells. *Cancer Biology & Therapy*. 2010; 10(7):703-711.

190. Ghimirey N, Steele C, Czerniecki BJ, Koski GK, Showalter LE. Sunitinib combined with Th1 cytokines potentiates apoptosis in human breast cancer cells and suppresses tumor growth in a murine model of HER-2^{pos} breast cancer. *International Journal of Breast Cancer*. 2021; 2021. doi:https://doi.org/10.1155/2021/8818393.

191. Wu Y, Hooper AT, Zhong Z, Witte L, Bohlen P, Rafii S, Hicklin DJ. The vascular endothelial growth factor receptor (VEGFR-1) supports growth and survival of human breast carcinoma. *International Journal of Cancer*. 2006; 119(7):1519-1529.

192. Lee T-H, Seng S, Sekine M, Hinton C, Fu Y, Avraham HK, Avraham S, . Vascular endothelial growth factor mediates intracrine survival in human breast carcinoma cells through internally expressed VEGFR1/FLT1. PLoS *Medicine*. 2007; 4(6):e186. doi:https://doi.org/10.1371/journal.pmed.0040186.

193. Chinchar E, Makey KL, Gibson J, Chen F, Cole SA, Megason GC, Vijayakumar S, Miele L, Gu J-W. Sunitinib significantly suppresses the proliferation, migration, apoptosis resistance,

tumor angiogenesis and growth of triple-negative breast cancers but increases breast cancer stem cells. Vascular Cell. 2014; 6(1):1-12.

194. Garuti L, Roberti M, Bottegoni G. Multi-kinase inhibitors. *Current Medicinal Chemistry*. 2015; 22(6):695-712.

195. Yan J-D, Liu Y, Zhang Z-Y, Liu G-Y, Xu J-H, Liu L-Y, *et al*. Expression and prognostic significance of vegfr-2 in breast cancer. Pathology-Research and Practice. 2015; 211(7):539-43.

196. Carvalho I, Milanezi F, Martins A, Reis RM, Schmitt F. Overexpression of platelet-derived growth factor receptor α in breast cancer is associated with tumour progression. *Breast Cancer Research*. 2005; 7(5):1-8.

197. Kim S, You D, Jeong Y, Yoon SY, Kim SA, Lee JE. Inhibition of platelet-derived growth factor receptor synergistically increases the pharmacological effect of tamoxifen in estrogen receptor α positive breast cancer. *Oncology Letters*. 2021; 21(4):1-8.

198. Saraste A, Pulkki K. Morphologic and biochemical hallmarks of apoptosis. *Cardiovascular Research*. 2000; 45(3):528-537.

199. Korashy HM, Maayah ZH, Al Anazi FE, Alsaad AM, Alanazi IO, Belali OM, *et al*. Sunitinib inhibits breast cancer cell proliferation by inducing apoptosis, cell-cycle arrest and DNA repair while inhibiting NF-κB signaling pathways. *Anticancer research*.. 2017; 37(9):4899-909.

200. Ni H, Guo M, Zhang X, Jiang L, Tan S, Yuan J, *et al*. Vegfr2 inhibition hampers breast cancer cell proliferation via enhanced mitochondrial biogenesis. *Cancer Biology & Medicine*. 2021; 18(1):139.

201. Wechman SL, Emdad L, Sarkar D, Das SK, Fisher PB. Vascular mimicry: Triggers, molecular interactions and *in vivo* models. *Advances in Cancer research*. 2020; 148:27-67.

202. Krakhmal NV, Zavyalova M, Denisov E, Vtorushin S, Perelmuter V. Cancer invasion: Patterns and mechanisms. *Acta Naturae*. 2015; 7(2 (25)):17-28.

203. Xu W, Yang Z, Lu N. A new role for the PI3K/Akt signaling pathway in the epithelial-mesenchymal transition. *Cell Adhesion & Migration*. 2015; 9(4):317-324.

204. Babina IS, McSherry EA, Donatello S, Hill AD, Hopkins AM. A novel mechanism of regulating breast cancer cell migration via palmitoylation-dependent alterations in the lipid raft affiliation of CD44. *Breast Cancer Research*. 2014; 16(1):1-14.

205. Ring A, Kaur P, Lang JE. Ep300 knockdown reduces cancer stem cell phenotype, tumor growth and metastasis in triple negative breast cancer. *BioMed Central Cancer*. 2020; 20(1):1-14.

206. Stalker L, Pemberton J, Moorehead RA. Inhibition of proliferation and migration of luminal and claudin-low breast cancer cells by pdgfr inhibitors. *Cancer Cell International*. 2014; 14(1):1-9.

207. Sommer AK, Falcenberg M, Ljepoja B, Fröhlich T, Arnold GJ, Wagner E, et al. Downregulation of GRK5 hampers the migration of breast cancer cells. *Scientific report.* 2019; 9(1):15548.

208. Nisar MA, Zheng Q, Saleem MZ, Ahmmed B, Ramzan MN, Ud Din SR, Tahir N, Liu S, Yan Q. Il-1β promotes vasculogenic mimicry of breast cancer cells through p38/MAPK and PI3K/Akt signaling pathways. *Frontiers in Oncology*. 2021; 11:618839. doi:https://doi.org/10.3389/fonc.2021.618839.

209. Azad T, Janse van Rensburg H, Lightbody E, Neveu B, Champagne A, Ghaffari A, Kay VR, Hao Y, Shen H, Yeung B, Croy BA, Guan KL, Pouliot F, Zhang J, Nicol CJB, Yang X. A LATS biosensor screen identifies VEGFR as a regulator of the hippo pathway in angiogenesis. *Nature Communications*. 2018; 9(1):1-15.

210. Sadremomtaz A, Kobarfard F, Mansouri K, Mirzanejad L, Asghari SM. Suppression of migratory and metastatic pathways via blocking VEGFR1 and VEGFR2. *Journal of Receptors and Signal Transduction*. 2018; 38(5-6):432-441.

211. Liu Q, Cai J, Nichols RG, Tian Y, Zhang J, Smith PB, . A quantitative HILIC–MS/MS assay of the metabolic response of Huh-7 cells exposed to 2, 3, 7, 8-tetrachlorodibenzo-p-dioxin. Metabolites. 2019; 9(6):118. doi:https://doi.org/10.3390/metabo9060118.

212. Rahman AMA, Pawling J, Ryczko M, Caudy AA, Dennis JW. Targeted metabolomics in cultured cells and tissues by mass spectrometry: Method development and validation. *Analytica Chimica Acta*. 2014; 845:53-61.

213. Bino RJ, Hall RD, Fiehn O, Kopka J, Saito K, Draper J, Nikolau BJ, Mendes P, Roessner-Tunali U, Beale MH, Trethewey RN, Lange BM, Wurtele ES, Summer LW. Potential of metabolomics as a functional genomics tool. *Trends in Plant Science*. 2004; 9(9):418-425.

214. Semreen MH, Alniss HY, Grgic SR, El-Awady RA, Almehdi AH, Mousa MK, Hamoudi RA. Comparative metabolomics of MCF-7 breast cancer cells using different extraction solvents assessed by mass spectroscopy. *Scientific Reports*. 2019; 9(1):1-9.

215. Jandera P. Stationary and mobile phases in hydrophilic interaction chromatography: A review. *Analytica Chimica Acta*. 2011; 692(1-2):1-25.

216. Sandi A, Bede A, Szepesy L, Rippel G. Characterization of different RP-HPLC columns by a gradient elution technique. *Chromatographia.* 1997; 45(1):206-214.

217. Yuan M, Breitkopf SB, Yang X, Asara JM. A positive/negative ion–switching, targeted mass spectrometry–based metabolomics platform for bodily fluids, cells, and fresh and fixed tissue. *Nature Protocols*. 2012; 7(5):872-881.

218. Peers C, Brahimi-Horn MC, Pouysségur J. Hypoxia in cancer cell metabolism and pH regulation. *Essays in Biochemistry*. 2007; 43:165-178.

219. Block KI, Gyllenhaal C, Lowe L, Amedei A, Amin AR, Amin A, Aqulino K, Arbiser J, Arreola A, Arzumanyan A, Ashraf SS, Azmi AS, Benencia F, Bhakta D, Bilsland A, Bishayee A, Blain WS, Block PB, Boosani CS, Carey TE, Zollo M. Designing a broad-spectrum integrative approach for cancer prevention and treatment. *Seminars in Cancer Biology*; 2015;25:S276-S304.

220. Abdel-Wahab AF, Mahmoud W, Al-Harizy RM. Targeting glucose metabolism to suppress cancer progression: Prospective of anti-glycolytic cancer therapy. *Pharmacological Research*. 2019; 150:104511. doi:https://doi.org/10.1016/j.phrs.2019.104511.

221. Lunt SY, Vander Heiden MG. Aerobic glycolysis: Meeting the metabolic requirements of cell proliferation. 2011; 27(1):441-464.

222. Zheng J. Energy metabolism of cancer: Glycolysis versus oxidative phosphorylation. *Oncology Letters*. 2012; 4(6):1151-1157.

223. Chen C-L, Chu J-S, Su W-C, Huang S-C, Lee W-Y. Hypoxia and metabolic phenotypes during breast carcinogenesis: Expression of hif-1α, glut1, and caix. *Virchows Archiv*. 2010; 457(1):53-61.

224. Wike-Hooley J, Haveman J, Reinhold H. The relevance of tumour ph to the treatment of malignant disease. *Radiotherapy and Oncology*. 1984; 2(4):343-66.

225. Tavares-Valente D, Sousa B, Schmitt F, Baltazar F, Queirós O. Disruption of ph dynamics suppresses proliferation and potentiates doxorubicin cytotoxicity in breast cancer cells. *Pharmaceutics*. 2021; 13(2):242.

226. Matuszcak C, Lindner K, Haier J, Hummel R. Proton pump inhibitors as chemosensitizer: New indication for a well-known medication. *Cancer Cell & Microenvironment*. 2015; 2

227. Moellering RE, Black KC, Krishnamurty C, Baggett BK, Stafford P, Rain M, *et al*. Acid treatment of melanoma cells selects for invasive phenotypes. *Clinical & experimental metastasis.* 2008; 25(4):411-25.

Appendix I: PhD committee letter

UNIVERSITEIT VAN PRETORIA
UNIVERSITY OF PRETORIA
YUNIBESITHI YA PRETORIA

Faculty of Health Sciences

14 May 2019

Dr P Mabeta
Department of Physiology
Faculty of Health Sciences

Dear Dr P Mabeta

STUDENT: SEKOBA N (PHD PHYSIOLOGY)

TITLE: Effects of vascular endothelial growth factor receptor-1 inhibition on vasculogenic mimicry and the metabolic profile of breast cancer cells *in vitro*

The above-mentioned student's protocol has been approved by the PhD committee.

We wish the student all the best with her studies.

Kind regards

PROF V STEENKAMP
CHAIR: PhD COMMITTEE

Pharmacology Dept., BMS Building
University of Pretoria, Private Bag X323
Arcadia 0007, South Africa
Tel +27 (0)12 319 2254
Email: vanessa.steenkamp@up.ac.za

Fakulteit Gesondheidswetenskappe
Lefapha la Disaense tša Maphelo

Appendix II: Ethics letter

UNIVERSITEIT VAN PRETORIA
UNIVERSITY OF PRETORIA
YUNIBESITHI YA PRETORIA

Faculty of Health Sciences

Institution: The Research Ethics Committee, Faculty Health Sciences, University of Pretoria complies with ICH-GCP guidelines and has US Federal wide Assurance.

- FWA 00002567, Approved dd 18 March 2022 and Expires 18 March 2027.
- IORG #: IORG0001762 OMB No. 0990-0278 Approved for use through August 31, 2023.

Faculty of Health Sciences **Research Ethics Committee**

20 May 2022

Approval Certificate
Annual Renewal

Dear Ms NP Sekoba,

Ethics Reference No.: 348/2019 – Line 3
Title: Effects of vascular endothelial growth factor receptor-1 inhibition on vasculogenic mimicry and the metabolic profile of breast cancer cells in vitro

The **Annual Renewal** as supported by documents received between 2022-04-13 and 2022-05-20 for your research, was approved by the Faculty of Health Sciences Research Ethics Committee on 2022-05-20 as resolved by its quorate meeting.

Please note the following about your ethics approval:

- Renewal of ethics approval is valid for 1 year, subsequent annual renewal will become due on 2023-05-20.
- Please remember to use your protocol number (348/2019) on any documents or correspondence with the Research Ethics Committee regarding your research.
- Please note that the Research Ethics Committee may ask further questions, seek additional information, require further modification, monitor the conduct of your research, or suspend or withdraw ethics approval.

Ethics approval is subject to the following:

- The ethics approval is conditional on the research being conducted as stipulated by the details of all documents submitted to the Committee. In the event that a further need arises to change who the investigators are, the methods or any other aspect, such changes must be submitted as an Amendment for approval by the Committee.

We wish you the best with your research.

Yours sincerely

On behalf of the FHS REC, Dr R Sommers
MBChB, MMed (Int), MPharmMed, PhD
Deputy Chairperson *of the Faculty of Health Sciences Research Ethics Committee, University of Pretoria*

The Faculty of Health Sciences Research Ethics Committee complies with the SA National Act 61 of 2003 as it pertains to health research and the United States Code of Federal Regulations Title 45 and 46. This committee abides by the ethical norms and principles for research, established by the Declaration of Helsinki, the South African Medical Research Council Guidelines as well as the Guidelines for Ethical Research: Principles Structures and Processes, Second Edition 2015 (Department of Health)

Research Ethics Committee
Room 4-60, Level 4, Tswelopele Building
University of Pretoria, Private Bag x323

Fakulteit Gesondheidswetenskappe
Lefapha la Disaense tša Maphelo

Appendix III: Language editor certificate

Our team comprises enthusiastic and committed language specialists

ProCom language consultancy

Professional Communicators and Language Specialists

ZETHUSHOF, 620 PARK STREET
0007 ARCADIA
+27641001099 josemuta@gmail.com

SUITE 8, 1ST FLOOR
MIZRAHI HOUSE
33 ROBSON MANYIKA STREET
+263778915424

EDITING AND TRANSLATION SERVICES

Date: 04 January 2023

CERTIFICATE OF ENGLISH LANGUAGE EDITING

To whom it may concern

This is to certify that thesis paper with the provisional title **Effects of vascular endothelial growth factor receptor-1 inhibition on vasculogenic mimicry, and the metabolic profile of breast cancer cells *in vitro* by Nare Pretty Sekoba, (student number: 11213354), A thesis submitted in partial fulfilment for the degree of Doctor of Philosophy (Physiology) In the Department of Physiology, School of Medicine, Faculty of Health Sciences University of Pretoria** has been edited for language by ***ProCom Language Consultancy***. Neither the research content nor the authors' intentions were altered in any way during the editing process.

ProCom Language Consultancy guarantees the quality of the English language in this paper, provided our editor's suggestions are accepted and further changes made to the paper are referred back to our editing team.

Mutangadura J. (Dr.) Author Services—ProCom Language Services

Affiliated to:

MEMBER OF THE Professional EDITORS Guild

ENGLISH ACADEMY OF SOUTHERN AFRICA

MUTANGADURA J. DRS, BA Hons, MA Applied Language: (UZ), DTech: Language Practice, (TUT), PhD: Communication Science. (UNISA).

Appendix IV: Turnitin report

Effects of vascular endothelial growth factor receptor-1 inhibition on vasculogenic mimicry and the metabolic profile of breast cancer cells in vitro

ORIGINALITY REPORT

10%	10%	5%	2%
SIMILARITY INDEX	INTERNET SOURCES	PUBLICATIONS	STUDENT PAPERS

PRIMARY SOURCES

1	repository.up.ac.za Internet Source	5%
2	link.springer.com Internet Source	1%
3	Rowshan Ara Islam, Sazzad Hossain, Ezharul Hoque Chowdhury. "Potential Therapeutic Targets in Energy Metabolism Pathways of Breast Cancer", Current Cancer Drug Targets, 2017 Publication	1%
4	www.science.gov Internet Source	1%
5	"Encyclopedia of Cancer", Springer Science and Business Media LLC, 2017 Publication	1%
6	onlinelibrary.wiley.com Internet Source	1%
7	coek.info	

	Internet Source	1%
8	pdfs.semanticscholar.org Internet Source	1%

Exclude quotes	On	Exclude matches	< 1%
Exclude bibliography	On		